THE PEOPLE'S DEMOCRATIC REPUBLIC OF ALGERIA
MINISTRY OF HIGHER EDUCATION AND SCIENTIFIC RESEARCH

MEDEA UNIVERSITY

Faculty of Technology

Department of Electrical Engineering

Master's Thesis

Presented for the purpose of obtaining a Master's degree
In Electrical Engineering
Option: Renewable Energy

Topic:

Active and reactive power control of DFIG Using the Backstepping Controller

Studied by:

Aymen Lachemat

Benaissa Mohamed Houssam Eddine

Proposed and supervised by:

Supervisor: Dr. Boulkhrachef Salah

Co-supervisor: Dr. Moualdia.A

Class of 2023

ABSTRACTS

ملخص:

الهدف الرئيسي من هذا العمل هو تنظيم تبادل الطاقة النشطة والمتفاعلة بين المولد غير المتزامن مزدوج التغذية والشبكة من خلال العمل على الإشارات من الدوار بواسطة مموج للتوتر الكهربائي بتقنية النبضة معدلة العرض.يقدم هذا العمل دراسة نظام تحويل طاقة الرياح ذو مولد غير متزامن مزدوج التغذية، وذلك باستخدام طريقة الحل بالخطوات (Backstepping). تم اختيار عنصر التحكم بالخطوات لقدرته على التعامل بفعالية مع قضايا عدم اليقين في النموذج. تظهر نتائج المحاكاة التي تم الحصول عليها فعالية نهج التحكم بالخطوات في تحسين أداء نظام طاقة الرياح.

كلمات مفتاحية: طاقة الرياح، مولد غير متزامن مزدوج التغذية، التحكم بالخطوات، بتقنية النبضة معدلة العرض، التحكم في الطاقة.

Abstract:

The main objective of this work is to regulate the exchange of active and reactive power between the double-fed asynchronous generator and the grid by acting on the signals from the rotor via a Pulse Width Modulation (PWM) voltage source inverter. This work presents the study of a wind energy conversion system based on a double-fed asynchronous generator (DFIG), using the Backstepping command. The Backstepping control is chosen for its ability to handle model uncertainty problems effectively. The simulation results obtained show the effectiveness of the Backstepping control approach to improve the performance of the wind power system.

Keywords: Wind energy, Double-fed asynchronous generator (DFIG), Backstepping control, Pulse Width Modulation (PWM), Power control.

Résumé:

L'objectif principal de ce travail est de réguler l'échange de puissance active et réactive entre le générateur asynchrone à double alimentation et le réseau en agissant sur les signaux du rotor via un onduleur de tension à modulation de Largeur d'Impulsion (MLI).Ce travail présente l'étude d'un système de conversion d'énergie éolienne à base d'un générateur asynchrone à double alimentation (MADA), en utilisant la commande Backstepping. Le contrôle Backstepping est choisi pour sa capacité à gérer efficacement les problèmes d'incertitude de modèle Les résultats de simulations obtenus montrent l'efficacité de l'approche de contrôle Backstepping pour améliorer les performances du système d'énergie éolienne.

Mots-clés: Energie éolienne, Générateur asynchrone à double alimentation (GADA), Commande Backstepping, modulation de Largeur d'Impulsion (MLI), Contrôle des puissances.

Acknowledgments

First of all, we thank ALLAH, the Almighty for giving me the will, health and courage to carry out this work.

We thank very much Doctor: BOULKHRACHEF Salah and Dr. Moualdia who having ensured the co-direction of this thesis, for these precious advices along my memory work. We cannot thank him enough for his interest in this work and for the long hours of discussion that he reserved for us with uneven. And all the teachers of the Electrical department. We would also like to thank all the members of the jury who were kind enough to examine this modest work. We are certain that we can count on their vast knowledge and their constructive critical spirit to help us, through their comments and discussions, to better understand some of the problems encountered during this research work. It is difficult, in a small space, to thank all the people who have had an influence on our everyday life during the time of making our graduation thesis. These people will recognize each other easily and will know how great our tenderness and our friendship are for them. This work would not have been possible without the continued support of our family and without their education based on moral values based on respect for others and the work

Dedication

First, I would like to thank Allah for giving me strength and energy to
Accomplish the Work
I wish to express my sincere gratitude to, my supervisor
Dr.Boulkhrachef Salah for his
Constant Comprehension and Piece of Advice
I have the honor to dedicate this great gratitude to, my family for their help
And Encouragement
I dedicate this work to:
My Dear mother Naima and My beloved father Laid
Thank you for all your encouragements, love and your help. May Allah bless you now, and forever
To my brother Houssam and My sisters Amina and Sirine
To my Best freind Lina and her family
To my best friend Yahia and his family
To all my closest friends Zohir, Houssam, Rachid, Oussama
And
To all my teachers Special gratitude to all those extraordinary people
Who have stood by my side
In every hard moments

Aymen

Dedication

I would like to dedicate this Master's thesis to my family, with a special mention of my father. His words, 'If you cannot raise my head, at least do not bow it,' have resonated deeply within me. Thank you for instilling this powerful mantra in the back of my mind.

To my supportive mother, thank you for always being there to lift me up whenever I found myself in tears. Your unwavering presence and belief in me have given me the strength to face any challenge that comes my way. Everything I have achieved and will achieve is a result of your love and unwavering support.

I would also like to express my heartfelt gratitude to my teachers, whose guidance and expertise have played a vital role in shaping my academic journey. Your knowledge, dedication, and passion for teaching have inspired me to reach new heights. Your mentorship and encouragement have been invaluable, and I am deeply grateful for all the lessons I have learned under your guidance.

Furthermore, I want to dedicate this thesis to my friends and comrades who have made this journey possible and memorable. Thank you for standing by my side through thick and thin, for your unwavering support and camaraderie. Your presence has made this experience all the more meaningful.

This thesis is a testament to the love, belief, and support of my family, friends, and teachers. It is because of all of you that I have reached this milestone, and I am forever grateful.

Houssam

Notations and symbols

V_{vent}: wind speed.
$P_{VENT:}$ wind power.
V1: the wind speed upstream of the wind turbine.
V2: the wind speed downstream of the wind turbine.
V: the air velocity passing through the wind turbine.
S1: the upstream section of the air duct.
S2: the downstream section of the air duct.
F: the force exerted on the blades of a variable-pitch wind turbine.
ρ: The air density.
R: the radius of the swept area by the turbine.
$P_{arer:\ the}$ power absorbed by the wind turbine.
E: the kinetic energy of the mass of air passing through the wind turbine.
C_p: the power coefficient.
t: the relative velocity of the wind turbine.
$\Omega_{turbine}$: the rotational speed of the turbine.
Ω_{mee}: the rotational speed of the generator shaft.
K: mechanical multiplier (gearbox).
β: pitch angle (blade pitch angle).
i: incidence angle (angle of attack).
V_{rot}: the wind component due to the rotation of the wind turbine.
V_{res}: the resultant wind vector.
F_{res}: the force generated by the wind acting on the blade.
F_{ax}: the force representing axial thrust.
F_{rot}: the force causing the displacement of the blade.
T_T: the torque of the turbine.
$C_T(\lambda)$:the torque coefficient.
s,r: the corresponding indices for stator winding and rotor winding are typically referred to as (s) for stator and (r) for rotor .
sa, sb, sc : phases of the stator winding.
Ar, Br, Cr: rotor phases.
d , q : rotating field reference faram axes .
θ : angle between the axis of the first stator winding phase and the axis of the rotor .
θ_S : angle between the axis of the first phase of the stator winding and the d-axis .
θ_r : angle between the axis of the first phase of the rotot and the d-axis.
g: slip of the machine.
$V_{abs\ s}$: voltage of the three phases of the stator winding.
$V_{dq\ s}$: voltages of the stator winding in the d,q-axis.
$i_{abc\ s}$: currents of the three phases of the stator winding.
$i_{dq\ s}$: currents of the stator winding in the d,q-axis .
$i_{ABC\ r}$: currents of the three rotor phase .
$i_{dq\ r}$:currents of the stator winding in the d,q-axis .
Lss, Lrr : stator and rotor self- inductances .

Ms, Mr : mutual inductance between stator and rotor phases
Msr : maximum value of the mutualinductance between stator and rotor phases.
Rs, Rr : stator and rotor resistances per phase .
Is , Ir : stator and rotor leakage inductances .
τ_r : rotor time constant.
σ:the winding distribution factor .
$\Psi_{s\,abc}$: flux of the three phases of the stator winding .
$\Psi_{r\,ABC}$: flux of the three phases of the rotor winding.
$\Psi_{s\,dq}$: flux of the stator winding in the d,q-axis.
$\Psi_{r\,dq}$:rotor flux in the d,q-axis.
Ψ_m : magnetizing flux.
C_{em} : electromagnetic torque .
U_C : input voltage of an inverter level.
Cr : load torque.
f_r : coefficient of visxous friction .
Ω : rotational speed of the machine .
J: inertia of the machine.
p : number of pole pairs .
P: maplace perator.
N_r, N_s: number of turns of the rotor and stator windings.
ω_r, ω_S, ω : electrical frequencies respectively of the rotor , the stator , and the slip .
P_S : active power flowing through the stator .
P_r:active power flowing through the rotor .
Q_S: reactive power flowing through the stator.
Q_r: reactive power flowing through the rotor.
R: inference rule.
e: the error .

Table of Figure

Chapter I: Introduction to Wind Turbine Technology

Figure I. 1 : Annual map of the Average wind speed at 10m from the ground (m/s) [7]. 3
Figure I . 2: Conversion of kinetic energy from the wind 5
Figure I. 3 : Type of Wind Turbine 6
Figure I . 4 : The Tower 6
Figure I . 5 : The nacelle of the wind turbine 7
Figure I . 6 : The Gear box of the wind turbine 7
Figure I . 7 : Chaîne de fabrication de générateurs d'éoliennes 8
Figure I . 8 : The Anemometer of the wind turbine 8
Figure I . 9 : The multiplier 9
Figure I . 10 : Control system (command). 9
Figure I . 11 : The concrete foundation 10
Figure I . 12 : Wind turbine blades 10
Figure I . 13 : The hub of the wind turbine 11
Figure I . 14 : Demonstration of Betz's law 12
Figure I . 15 : Power coefficient 13
Figure I . 16 : Power coefficient for different types of wind turbines. 14
Figure I . 17 : Force balance on a blade section 15
Figure I . 18 : Airflow on a "stall" blade profile 16
Figure I . 19 : Variation of the pitch angle of a blade. 17
Figure I . 20 : Influence of the pitch angle on the power coefficient 17
Figure I . 21 : Variation of maximum wind power as a function of wind speed. 18
Figure I . 22 : Diagram of the wind turbine 19
Figure I . 23 : Simplified mechanical model of the turbine. 20
Figure I . 24 : Aerodynamic coefficient as a function of the turbine speed ratio (λ) for a 1.5 MW wind turbine [15]. 21
Figure I . 25 : Block diagram of the turbine model. 22

Chapter II: Modeling and Functioning of the DFIG

Figure II. 1 : Structure of the stator and rotor contacts of the DFIG 24
Figure II. 2 : Structure of the stator and rotor contacts of the DFIG 24
Figure II. 3 : Different Operating Modes of the Double-Fed Asynchronous Machine (DFIG) 25
Figure II. 4 : Schematic representation of a DFIG model 26
Figure II. 6 : Diagram of the static converter. 32
Figure II. 7 : Diagram of three-phase diode rectifier. 33
Figure II. 8: Representation of a filter. 33
Figure II. 9: Two-level three-phase NPC inverter structure. 35
Figure.II.10: The rotor current along the d-axis. 37
Figure.II.11: The rotor current along the q-axis. 37
Figure.II.12: active power of the stator. 37
Figure.II.13:reactive power of the stator.. 38
Figure.II.14: Active power of the rotor.. 38
Figure.II.15: reactive power of the rotor.. 38
Figure.II.16: Electromagnetic torque. 38
Figure.II.17: The rotor current along the d-axis. 39
Figure.II.18: The rotor current along the q-axis. 39
Figure.II.19: active power of the stator. 39
Figure.II.20:reactive power of the stator.. 39
Figure.II.21: Active power of the rotor.. 40

Figure.II.22: reactive power of the rotor.. 40
Figure.II.23: Electromagnetic torque. 40
Figure.II.24: The rotor current along the d-axis. 41
Figure.II.25: The rotor current along the q-axis. 41
Figure.II.26: active power of the stator. 41
Figure.II.27:reactive power of the stator.. 41
Figure.II.28: Active power of the rotor.. 42
Figure.II.29: reactive power of the rotor.. 42
Figure.II.30: Electromagnetic torque. 42
Figure.II.31: The rotor current along the d-axis. 43
Figure.II.32: The rotor current along the q-axis. 43
Figure.II.33: active power of the stator. 43
Figure.II.34:reactive power of the stator.. 43
Figure.II.35: Active power of the rotor.. 44
Figure.II.36: reactive power of the rotor.. 44
Figure.II.37: Electromagnetic torque. 44

Chapter III : VECTOR CONTROL OF THE DFIG

Figure III. 1 : Principle of vector control 44
Figure III. 2 : Block diagram of the DFIG (Doubly-Fed Induction Generator) 47
Figure III. 3 : Flux-oriented control block. 47
Figure III. 4 : Indirect control block diagram 48
Figure III. 5 : Regulation loop of the direct component of the stator current. 48
Figure III. 6 : Active and reactive power of the stator. 50
Figure III. 7 : The rotor current along the d-axis and q-axis 50
Figure III. 8 : Active and reactive power of the rotor 51
Figure III. 9 : The stator flux along the d and q axes 51
Figure III. 10 : Rotor voltages and currents. 51
Figure III. 11 : Electromagnetic torque 52

Chapter IV : Backstepping Control of the DFIG

Figure IV. 1 : Diagram of the indirect control of the stator powers of the DFIG, ... 55
Figure IV. 2 : Bloc diagram of the Backstepping iqrcurrent controller 58
Figure IV. 3 : Active power of the stator. 59
Figure IV. 4 : Reactive power of the stator. 59
Figure IV. 5 : Rotor current along the d-axis. 59
Figure IV. 6 : Rotor current along the q-axis. 60
Figure IV. 7 : Active power of the rotor. 60
Figure IV. 8 : Reactive power of the rotor. 60
Figure IV. 9 : Stator flux along the q-axis. 61
Figure IV. 10 : Stator flux along the d-axis. 61
Figure IV. 11 : Rotor Voltages. 61
Figure IV. 12 : Electromagnetic torque 62
Figure IV. 13 : the active power of the stator using a PI controller and the backsteppingcommand 63
Figure IV. 14 : comparing the reactive power of the stator using a PI controller and the Backstepping command 63
Figure IV. 15 : comparing the Rotor current along the d-axis. Using a PI controller and the . 63
Figure IV. 16 : comparing the Rotor current along the q-axis. Using a PI controller and the . 64
Figure IV. 17 : comparing The Rotor Voltages using a PI controller and the command Backstepping 64

Table of Contents

General Introduction 1
I.1 Introduction: 2
I.2 General Information on wind energy: 2
I.3 Estimation of wind resources in Algeria 3
I.4 Definition of Wind Energy: 3
I.5 Advantages and Disadvantages of wind energy 4
I.5.1. Advantages: 4
I.5.2. Disadvantages: 4
I.6 Different Types of Wind Turbines 5
I.6.1 Vertical Axis Wind Turbines 5
I.6.2 Horizontal Axis Wind Turbines 5
I.7 Main components of a wind turbine: 6
I.7.1 The tower 6
I.7.2 The nacelle of the wind turbine: 7
I.7.2.1 Slow Shaft: 7
I.7.2.2 a Gear box: 7
I.7.2.3 The cooling system: 7
I.7.2.4 the Generator: 8
I.7.2.5 Anemometer: 8
I.7.2.6 The multiplier 8
I.7.3. The control system: 9
I.7.4. The concrete foundation 10
I.7.5.The rotor and blades: 10
I.7.6 The hub: 11
I.8 operating principle: 11
I.9 Wind energy conversion 11
I.9.1 BETZ's Law 12
I.9.2 Mechanical energy production 14
I.10 Control system 15
I.10.1 Balance of forces on the blade 15
I.10.2 Energy conversion adjustment means 15
I.10.2.1 “Stall” aerodynamic stall system 15

I.10.2.2 “Pitch” blade orientation system: 16
I.11 The continuously variable wind speed: 17
I.12 Wind turbine modeling 18
I.12.1 simplifying assumptions for the mechanical modeling of the turbine 19
I.12.2 Wind speed modeling 20
I.12.3 Turbine modeling 20
I.12.4 Multiplier model 22
I.12.5 Dynamic equation of the generator shaft 22
I.13 Conclusion 23
II.1. Introduction: 23
II.2.Definition of the double-fed asynchronous machine: 23
II.3. Machine structure: 24
II.4. Principle of operation of the double-fed asynchronous machine: 24
II.5 Modeling of the Doubly Fed Induction Machine: 26
II.5.1 Assumptions made for simplification: 26
II.5.2 Model of the DFIG in the abc frame: 26
II.5.3 The Park Transformation: 28
II.5.3.1 Electric and magnetic equations in the (d, q) axis system: 30
II.5.4 Choice of reference frame: 30
II.5.5 Two-phase model of the DFIG related to the rotating field: 31
II.5.6 State space representation: 31
II.6 modeling of the DFIG power supply: 32
II.6.1 Rectifier Modeling: 32
II.6.2 Filter Modeling: 33
II.6.3 modeling of the inverter: 34
II.6.4 Double-fed asynchronous machine simulation with the inverter struchure: 36
II.7. Conclusion: 45
III.1 Introduction: 42
III.2 Vector Control: 42
III.2.1 Advantages of vector control: 42
III.2.2 Disadvantages of vector control: 42
III.3 Principle of vector control: 43
III.4 Model for independent power control: 44
III.5 Synthesis of current PI controllers: 48
III.6 Simulation of indirect power control 49

III.9. Conclusion: 52
IV.1.Introduction: 54
IV.2.Basic Concepts and Principles: 54
IV.2.1. Virtual Control: 54
IV.2.2. Stabilizing Functions: 54
IV.3. Backstepping Control [26] 55
IV.3.1. Lyapunov Method: 56
IV.3.2. Rotor currents control: 57
IV.4. simulation results: 58
IV.5.Comparison between Backstepping and the PI Controller: 62
IV.5.1 Backstepping: 62
IV.5.2 PI Controller (Proportional-Integral): 63
IV.6.Conclusion: 65
General Conclusion: 66
Annexe 67
Bibliography 68

General Introduction

General Introduction

The asynchronous machine, highly appreciated in industrial applications for its robust electromechanical construction and low cost, requires specific and complex control structures that are used in high-performance variable speed drive systems. In the field of variable speed applications [1], there is a new and original solution that utilizes an alternating current machine operating in a somewhat unique mode [1]. This is the doubly fed asynchronous machine (DFIG), a three-phase asynchronous machine with a wound rotor that can be powered by two voltage sources [2]. The doubly fed asynchronous machine has been the subject of extensive research, mainly for its operation as a generator in wind energy applications and for high-power drive applications. Our work focuses on its operation as a generator, aiming to improve the dynamic performance of the DFIG using non-linear control theory.

Significant interest has been given to this machine due to the degrees of freedom it offers, as its rotor is accessible, allowing it to be powered by a converter on both the stator and rotor sides, and enabling a wider speed range (sub-synchronous, synchronous, super-synchronous) [3]. Analogous to the induction machine, the principle of vector control based on classical PI controllers has been the most commonly used solution for controlling the DFAM. However, the simplicity of PI controllers comes with some drawbacks that limit performance, such as sensitivity to parameter variations and the linear nature of PI controllers, whose validation conditions are only satisfied under steady-state conditions, etc. [4].

On the other hand, given the nonlinear nature of the DFIG dynamics, it was natural for several researchers to turn to non-linear control theory to improve the dynamic performance of this machine. Among the various variants of non-linear control, one stands out as being both more efficient in terms of computation and development costs: backstepping control. This technique is based on Lyapunov stability theory, which enhances the stability aspect of the control [5].

Therefore, the objective of this work is to use one of the principles of backstepping control for the control of the DFIG. In addition to the general introduction, this work consists of four chapters:”

The first chapter provides an introduction to wind turbines, highlighting their evolution and advancements over time.

In the second chapter, the focus shifts to the modeling and functioning of the DFIG system.

Moving forward, the third chapter explores Vector Control of the DFIG

The final chapter will be dedicated to the presentation of the principle of Backstepping control and its application on the DFIG to control the active and reactive powers on the stator side.

CHAPTER I

Introduction to Wind Turbine Technology

I.1 Introduction:

Wind sensor technology has undergone significant advancements since the inception of windmills. Profiled blade wind turbines were first developed in the early 1940s and proved successful in generating electricity. Both vertical and horizontal axis sensors are utilized to capture wind energy, and the efficiency of these sensors is increasing over time. The conversion of mechanical energy into electrical energy is a crucial aspect of wind turbines, and various devices are employed, primarily using synchronous and asynchronous machines. To enhance the profitability of wind installations, control strategies must be in place for these machines, along with possible network connection interfaces, to capture maximum energy over a broad range of wind speed variations.

I.2 General Information on wind energy:

In the 9th century, the first wind turbines were utilized in what is now Iran, Afghanistan, and Pakistan. These early wind turbines served the purpose of grinding grain and pumping water. Similarly, wind turbines were employed in Europe from the 11th century onwards. Initially, vertical-axis windmills resembling the Panemone windmills of Iran were prevalent. However, horizontal-axis windmills gained popularity in Europe, and by the 14th century, they were employed for various tasks such as grinding grain, sawing wood, and pumping water.

In the 19th century, wind turbines began to be used for electricity generation. Professor James Blyth constructed the first wind turbine for electricity in Scotland in 1887, which was a small vertical-axis turbine powering the lighting in his holiday cottage. In 1888, Charles Brush erected a larger horizontal-axis wind turbine in Ohio, which supplied power to his home and laboratory. During the early 20th century, wind turbines were employed for electricity generation in multiple countries, including Denmark, the United States, and the Netherlands. However, due to slow technological development and high costs, their widespread usage was limited.

The oil crisis in the 1970s renewed interest in wind energy as the high cost of oil made wind-generated electricity more economically viable. Consequently, various countries began investing in wind energy research and development. In the 1980s, the cost of wind turbines decreased, leading to an increase in installations worldwide. The wind energy industry continued to expand in the 1990s, with wind turbines becoming a significant electricity source in many countries. Throughout the 2000s, wind turbines further established themselves as major contributors to electricity generation worldwide.

Presently; wind turbines play a vital role in generating electricity in both onshore and offshore wind farms. Onshore wind farms are situated on land, while offshore wind farms are located in the ocean. Wind turbines offer numerous advantages as a clean, renewable, and reliable energy source. They produce no greenhouse gases or pollutants and do not necessitate water or fuel. With declining costs, wind energy is projected to grow substantially, playing a pivotal role in transitioning towards a clean energy future. [6]

I.3 Estimation of wind resources in Algeria

As for Algeria, the wind resource varies greatly from one location to another. This is mainly due to the diverse topography and climate of the country. Indeed, our vast country is divided into two distinct geographical zones. The Mediterranean north is characterized by a 1200 km coastline and mountainous terrain, represented by the Tell Atlas and the Saharan Atlas ranges. In between, there are plains and high plateaus with a continental climate. The south, on the other hand, is characterized by a Saharan climate.

The southern part of Algeria is characterized by higher wind speeds compared to the north, especially in the southwest where speeds exceed 4 m/s and even reach values exceeding 6 m/s in the Adrar region. In the northern regions, the average wind speed is generally lower. However, there are microclimates observed in coastal sites such as Oran, Bejaia, and Annaba, as well as in the high plateaus of Tiaret and El Kheiter, and in the region bounded by Bejaia in the north and Biskra in the south [7].

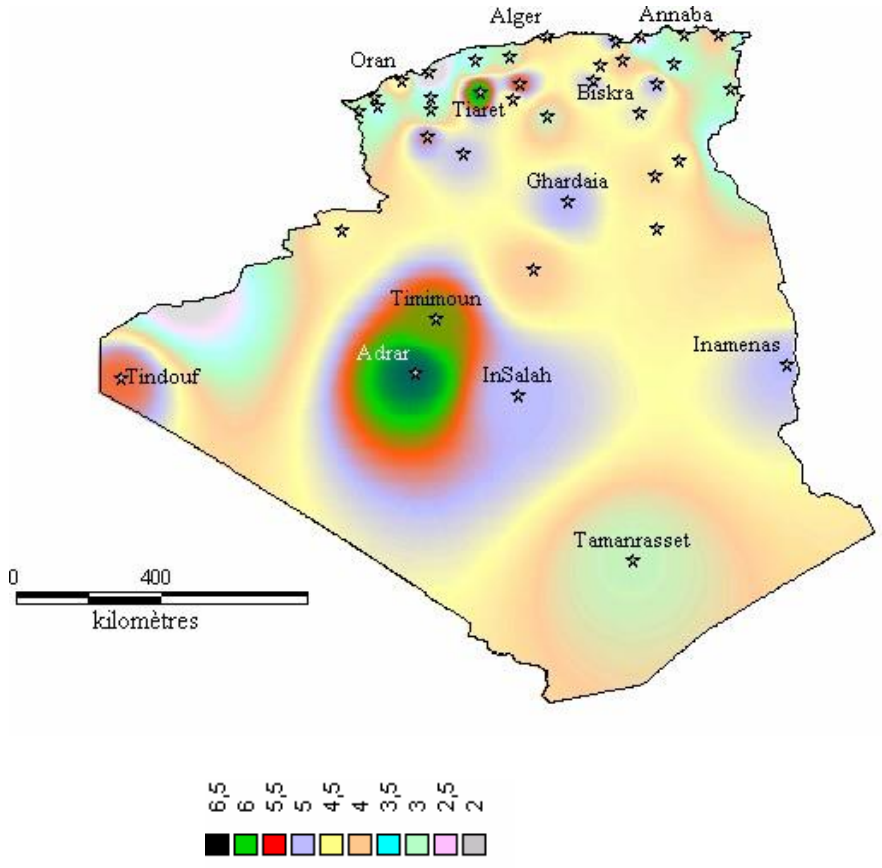


Figure I. 1 : Annual map of the Average wind speed at 10m from the ground (m/s) [7].

I.4 Definition of Wind Energy:

A wind turbine, more commonly called a windmill, is a device that converts a portion of the kinetic energy of the wind (moving fluid) into mechanical energy available on a transmission shaft, and then into electrical energy through a generator. Figure (I.1)

The wind energy is an "un-degraded" renewable energy source, which does not produce any atmospheric emissions or radioactive waste. However, due to its temporal variability and complexity in harvesting, wind energy requires large-scale wind turbines (up to 60 meters for several-megawatt turbines) installed in geographically unobstructed areas to avoid turbulence [8].

Wind energy is a new means of decentralized electricity production that offers a viable alternative to nuclear power, without necessarily claiming to replace it, since the amount of energy produced is significantly lower. Wind turbines can be installed on land or increasingly, offshore where the wind is more consistent. This makes the turbines less visible and less noisy, reducing their environmental impact.

I.5 Advantages and Disadvantages of wind energy

I.5.1. Advantages:

- Wind energy is a clean and renewable energy that produces no pollution or waste. In addition, it repays its energy debt, that is to say the energy necessary for its manufacture, in a few months;
- Wind energy is abundant: the wind is inexhaustible. It is therefore a real renewable resource;
- the wind industry has significant potential in terms of manufacturing and installation jobs;
- Beyond the economic and environmental situation, wind energy is of particular interest because it can promote the diversification and energy independence of a country.

I.5.2. Disadvantages:

- Visual and noise pollution. Disturbance of electromagnetic waves (television, radio, portable) are obstacles to installation in private homes and this obliges the installation of wind turbines far from dwellings;
- From a technical point of view, wind power has some disadvantages compared to other types of electrical energy production:
- Wind energy is intermittent and difficult to predict;
- Its insertion in electrical networks leads to specific problems and constraints that must be taken into account by network operators. Indeed, as long as this type of production remains marginal, the constraints are limited. Also for a long time, wind farms often had the only "constraints" to produce when it was possible to produce and not to degrade the quality of voltage on the networks.
- Today, due to the significant and ever-increasing development in terms of installed power of wind farms, they are subject to increasingly stringent technical requirements imposed by grid connection rules defined at the initiative of managers of networks.

I.6 Different Types of Wind Turbines

According to the geometric arrangement of the shaft on which the propeller is mounted, wind turbines are classified into two types [8]:

I.6.1 Vertical Axis Wind Turbines

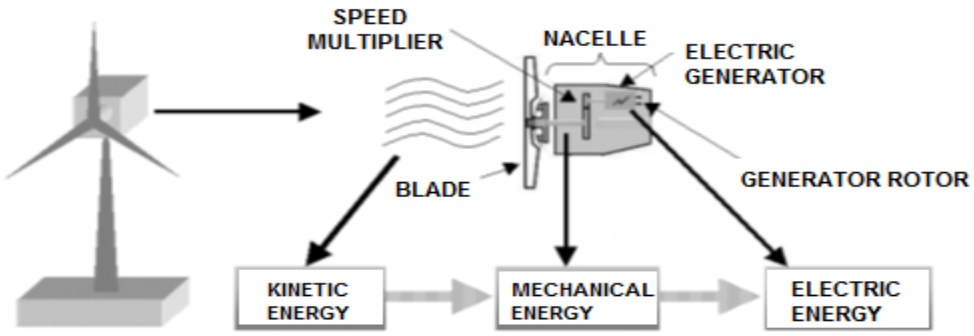


Figure I . 2: Conversion of kinetic energy from the wind

The most well-known ones are called "Darrieus" turbines (named after their inventor Georges Darrieus). Vertical-axis wind turbines were the first structures developed to generate electricity. In this type, the shaft is perpendicular to the ground, which has the advantage of not requiring a blade orientation system. Additionally, the mechanical components such as the gearbox and generator are located at ground level, eliminating the need for a tower. This design facilitates maintenance interventions (Figure I.2).

In summary, this particular type of wind turbine has been the subject of numerous research studies. It offers the advantage of not requiring a blade orientation system and having a mechanical component at ground level, which facilitates maintenance. However, some of these turbines need to be manually started, and the tower often experiences significant mechanical stress, leading manufacturers to largely abandon them (except for very low power applications) in favor of horizontal-axis wind turbines.

I.6.2 Horizontal Axis Wind Turbines

Although they require a blade orientation mechanism, horizontal-axis wind turbines are the most commonly used. In this type of turbine, the shaft is parallel to the ground. Horizontal-axis turbines have surpassed vertical-axis turbines because they are more cost-effective and less exposed to mechanical constraints. The generator is placed in the nacelle, close to the rotor and shaft, reducing mechanical stresses. Additionally, the position of the receiver several meters above the ground captures stronger and more consistent winds compared to ground-level. Typically, horizontal-axis turbines for electricity production use between 1 and 3 blades.

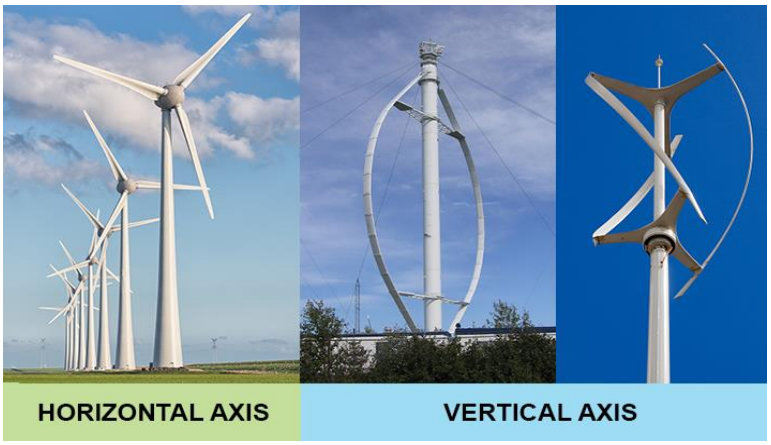


Figure I. 3 : Type of Wind Turbine

In addition to the visual aspect of wind turbines, their impact on the environment is reduced. A wind turbine covers only a very small percentage of the total surface area of the site on which it is located, allowing most sites to maintain their industrial or agricultural activities. Their noise pollution is also relatively low. Wind turbines are divided into three categories according to their rated power:

- Small wind turbines: less than 40 KW.
- Medium wind turbines: from 40 to a few hundred KW.
- Large wind turbines: greater than 1 MW.

I.7 Main components of a wind turbine:

A wind turbine is generally made up of three main elements: the tower or mast, the nacelle, and the rotor-blade assembly.

I.7.1 The tower

The tower of a wind turbine is typically a supporting element that is made of steel tube or lattice structure. Its height is designed to minimize the effects of ground-level disturbances. The tower has a conical shape, resembling a truncated cone, and contains electrical energy transport cables, control elements, connection devices to the distribution network, and access to the nacelle.



Figure I . 4 : The Tower

I.7.2 The nacelle of the wind turbine:

It groups together the entire system for transforming wind energy into electrical energy and various control actuators

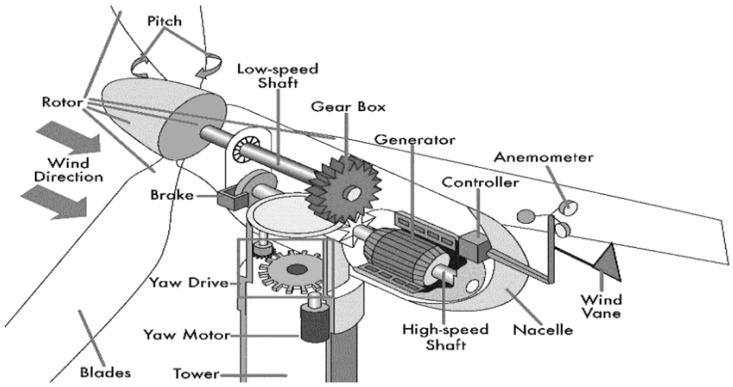


Figure I . 5 : The nacelle of the wind turbine

I.7.2.1 Slow Shaft:

It connects the hub to the gearbox and contains a hydraulic system allowing aerodynamic braking if necessary.

I.7.2.2 a Gear box:

The gearbox of a wind turbine is responsible for adjusting the speed of the blades to match that of the electrical generator, which typically operates at around 1500 rpm. Additionally, the gearbox is equipped with a mechanical disk brake that can be used in case of emergency if the aerodynamic brake fails, or during maintenance of the wind turbine.

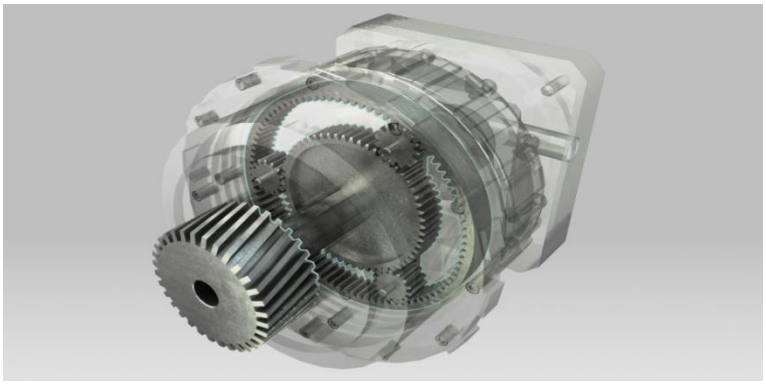


Figure I . 6 : The Gear box of the wind turbine

I.7.2.3 The cooling system:

It usually includes an electric fan used to cool the generator and an oil cooler for the gearbox. There are some types of wind turbines that have a water cooling system.

I.7.2.4 the Generator:

The generator in a wind turbine is responsible for converting the mechanical energy available on the output shaft of the gearbox into electrical energy. This can be achieved using two different types of machines: an asynchronous generator or a synchronous generator.

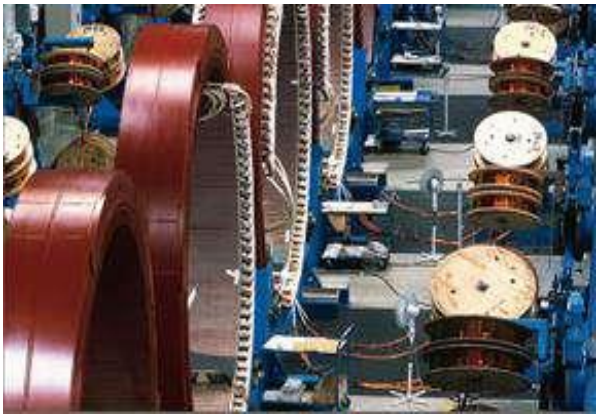


Figure I . 7 : Chaîne de fabrication de générateurs d'éoliennes

.

I.7.2.5 Anemometer:

The control system of a wind turbine uses the electrical signals generated by the anemometer to start the turbine when the wind speed reaches around 5m/s. Likewise; the system automatically stops the turbine if the wind speed exceeds 25m/s, as a safety measure to protect the turbine.



Figure I . 8 : The Anemometer of the wind turbine

I.7.2.6 The multiplier

The gearbox connects the (primary) shaft of the wind turbine to the (secondary) shaft of the electric generator. It transforms high-torque, slow-speed power into low-torque, high-speed power.

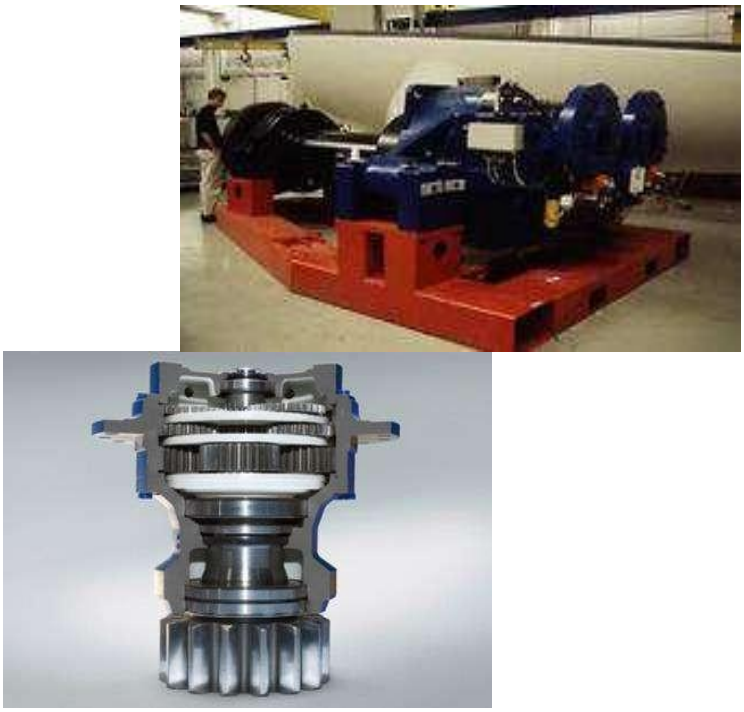


Figure I . 9 : The multiplier

I.7.3. The control system:

It includes a computer that constantly monitors the status of the wind turbine while controlling the orientation device. In the event of the gearbox or generator overheating, the system automatically shuts down the wind turbine and signals this to the operator's computer via a telephone modem [9].



Figure I . 10 : Control system (command).

I.7.4. The concrete foundation

A solid foundation ensuring the resistance of the assembly in high winds and/or in icing conditions.



Figure I . 11 : The concrete foundation

I.7.5.The rotor and blades:

The rotor of a wind turbine consists of blades that are mounted on a hub, and its primary function is to convert the kinetic energy of the wind into mechanical energy. The maximum efficiency of the rotor is about 59% according to the Betz limit. The number of blades has relatively little impact on the performance of a wind turbine. While more blades provide greater starting torque, they result in a smaller rotational speed. Single and double-bladed turbines are lighter but produce fluctuations that are more mechanical, have lower energy efficiency, and are noisier since they rotate faster. They also cause more significant visual disturbances, as noted by landscape architects. Additionally, an even number of blades should be avoided for stability reasons.

The blade itself is a technically challenging component to manufacture, as it must comply with specific geometric rules regarding the aerodynamic profile. Additionally, it must be made of a material strong enough to withstand the pressure forces exerted by the wind and external aggressions, such as pollution or certain particles found in the air.

The blades are made of fiberglass or composite materials such as carbon fiber, which is lightweight and strong (Fig. I.11).

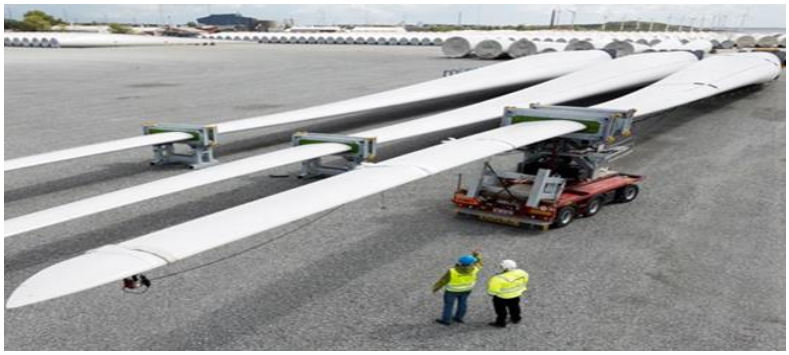


Figure I . 12 : Wind turbine blades

I.7.6 The hub:

The hub of a wind turbine is a critical component that must endure considerable stress, especially during start-up and abrupt changes in wind velocity. For this reason, the hub is typically constructed through molding rather than welding to ensure its strength and durability.

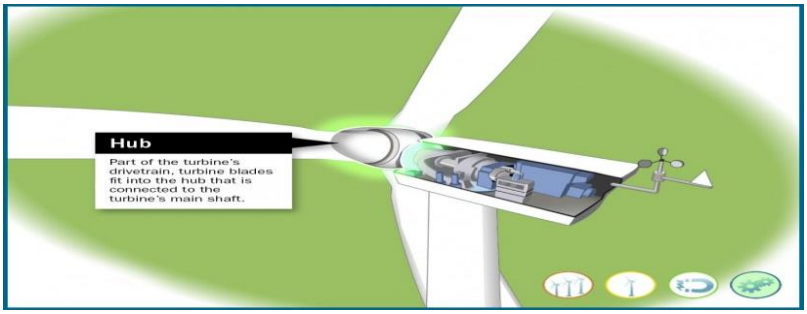


Figure I . 13 : The hub of the wind turbine

I.8 operating principle:

At the height of the nacelle, a wind blows at speed V_{wind}. As long as this speed is below the threshold speed, the blades are in a feathered position (their surface is perpendicular to the direction of the wind) and the system is at a standstill. When the anemometer detects the threshold speed, a signal is sent by the control system to start the wind turbine. The orientation mechanism rotates the nacelle to face the wind; the blades are then set at the optimal pitch angle and begin to rotate. A power P_{wind} is then captured and transmitted to the shaft with a coefficient of performance. After passing through the gearbox, this same power is transmitted to the generator shaft at a higher speed. Finally, this mechanical power is converted into electrical power output by the generator. There are two cases: either the wind turbine is connected to the distribution grid (directly or through static converters), or it autonomously powers an isolated load through or without static converters [10].

I.9 Wind energy conversion

Wind energy conversion refers to the process of transforming the kinetic energy of the wind into usable electrical energy. It is achieved using wind turbines, which capture the energy of the wind through rotating blades. When the wind blows, the blades spin, and this rotational motion is then converted into electricity using an integrated generator. Wind energy conversion is a form of renewable energy that offers sustainable electricity generation with environmental benefits.

I.9.1 BETZ's Law

According to Betz's theorem, the speed of the wind crossing the surface swept by the rotor is assumed to be equal to the average of the mean speed of the undisturbed wind upstream of the wind turbine] and its speed after passing through the plane of rotor (see figure I.13) [11]

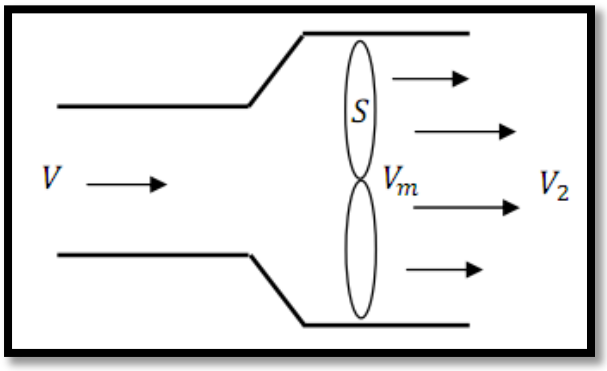


Figure I . 14 : Demonstration of Betz's law

Consider the horizontal axis wind system shown in Figure (I-10) on which the wind speed V1 upstream of the wind generator and the speed V2 downstream have been shown.

Designating by V the speed of the air crossing the wind turbine, by S1 and S2 the upstream and downstream sections of the air tube and by S the surface swept by the propeller. The equality, which translates the incompressibility of the air and the permanence of the flow, is written [12]:

$$S_1V_1 = S = S_2V_2 \qquad (\mathrm{I}.1)$$

The force exerted by the air on the aero generator according to the EULER theorem:

$$F = \rho.SV.(V_1 - V_2) \qquad (I.2)$$

Hence the power absorbed by the aero generator:

$$P_{aero} = F.V = \rho.SV^2(V_1 - V_2) \qquad (I.3)$$

The power absorbed by the wind turbine is also equal to the variation of the kinetic energy Ec of the mass of air passing through it, from which:

$$\frac{\Delta E_c}{\Delta t} = \frac{1}{2}\rho.SV.\left({V_1}^2 - {V_2}^2\right) = P_{aero} = \rho.SV^2.(V_1 - V_2) \qquad (\mathrm{I}.4)$$

We can deduce:

$$V = (V_1 + V_2)/2 \qquad (\mathrm{I}.5)$$

By replacing the expression of V in relations (I.2) and (I.3), we obtain:

$$F = \frac{1}{2}\rho.S\left({V_1}^2 - {V_2}^2\right) \quad \text{(I. 6)}$$

$$P_{aero} = \frac{1}{4}.\rho.S\left({V_1}^2 - {V_2}^2\right).(V_1 - V_2) \quad \text{(I. 7)}$$

A theoretically undisturbed wind would cross the same surface S without a decrease in speed, i.e. at speed V1, the corresponding power P_{mt} would then be:

$$P_{mt} = \rho.S.V_1^3/2 \quad \text{(I. 8)}$$

The ratio between the power extracted from the wind and the total power theoretically available is:

$$\frac{P_{aero}}{P_{mt}} = \frac{\left(1 + \frac{V_1}{V_2}\right).(1 - (\frac{V_1}{V_2})^2)}{2} = Cp \quad \text{(I. 9)}$$

If we represent the characteristic corresponding to equation (I.9), we see that the ratio P_{aero}/P_{mt}also called power coefficient Cp has a maximum for $\frac{V_1}{V_2} = \frac{16}{25}$ which equals 0.59 (Figure I.14). This limit is actually never reached and each wind turbine is defined experimentally by its own power coefficient expressed as a function of the relative speed λ representing the ratio between the speed of the end of the blades of the wind turbine and the speed of the wind. .

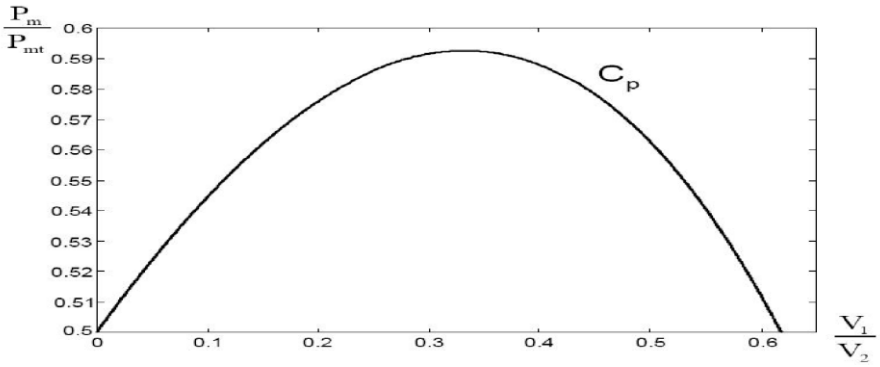


Figure I . 15 : Power coefficient

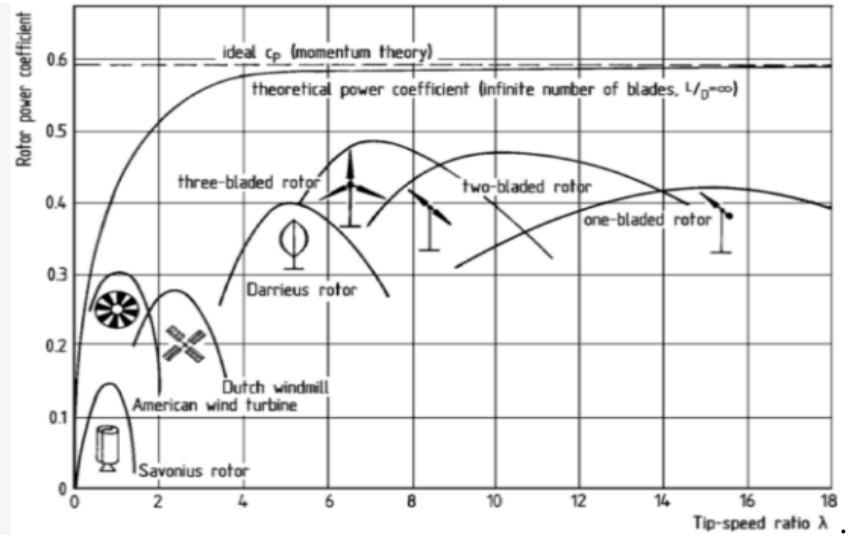


Figure I . 16 : Power coefficient for different types of wind turbines**.**

Slow-running wind turbines are equipped with a large number of blades (between 20 and 40); their high inertia generally imposes a diameter limitation of around 8 m. Their power coefficient (Figure I.15) quickly reaches its maximum value during the increase in speed but also decreases rapidly thereafter. Fast-paced wind turbines are much more widespread and almost all dedicated to the production of electrical energy.

They generally have between one and three fixed or adjustable blades to control the speed of rotation. The blades can reach lengths of 45 m for wind turbines of several megawatts [12].

Three-bladed wind turbines are the most common because they represent a compromise between the vibrations caused by the rotation and the cost of the wind generator. Moreover, their coefficient of power (Figure I.15) reaches high values and decreases slowly as the speed increases.

I.9.2 Mechanical energy production

By combining equations (I.8) and (I.9), the mechanical power P_{aero} available on the shaft of a wind turbine is expressed as follows:

$$P_{aero} = \left(\frac{P_{aero}}{P_{mt}}\right).P_{mt} = C_P(\lambda).P_{mt} = \frac{1}{2}C_P(\lambda).\rho.\pi.R^2V_1^3 \qquad \text{(I.10)}$$

With:

$$\lambda = \frac{\Omega_{turbine}.R}{V_1} = \frac{\Omega_{mec}.R}{K.V_1} \qquad \text{(I.11)}$$

$\Omega_{turbine}$: Rotation speed of the turbine.

Ω_{mec} : Speed of rotation of the shaft of the generator.

P : the air density equal to 1.225 kg.m^(-3).

R : radius of the aero generator. Given the ratio of the speed multiplier K.

This relationship makes it possible to establish a set of characteristics giving the power available as a function of the rotational speed of the generator for different wind speeds.

I.10 Control system

I.10.1 Balance of forces on the blade

The figure (I.13) represents the section of a wind turbine blade. The vector V represents the speed of the wind arriving in front of this blade, the vector V_{rot} represents the component of wind due to the rotation of the aero generator. The resultant of these two vectors is calledV_{res}.

The action of the wind on the blade produces a force F_{res} , which breaks down into an axial thrust F_{ax}directly compensated by the mechanical resistance of the mast and a thrust F_{rot}in the direction of rotation that actually produces the displacement.

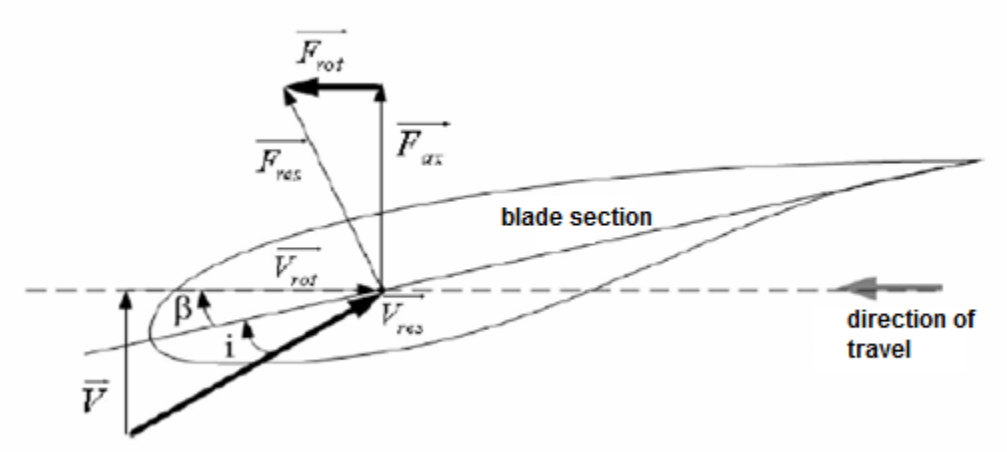


Figure I . 17 : Force balance on a blade section

.

Each wind turbine is thus sized so that this force reaches its nominal value for a given nominal wind speed. When the wind speed becomes too high,

The power extracted by the wind turbine must be canceled or limited to its nominal value. It should be noted that β and i are respectively the pitch angle and the angle of incidence

I.10.2 Energy conversion adjustment means

In the operating phase, given the very fluctuating nature of the wind and the limited resistance of the structure, two types of adjustment are required. In fact, to guarantee maximum (optimal) capture of the incident energy, the speed of the wind turbine must be constantly adjusted to the wind speed and the angle of incidence of the blades.

I.10.2.1 "Stall" aerodynamic stall system

It is a regulator by aerodynamic stall, in other words the geometric behavior of the blades can be evaluated according to the ratio between the two speeds of the wind and the

turbine, which allows the stall from a certain wind speed. This stall depends in particular on the pitch angle of the blades which can be manufactured with a variable pitch depending on the position along the blade and also allowing an end braking mechanism. This technique of "Stall Control" also has some advantages:

- No pitch angle control system
- Simpler and less expensive construction of the rotor.
- Easier maintenance and better reliability.

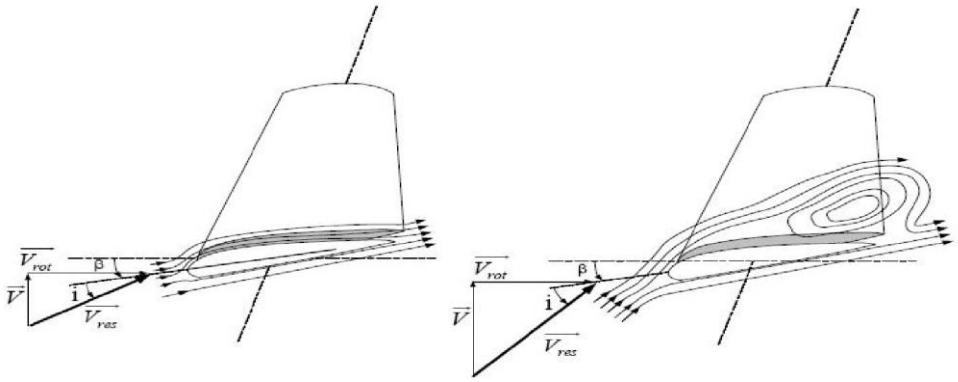


Figure I . 18 : Airflow on a "stall" blade profile

I.10.2.2 "Pitch" blade orientation system:

It is a control system that varies the pitch angle of the blades (blade pitch) around their longitudinal axis based on the wind speed and the active power to be extracted. By utilizing Pitch Control, the power coefficient (cp) no longer varies based on λ as before, but instead varies according to the wind speed at a constant rotation speed. This enables the maintenance of constant power at its maximum value within Zone 3 [13]. It should be noted that to adjust the pitch angle in Pitch Control within an automatic rotational speed control system, an electronic regulator with centrifugal masses or a regulator is required. or an electronic regulator with servomotors, which will allow for:

- Starting at a reduced vd wind speed.
- The regulation of the angular speed of the turbine for a wind speed higher than the nominal speed vn
- The optimization of the energy conversion regime when the wind speed evolves between vd and vn.
- Protection of the wind turbine against high wind speeds ($>vmax$) by feathering the blades without the need for a powerful braking system for emergency stops.

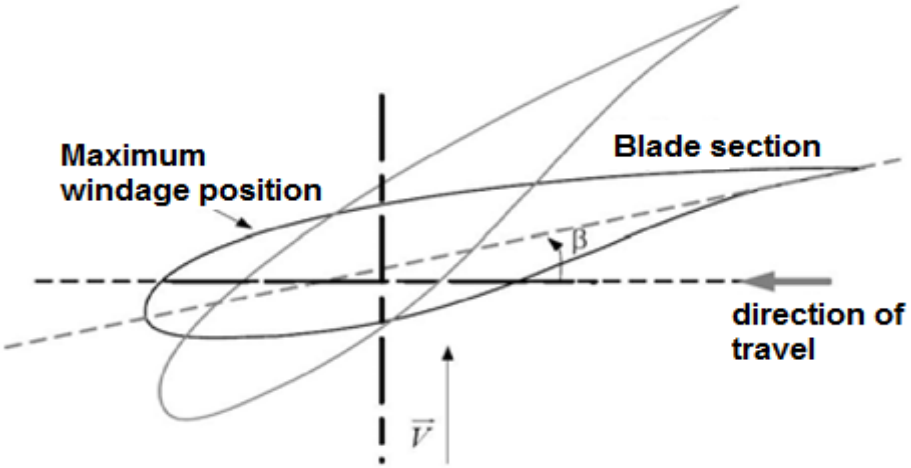


Figure I . 19 : Variation of the pitch angle of a blade**.**

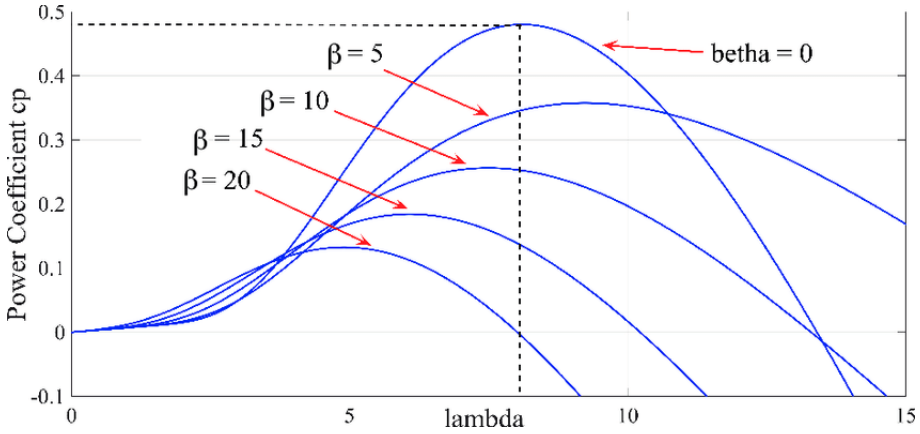


Figure I . 20 : Influence of the pitch angle on the power coefficient

In order to improve the effectiveness of capturing energy using Stall Control, one can integrate this mechanism with a two-speed rotation machine. This integration broadens the range of energy production, making it comparable to the results obtained with Pitch Control

Some wind turbines use a hybrid system called Stall Actif which combines the advantages of both systems where the aerodynamic stall is obtained gradually thanks to a minimal orientation of the blades requiring more economical and more robust means of adjustment than in the case of the Pitch Control system. .

I.11 The continuously variable wind speed:

The electrical configuration of a wind turbine has a great influence on its operation. Whether a wind turbine operates at fixed speed or variable speed depends on this configuration.

Fixed speed operation has the following characteristics:

- Simpler electrical system.
- Greater reliability.
- Little probability of excitation of the resonant frequencies of the elements of the wind

turbine.

- No need for an electronic control system.
- Cheaper.

And variable speed operation is characterized by:

- Increased energy efficiency;
- Reduction of torque oscillations in the power train;
- Reduction of the forces undergone by the power train;
- Generation of higher quality power.

Thus, the importance of operating at variable speed and the continuous adjustment of it to maintain the power coefficient (cp) at its maximum value becomes evident, especially if the electric generator is of the synchronous or asynchronous type directly connected to the grid. In this case, the speed remains relatively constant, and the aerodynamic efficiency can only be maximized at a specific wind speed (λopt).

A two-speed rotation system is possible, but electronically variable speed provides much more in terms of energy efficiency. Figure (I.17) shows that the position of the maximum power curve changes with the wind speed. Typically, direct or indirect speed control is necessary to optimize energy transfers effectively [14].

.

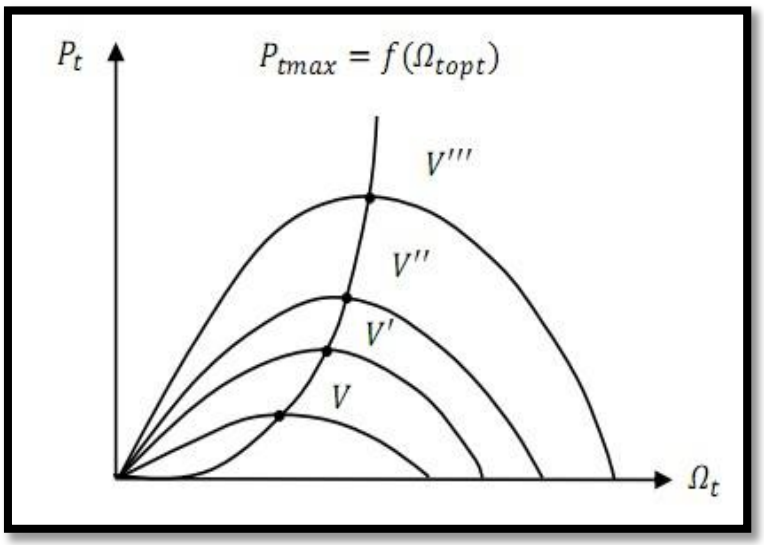


Figure I . 21 : Variation of maximum wind power as a function of wind speed.

I.12 Wind turbine modeling

The purpose of the wind system is to convert the kinetic energy of the wind into mechanical energy available on a transmission shaft and then into electrical energy via a generator. This system, in our case, is mechanically made up of five organs:

- Three oriental blades having their own coefficients of inertia..
- Elasticity and friction with respect to the air and with respect to the support of the turbine.
- A blade drive shaft with its own inertia, its own elasticity and its coefficient of

friction with respect to the multiplier.

- A speed and gain multiplier.
- A generator rotor having inertia and a coefficient of friction.

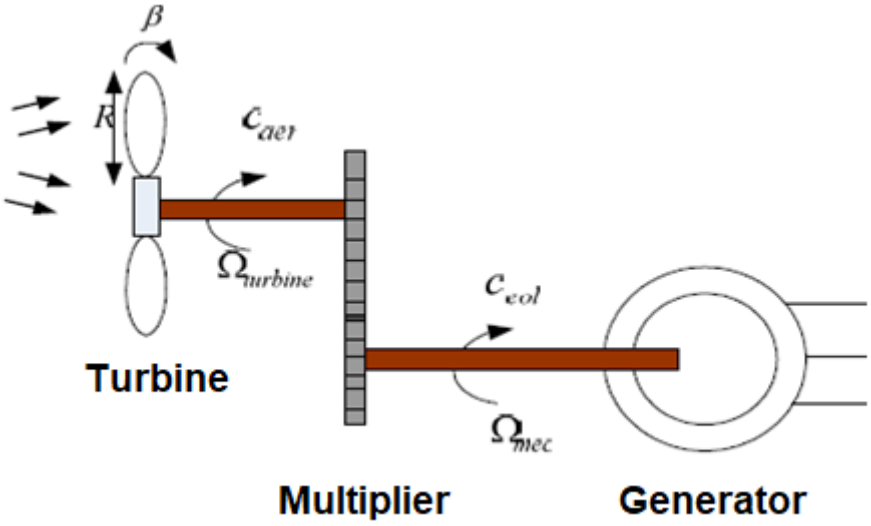


Figure I . 22 : Diagram of the wind turbine

I.12.1 simplifying assumptions for the mechanical modeling of the turbine

In electromechanical studies, the models commonly used are relatively simple and follow certain simplifying assumptions, including:

- Assuming that the blades are designed identically with the same values for parameters such as inertia, elasticity, and friction.
- Ignoring the low friction coefficients of the blades with respect to the air and support.
- Assuming that the wind speed is uniformly distributed across all the blades, allowing for the consideration of all the blades as a single mechanical system characterized by the sum of all individual mechanical systems**.**

A simple mechanical model is then obtained (see figure I.19) [15].

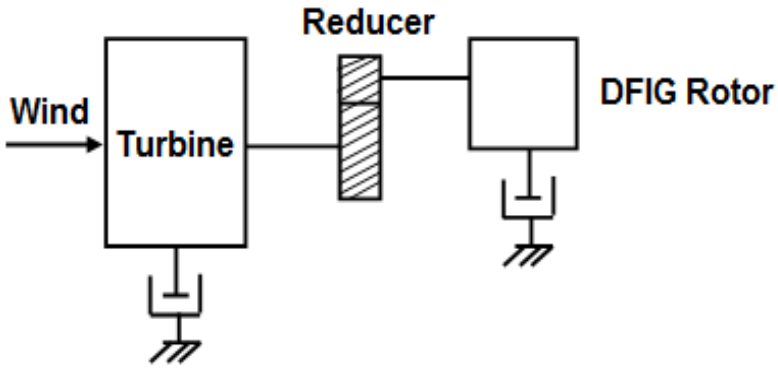


Figure I . 23 : Simplified mechanical model of the turbine.

I.12.2 Wind speed modeling

Wind is the primary driving force behind wind turbines. It is the input variable that the system is designed to harness. The kinetic energy of the wind is partially captured and converted into mechanical energy through the turbine, and then into electrical energy via the generator.

The dynamic characteristics of the wind are crucial to the analysis of the entire energy conversion process, as wind power, at optimal conditions, varies with the cube of the wind speed. Although wind speed is a three-dimensional vector, this model considers only the horizontal dimension. Therefore, the wind model's behavior can be significantly simplified. Wind speed V is typically represented by a scalar function that changes over time.

$$V = f(t) \qquad (I.12)$$

The wind function can be broken down into two main components, a slowly varying average and fluctuations [15]:

$$V(t) = V_0 + \sum_{i=1}^{n} A_i \, sin(\omega_i t + \varphi_i) \qquad (I.13)$$

For instance:

- V_0corresponds to the mean component;
- A_i, ω_i and $\varphi_i$denote the amplitude, pulsation, and initial phase of each fluctuating spectral component.

I.12.3 Turbine modeling

Previously, we saw that the relation (I.8) expresses the wind power of the wind as follows:

$$P_v = \frac{1}{2}\rho S V^3$$

In addition, the aerodynamic power at the level of the turbine rotor is written in the following form:

$$P_t = C_p P_v = \frac{1}{2} C_p(\lambda, \beta) \rho S V^3$$

The aerodynamic efficiency of a wind turbine is represented by the power coefficient C_p, which is influenced by the turbine's characteristics. Figure (I.20) displays the relationship between the coefficient and the speed ratio, as well as the blade orientation angle β for a 1.5 MW wind turbine analyzed in this study [15].

The speed ratio is defined as the ratio between the linear speed of the blades and the wind speed: $\lambda = \frac{\Omega_t R}{V}$

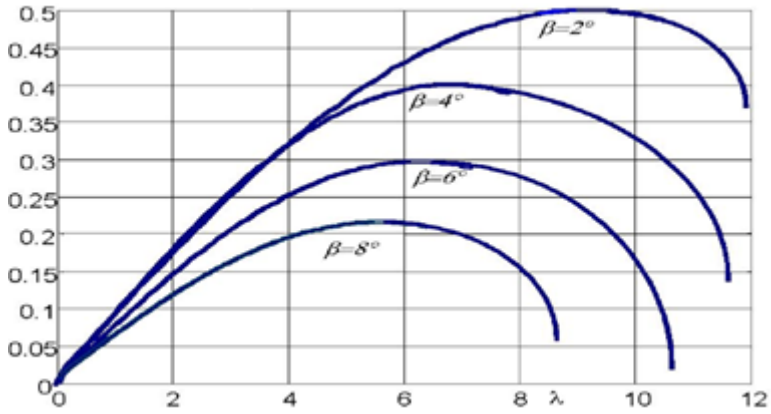


Figure I . 24 : Aerodynamic coefficient as a function of the turbine speed ratio (λ) for a 1.5 MW wind turbine [15].

From the readings taken on this 1.5 MW wind turbine, the expression of the power coefficient is interpolated in the following form [15]:

$$C_p(\lambda, \beta) = \big(0.5 - 0.00167(\beta - 2)\big) \sin\left[\frac{\pi(\lambda + 0.1)}{18.5 - 0.3(\beta - 2)}\right] - 0.00184(\lambda - 3)(\beta - 2) \quad (I.14)$$

Knowing the speed of the turbine, the aerodynamic torque is therefore directly determined by:

$$C_{aer} = \frac{P_t}{\Omega_t} = \frac{1}{2\Omega_t} C_p \rho S V^3 \quad (I.15)$$

Another coefficient known as the torque coefficient C_t can be defined; this relies on both the wind speed and the turbine's specific speed:

$$C_t = \frac{C_p}{\lambda} = C_p \frac{V}{R\Omega_t} \quad (I.16)$$

Thus, we can express it as follows:

$$C_{aer} = \frac{1}{2} C_t \rho S R V^2 \quad (I.17)$$

I.12.4 Multiplier model

The gain multiplier G is used to adjust the mechanical quantities, including speeds and torques, of both the turbine and the generator. These quantities can be expressed through the following mathematical equations:

$$\Omega_t = \frac{\Omega_e}{G} \qquad (I.18)$$

$$C_g = \frac{C_{aer}}{G} \qquad (I.19)$$

Here, $C_g$represents the impact of the turbine's torque on the generator shaft.

I.12.5 Dynamic equation of the generator shaft

By relating the mechanical parameters of the turbine to the generator shaft, we obtain the model defined by the following relationship:

$$J\frac{d\Omega_e}{dt} + f\Omega_e = C_g - C_{em} \qquad (I.20)$$

With:

$$J = \frac{J_t}{G^2} + J_e \qquad (I.21)$$

$$f = \frac{f_t}{G^2} + f_e \qquad (I.22)$$

Where:

J_t, f_t, J_e, f_e,J et f : It refers to the inertia and friction coefficient of the turbine, the generator, and the ones transmitted to the generator shaft, respectively

Using the equations described earlier, it is possible to create a physical model of the turbine, which takes the pitch angle of the blades, wind speed, and the electromagnetic torque supplied by the generator as inputs. Figure (I.21) illustrates this model.

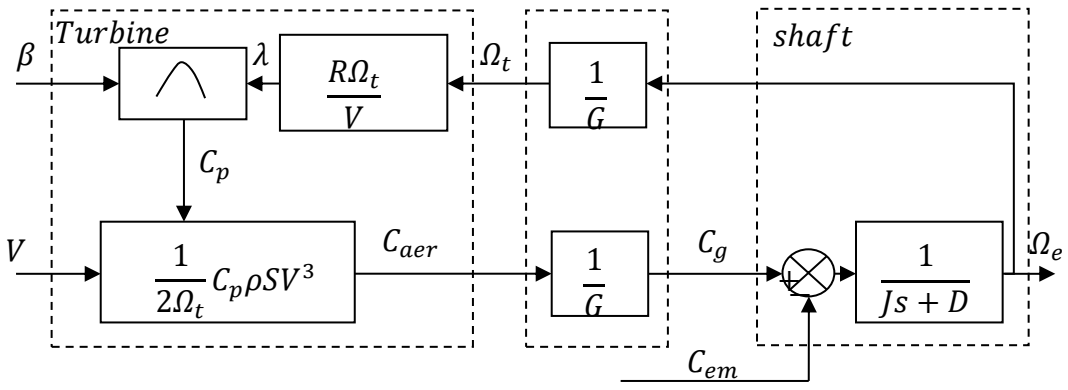


Figure I . 25 : Block diagram of the turbine model.

I.13 Conclusion

In this chapter, we take a closer look at the fascinating world of wind turbines and how they play a crucial role in generating electrical energy for various industries. We begin by exploring the process of converting the kinetic energy of wind into mechanical energy, which is made possible by the turbine according to Betz's law. This law helps us understand the intricate workings of wind turbines.

To provide a clearer understanding, we break down the different components of the turbine and explain how they work together. We also dive into the methods used to regulate the turbine's rotation speed, such as the pitch and stall mechanisms. These mechanisms ensure optimal performance and safety of the turbine.

In order to predict and analyze the behavior of wind turbines, we establish a mathematical model based on their characteristic equations. This model helps us gain valuable insights into the turbine's performance and efficiency.

It's important to keep in mind that the success and profitability of a wind project heavily rely on the availability of suitable wind resources. The average wind speed at a particular location plays a vital role in determining the amount of energy that can be generated. In fact, the energy produced by a wind turbine is directly proportional to the cube of the wind speed. Therefore, an ideal site for wind energy production would have consistent and strong winds.

As we progress, we will explore the most commonly used generators for converting the mechanical energy of the turbine into electrical energy. Specifically, we will focus on the double-fed asynchronous generators, which are widely employed in this process. These generators play a crucial role in efficiently transforming the mechanical power harnessed by the turbine into usable electricity.

CHAPTER II
Modeling and Functioning of the DFIG

II.1. Introduction:

This chapter's main subject is on theoretical analysis of the double-fed synchronous machine. We will focus on understanding how it works, the different control strategies available and its ability to perform under various conditions.

Our understanding of these factors will enable us to optimize the machine's performance for various applications.

The double-fed asynchronous machine in the Park frame will be studied further for its important role in modeling. This requires considering it uses a dual power source. One power source provides variable frequencies to the rotor, while the other directly powers the stator from the network. By these features, we can accurately simulate the machine's operation and evaluate its performance in different scenarios.

We aim to provide comprehensive insights into the double-fed asynchronous machine through this thorough theoretical examination. Engineers and researchers will gain insight into control tactics, design considerations, and performance enhancement by utilizing this knowledge to make informed decisions. We aim to aid in the creation of this innovative device and its utilization in various fields.

II.2.Definition of the double-fed asynchronous machine:

A doubly-fed asynchronous machine, also known as a doubly-fed induction machine (DFIM) or doubly-fed induction generator (DFIG), is an electrical machine used in a variety of applications such as wind turbines and variable speed drives.

A machine consists of a stator and a rotor. The stator is the stationary part and consists of a three-phase winding that is connected to the mains or power supply. The rotor, on the other hand, is the rotating part and also has three-phase windings. However, unlike conventional induction machines, the rotors of doubly fed asynchronous machines are not directly connected to the mains supply. A unique feature of a doubly fed asynchronous machine is that its rotor windings are connected to the power supply through a series of power electronic converters. These converters allow the rotor to be supplied with variable frequency and voltage, allowing the speed and torque of the machine to be controlled.

By controlling the frequency and voltage supplied to the rotor, the machine can operate at different speeds and accommodate different load conditions. This makes them suitable for applications requiring adjustable speed and precise torque control.

Dual-fed asynchronous machines offer advantages such as increased energy efficiency, greater operational flexibility and improved control options compared to traditional fixed-speed machines. It is especially used in wind turbines, enabling them to collect more energy from different wind speeds and efficiently transfer it to the power grid.

Overall, a secondary fed asynchronous machine is a versatile electrical machine that combines the advantages of an asynchronous machine (induction machine) and power electronics for improved control and performance in a wide variety of applications.

II.3. Machine structure:

The double-fed asynchronous machine has a stator similar to that of conventional three-phase machines. It is typically composed of stacked magnetic laminations with slots for inserting the windings. The rotor of this machine consists of three windings connected in a star configuration, with their ends connected to conductive rings that come into contact with brushes as the machine rotates. The structure of the double-fed asynchronous machine allows its physical behavior to be considered similar to that of a synchronous machine, with the difference being that the rotor is no longer a current-fed pole wheel or a permanent magnet, but rather a three-phase winding fed with alternating current. This is why it is also referred to as a generalized machine. There is no need for an external power supply to generate the excitation magnetic field. This operation can be summarized as "Synchronous machine with alternative excitation".

Figure (II.1) shows the structure of the stator and the rotor contacts of the double-fed asynchronous machine.

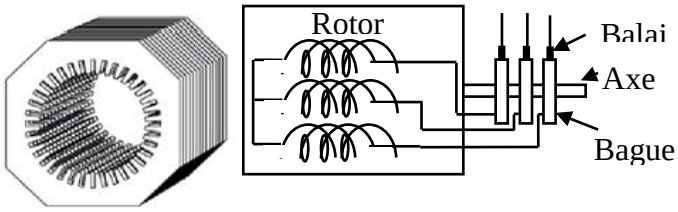


Figure II. 1 : Structure of the stator and rotor contacts of the DFIG

II.4. Principle of operation of the double-fed asynchronous machine:

For the operation of the Double-Fed Asynchronous Machine (DFAM), it is excited simultaneously at the stator and the rotor, respectively, with two frequencies imposed by two power sources. A certain synchronization between the two fields is required to ensure machine stability. The synchronous characteristic of this type of machine remains in the sense that the rotor speed will not be synchronized with the stator field speed or the rotor field speed, but it will be determined by their linear combination.

To ensure stable operation of the asynchronous machine in a steady state, the magneto motive force vectors of the stator and rotor must remain stationary concerning each other in space. As the stator-winding vector $fmms$ rotates in space with an angular velocity $\omega_s = 2.\pi.f_s$ and the rotor rotates at a speed ω_r , the rotor-winding vector must rotate at a speed ω_{gl} relative to the rotor to fulfill this condition. The speed must be such that:

$$\omega_{gl} = \omega_s - \omega_r = \omega_s \cdot g \qquad \text{(II.1)}$$

Where: g is the slip and

ω_{gl} is the slip angular velocity.

When the machine's speed is below the synchronism speed, the directions of rotation for the two vectors are the same. However, if the speed surpasses the synchronism speed, the directions become opposite to each other.

To enable the rotation of the resulting vector $fmms$ concerning the rotor, the current in the rotor winding must have a frequency f_r , which is determined based on $\omega_{gl} = 2.\pi.f_r$.

In other words:

$$f_r = g.f_s \tag{II.2}$$

Figure (II.2.A) shows the operation of the motor in hyposynchronous mode, where the power Pr is supplied by the rotor. This mode is commonly known as slip energy recovery. As the speed increases, causing the motor to operate in hypersynchronous mode, the power Pr is absorbed by the rotor, as illustrated in Figure (II.2.B).

In the case where the machine operates in hyposynchronous generator mode, as shown in Figure (II.2.C), the power Pr is absorbed by the rotor. If the speed increases to the point where the generator operates in hypersynchronous mode, in this case, the power Pr is supplied by the rotor, as depicted in Figure (II.2.D)

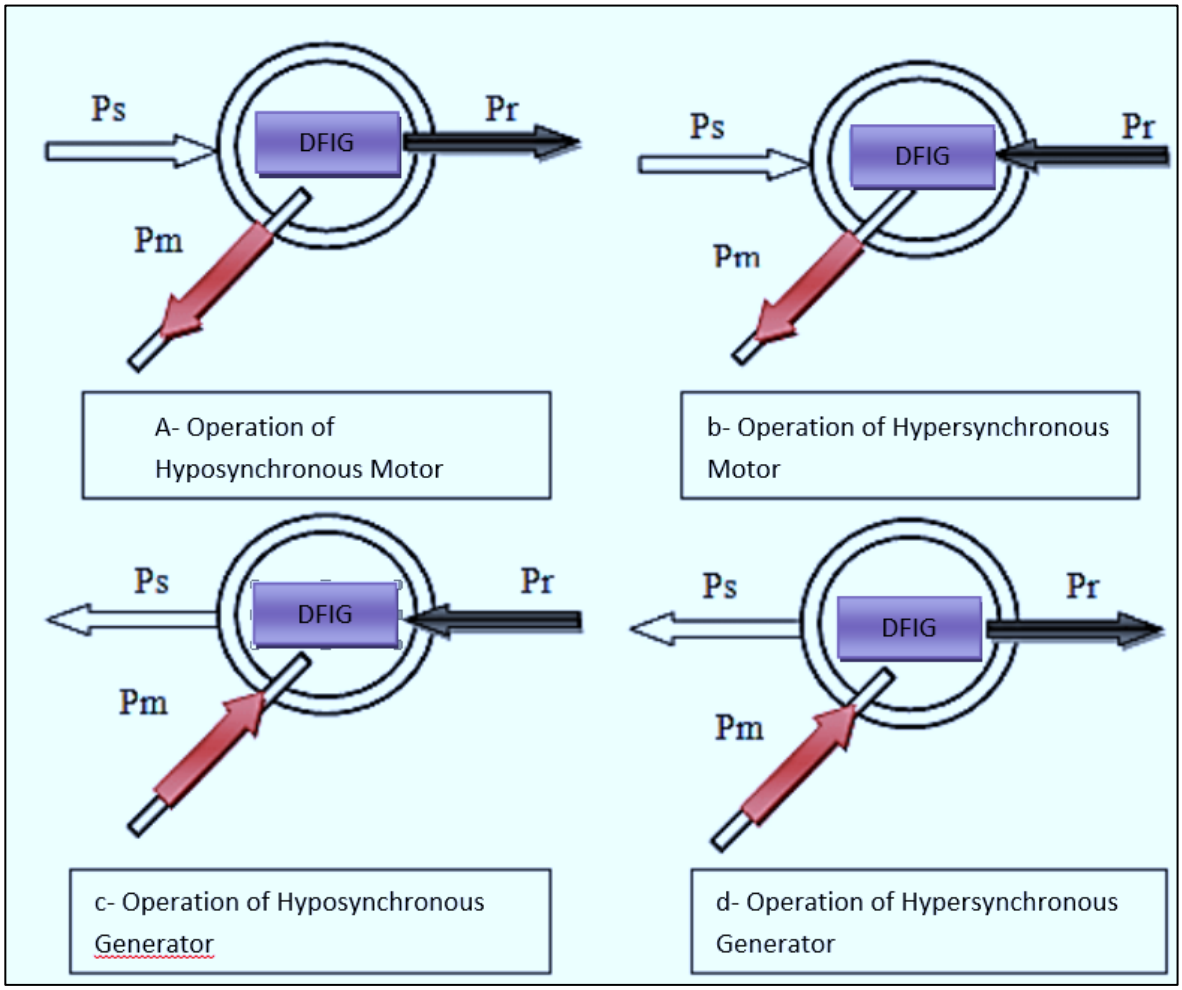


Figure II. 3 : Different Operating Modes of the Double-Fed Asynchronous Machine (DFIG)

II.5 Modeling of the Doubly Fed Induction Machine:

The asynchronous machine is represented in Figure (II.18) by its six windings in the electrical space. The angle θ measures the displacement of the rotor phase axis (OAR) relative to the fixed axis of the stator phase (OAS).

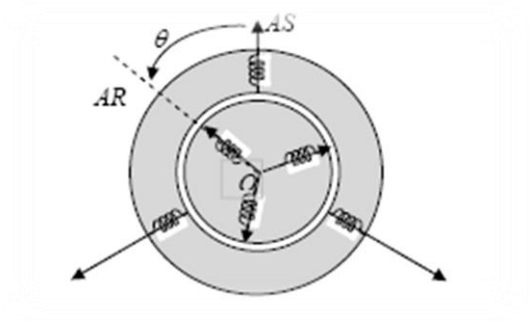


Figure II. 4 : Schematic representation of a DFIG model

.

II.5.1 Assumptions made for simplification:

To formulate the equation, we make the assumption that the winding is distributed to generate a sinusoidal m.m.f. with sinusoidal currents. Additionally, we assume that the operation is in an unsaturated regime, and we disregard hysteresis, eddy currents, and skin effect. Lastly, the homopolar regime is not considered as the neutral is not linked. These assumptions imply that:

- The fluxes can be added.

- The self-inductances remain constant.

- The mutual inductances between the stator and rotor windings have a sinusoidal variation concerning the electrical angle of their magnetic axes.

II.5.2 Model of the DFIG in the abc frame:

With the assumptions mentioned above, the electrical equations of the stator and rotor phases that describe the operation of the machine are written as follows:

$$\begin{cases} [V_S] = [R_S][I_S] + \dfrac{d}{dt}[\phi_S] \\ [V_r] = [R_r][I_r] + \dfrac{d}{dt}[\Phi_r] \end{cases} \tag{II.3}$$

With:

$$\begin{cases} [V_S] = [V_{as} \quad V_{bs} \quad V_{cs}]^T \\ [I_S] = [I_{as} \quad I_{bs} \quad I_{cs}]^T \\ [\Phi_S] = [\Phi_{as} \quad \Phi_{bs} \quad \Phi_{cs}]^T \end{cases} \tag{II.4}$$

Stator quantities:

$$\begin{cases}[V_r]=[V_{ar} \quad V_{br} \quad V_{cr}]^T \\ [I_r]=[I_{ar} \quad I_{br} \quad I_{cr}]^T \\ [\Phi_r]=[\Phi_{ar} \quad \Phi_{br} \quad \Phi_{cr}]^T \end{cases} \tag{II.5}$$

Rotor quantities:

The stator and rotor fluxes as a function of currents, self-inductances, and mutual inductances are expressed by the following equations:

$$\begin{cases}[\Phi_S]=[L_S].[I_S]+[M_{SS}].[I_S]+[M_{Sr}].[I_r] \\ [\Phi_r]=[L_r].[I_r]+[M_{rr}].[I_r]+[M_{rS}].[I_S] \end{cases} \tag{II.6}$$

Where:

$[R_s],[R_r]$: These are the matrices of stator and rotor resistances.

$[L_s],[L_r]$: The matrices of stator and rotor self-inductances.

$[M_{sr}],[M_{rs}]$ The matrices of mutual inductances between the stator and the rotor.

$[M_{ss}],[M_{rr}]$: These are the matrices of stator-stator and rotor-rotor mutual inductances.

With:

$$\begin{cases}[R_s]=R_s.[I]_{3\times3} \\ [R_r]=R_r.[I]_{3\times3} \end{cases} \tag{II.7}$$

$$\begin{cases}[L_s]=L_s.[I]_{3\times3} \\ [L_r]=L_r.[I]_{3\times3} \end{cases} \tag{II.8}$$

$$[M_{ss}]=M_{ss}.\begin{bmatrix} 0 & \cos(2.\pi/3) & \cos(2.\pi/3) \\ \cos(2.\pi/3) & 0 & \cos(2.\pi/3) \\ \cos(2.\pi/3) & \cos(2.\pi/3) & 0 \end{bmatrix} \tag{II.9}$$

$$[M_{rr}]=M_{rr}..\begin{bmatrix} 0 & \cos(2.\pi/3) & \cos(2.\pi/3) \\ \cos(2.\pi/3) & 0 & \cos(2.\pi/3) \\ \cos(2.\pi/3) & \cos(2.\pi/3) & 0 \end{bmatrix} \tag{II.10}$$

$$[M_{sr}]=M.\begin{bmatrix} \cos(\theta) & \cos(\theta-2.\pi/3) & \cos(\theta-4.\pi/3) \\ \cos(\theta-4.\pi/3) & \cos(\theta) & \cos(\theta-2.\pi/3) \\ \cos(\theta-2.\pi/3) & \cos(\theta-4.\pi/3) & \cos(\theta) \end{bmatrix} \tag{II.11}$$

$$[M_{rs}]=[M_{sr}]^T \tag{II.12}$$

With:

$[I]_{3*3}$: Is the identity matrix of order 3

M: Is the maximum mutual inductance between a stator phase and a rotor phase for $\theta = 0$.

Magnetic energy can be calculated from the following expression:

$$W_{mag} = \frac{1}{2}\left([I_s]^T[\phi_s]+[I_r]^T[\phi_r]\right) \tag{II.13}$$

The electromagnetic torque is expressed by the derivative of the electromagnetic energy with respect to the rotor's geometric angle of rotation [16]:

$$C_e = \frac{\partial W_{mag}}{\partial \theta_{geom}} = n_p \cdot \frac{\partial W_{mag}}{\partial \theta_{elect}} \tag{II.14}$$

One can deduce:

$$C_e = \frac{n_p}{2}[I_s]^T\left(\frac{d[M_{sr}]}{d\theta_{elect}}\right)[I_r] \tag{II.15}$$

The mechanical equation is given by:

$$J_m \frac{d\Omega r}{dt} + f_m \cdot \Omega_r = C_{em} - C_r \tag{II.16}$$

Where:

$$\Omega_r = \frac{\omega_r}{n_p} \tag{II.17}$$

"With: J_m moment of inertia of the machine, C_{em} electromagnetic torque, C_r resistive torque, and f_m coefficient of friction of the machine.

"We observe the complexity of the electrical equations and the mechanical equation of the asynchronous machine, which cannot be easily exploited due to the dimensions of the matrices involved in the calculations and the dependence of the inductance matrix on the position of the rotor axis relative to the stator axis, which varies over time.

II.5.3 The Park Transformation:

In order to investigate the control laws of an AC machine, we can model it in a rotating (d, q) reference frame whose orientation is arbitrary. This model is obtained after a virtual transformation of the three-phase machine into an equivalent two-phase machine [17]. This transformation, which allows the conversion from the three-phase to the two-phase system, is done by matching the real variables with their homopolar, direct and quadrature components, as shown in figure (II.4).

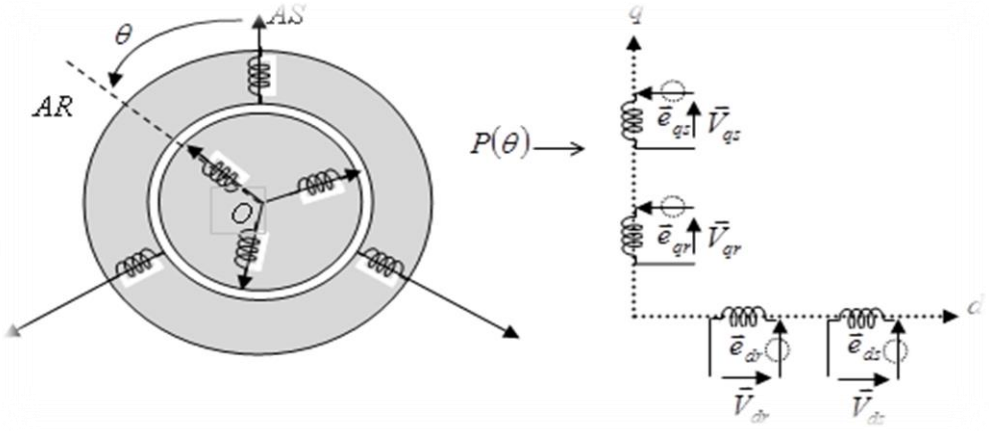


Figure II. 5 : Representation of the PMSM in the Park reference frame.

Therefore, for the conversion from the three-phase system to the two-phase system, we use the matrix $P(\theta)$:

$$\left[P(\theta)\right]=\frac{2}{3}\begin{bmatrix}\cos(\theta) & \cos(\theta-\frac{2\pi}{3}) & \cos(\theta-\frac{4\pi}{3})\\ -\sin(\theta) & -\sin(\theta-\frac{2\pi}{3}) & -\sin(\theta-\frac{4\pi}{3})\\ \frac{1}{2} & \frac{1}{2} & \frac{1}{2}\end{bmatrix} \tag{II.18}$$

The change of variables related to currents, voltages, and fluxes is defined by the transformation (II.16):

$$\begin{bmatrix}x_d\\ x_q\\ x_o\end{bmatrix}=\left[P(\theta)\right]\begin{bmatrix}x_a\\ x_b\\ x_c\end{bmatrix} \tag{II.19}$$

With x : The voltage, current or flux, and the following indices represent:

- 0 : index of the homopolar axis.
- d : index of the direct axis.
- q: index of the quadrature axis.

In addition, for the inverse transformation, we use the matrix $[P(\theta)]^{-1}$:

$$[P(\theta)]^{-1} = \begin{bmatrix} \cos(\theta) & -\sin(\theta) & 1 \\ \cos(\theta - \frac{2\pi}{3}) & -\sin(\theta - \frac{2\pi}{3}) & 1 \\ \cos(\theta - \frac{4\pi}{3}) & -\sin(\theta - \frac{4\pi}{3}) & 1 \end{bmatrix} \quad \text{(II.20)}$$

Thus, the real variables are obtained from the two-phase variables.

$$\begin{bmatrix} x_a \\ x_b \\ x_c \end{bmatrix} = [P(\theta)]^{-1} \begin{bmatrix} x_d \\ x_q \\ x_o \end{bmatrix} \quad \text{(II.21)}$$

II.5.3.1 Electric and magnetic equations in the (d, q) axis system:

The expressions of stator and rotor voltages along the (d, q) axes are given by:

$$\begin{cases} V_{ds} = R_s I_{ds} + \dfrac{d\Phi_{ds}}{dt} - \omega_{coor}\Phi_{qs} \\ V_{qs} = R_s I_{qs} + \dfrac{d\Phi_{qs}}{dt} + \omega_{coor}\Phi_{ds} \\ V_{dr} = R_r I_{dr} + \dfrac{d\Phi_{dr}}{dt} - (\omega_{coor} - \omega_r)\Phi_{qr} \\ V_{qr} = R_r I_{qr} + \dfrac{d\Phi_{qr}}{dt} + (\omega_{coor} - \omega_r)\Phi_{dr} \end{cases} \quad \text{(II.22)}$$

With:

ω_{coor} : Speed of the (d, q) axis system.

The expressions of the stator and rotor fluxes in the (d, q) system are:

$$\begin{cases} \Phi_{ds} = L_s I_{ds} + M I_{dr} \\ \Phi_{qs} = L_s I_{qs} + M I_{qr} \\ \Phi_{dr} = L_r I_{dr} + M I_{ds} \\ \Phi_{qr} = L_r I_{qr} + M I_{qs} \end{cases} \quad \text{(II.23)}$$

II.5.4 Choice of reference frame:

To study the transient regimes of electrical machines, it is recommended to choose a reference axis system that leads to the simplest possible differential system, as the final result is independent of the choice of coordinate system. The calculation can be more or less complex depending on the choice of reference frame. Starting from the (d, q) axis system, other axes can be obtained, which are special cases. In the following, the homopolar components are assumed to be zero:

- Reference frame fixed with respect to the stator: $\omega_{coor} = 0$

- Reference frame fixed with respect to the rotor: $\omega_{coor} = \omega_r$

- Reference frame fixed with respect to the rotating field: $\omega_{coor} = \omega_s$

This last representation, which corresponds continuous quantities to sinusoidal quantities in steady state, is necessary for the conception of vector control by flux orientation, and the action models depend on the position of the reference frame relative to the various flux axes.

II.5.5 Two-phase model of the DFIG related to the rotating field:

We express the voltages as:

$$\begin{cases} V_{ds} = R_s.I_{ds} + \dfrac{d\phi_{ds}}{dt} - \omega_s.\phi_{qs} \\ V_{qs} = R_s.I_{qs} + \dfrac{d\phi_{qs}}{dt} + \omega_s.\phi_{ds} \\ V_{dr} = R_r.I_{dr} + \dfrac{d\phi_{dr}}{dt} - (\omega_s - \omega_r)\phi_{qr} \\ V_{qr} = R_r.I_{qr} + \dfrac{d\phi_{qr}}{dt} + (\omega_s - \omega_r)\phi_{dr} \end{cases} \quad \text{(II.24)}$$

To study transient phenomena (starting, braking, load variation) with a variable rotor speed, it is necessary to add the equation of motion (II.14) to the system of differential equations modeling the machine [18]. The general form of the electromagnetic torque of a three-phase asynchronous machine modeled in the Park's coordinate system is given by the following relationship:

$$C_{em} = P(\phi_{ds}\mathrm{i}_{\mathrm{qs}} - \phi_{qs}i_{ds}) \quad \text{(II. 25)}$$

II.5.6 State space representation:

The equations (II.20) can be arranged in the form of state representation. We choose the state vector $x = \lfloor \phi_{ds}, \phi_{qs}, I_{dr}, I_{qr} \rfloor$, and we obtain the state equations in matrix form:

$$\begin{cases} L.\dfrac{dx}{dt} = A.x + B.U \\ y = C.x \end{cases} \quad \text{(II.26)}$$

Avec : $U = \left[V_{ds}, V_{qs}, V_{dr}, V_{qr}\right]^T$, $B = [I]_{4*4}$,

$$A=\begin{bmatrix} \frac{-R_s}{L_s} & \omega_s & \frac{R_s.M}{L_s} & 0 \\ -\omega_s & \frac{-R_s}{L_s} & 0 & \frac{R_s.M}{L_s} \\ 0 & \frac{M}{L_s}(\omega_s-\omega_r) & -R_r & \sigma.(\omega_s-\omega_r) \\ -\frac{M}{L_s}(\omega_s-\omega_r) & 0 & -\sigma(\omega_s-\omega_r) & -R_r \end{bmatrix} \quad L=\begin{bmatrix} 1 & 0 & 0 & 0 \\ 0 & 1 & 0 & 0 \\ \frac{M}{L_s} & 0 & \sigma & 0 \\ 0 & \frac{M}{L_s} & 0 & \sigma \end{bmatrix} \quad \text{(II.27)}$$

$$C=\begin{bmatrix} 1 & 0 & 0 & 0 \\ 0 & 1 & 0 & 0 \\ 0 & 0 & 0 & 0 \\ 0 & 0 & 0 & 0 \end{bmatrix}. \sigma = 1-(M^2/L_sL_r) \text{ : Coefficient of dispersion.}$$

II.6 modeling of the DFIG power supply:

In our study, we use various control structures that involve a double-fed asynchronous machine and a voltage inverter. The output voltage of the inverter is regulated using pulse width modulation (PWM) technique. Figure (II.22) illustrates the combination of rectifier, filter, and voltage inverter.

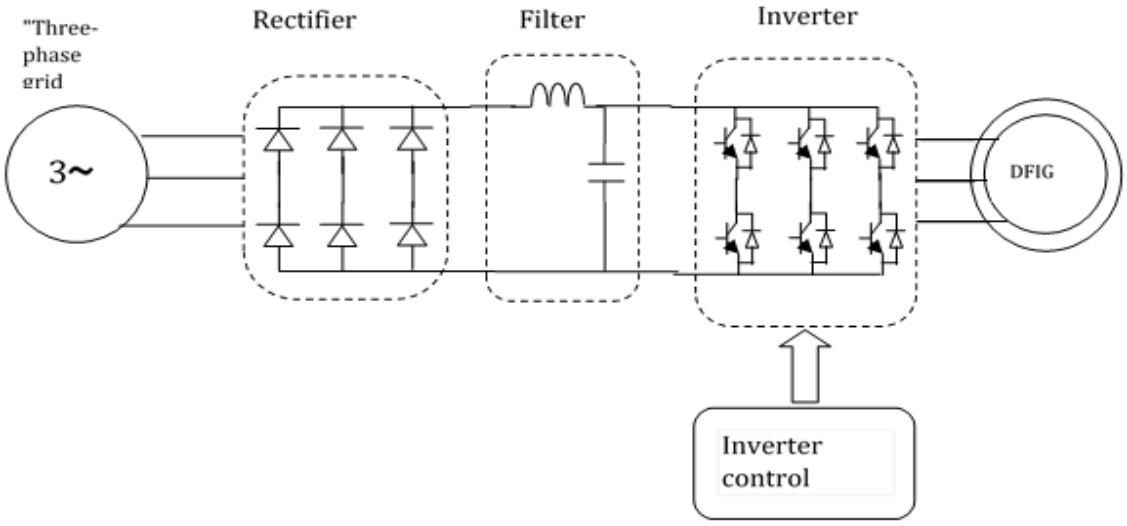


Figure II. 6 : Diagram of the static converter

II.6.1 Rectifier Modeling:

The rectifier is an "AC/DC" converter. Electrical energy conversion allows for the generation of a direct current source from an alternating current source [16].

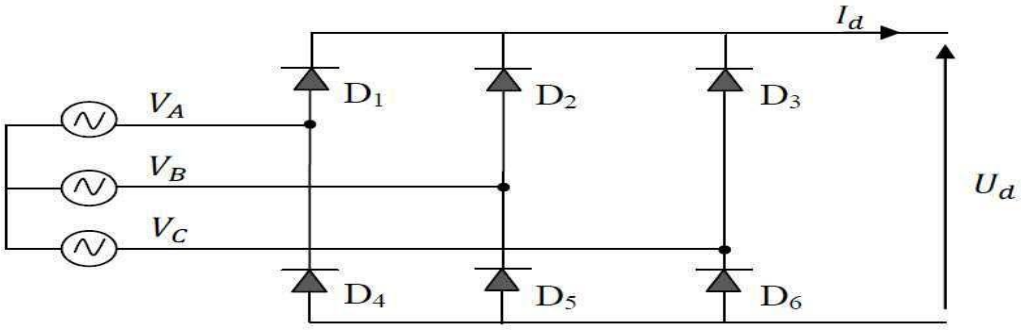


Figure II. 7 : Diagram of three-phase diode rectifier

"This rectifier consists of three common-cathode diodes D1, D2, D3 for the forward current Id and three common-anode diodes D4, D5, D6 for the return current Id. Assuming that the rectifier is powered by a balanced three-phase voltage grid:"

$$\begin{cases} U_a(t) = V_{max} sin(2\pi ft) \\ U_b(t) = V_{max} sin\left(2\pi ft - \frac{2\pi}{3}\right) \\ U_c(t) = V_{max} sin\left(2\pi ft + \frac{2\pi}{3}\right) \end{cases} \quad \text{(II-28)}$$

"And if we neglect the overlapping effect, the output voltage of the rectifier will be defined as follows:"

$$U_d(t) = Max[U_a(t), U_b(t), U_c(t)] - Min[U_a(t), U_b(t), U_c(t)] \quad \text{(II-29)}$$

The rectified voltage has ripple. To reduce these ripples, a low-pass filter should be placed between the rectifier and the inverter.

II.6.2 Filter Modeling:

The filter consists of an inductance L_{ft} in series with a capacitance C_{ft} in parallel, as shown in Figure (II.8).

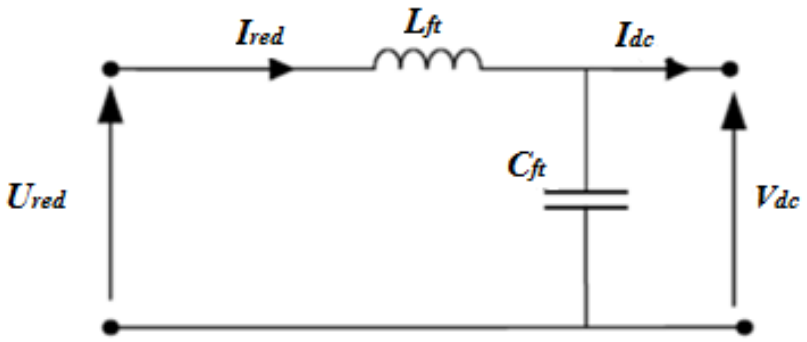


Figure II. 8: Representation of a filter

The model of the filter is defined by the following system of equations:

$$\begin{cases} \frac{d}{dt} i_{red} = \frac{1}{L_{ft}} (U_{red} - V_{dc}) \\ \frac{d}{dt} V_{dc} = \frac{1}{C_{ft}} i_c = \frac{1}{C_{ft}} (i_{red} - i_{dc}) \end{cases} \quad \text{(II-30)}$$

The transfer function of the filter is given by:

$$F(s) = \frac{V_{dc}(s)}{U_{red}(s)} = \frac{1}{1+\left(\sqrt{L_{ft}C_{ft}}s\right)^2} \quad \text{(II-31)}$$

"It is a second-order filter with a cutoff frequency equal to"

$$f_c = \frac{1}{\sqrt{L_{ft}C_{ft}}} \quad \text{(II-32)}$$

II.6.3 modeling of the inverter:

The voltage inverter is a static converter (DC-AC) consisting of three phases with voltage waveforms that are phase-shifted by 2π/3 and 4π/3, respectively. Typically, the switching cells are composed of transistors or GTO thyristors for high power applications. It allows for the imposition of variable amplitude and frequency voltage waveforms on the machine.

For a three-phase inverter, the switch controls of one arm are complementary. Therefore, each arm has two independent states. These two states can be considered as a Boolean variable F defined as follows:

- F a, b, c = 1: Upper half-bridge switch (a, b, or c) closed.

- F a, b, c = 0: Lower half-bridge switch (a, b, or c) open.

Figure.II.9 depicts a two-level three-phase voltage inverter. It consists of three arms with current-reversible switches that are controlled for closing and opening, implemented using a transistor (GTO or IGBT) and an ant parallel diode. To simplify the study of the inverter, the following assumptions are made:

- The switching of the switches is instantaneous.
- The voltage drop across the switches is negligible.
- The three-phase load is balanced, connected in a star configuration with an isolated neutral

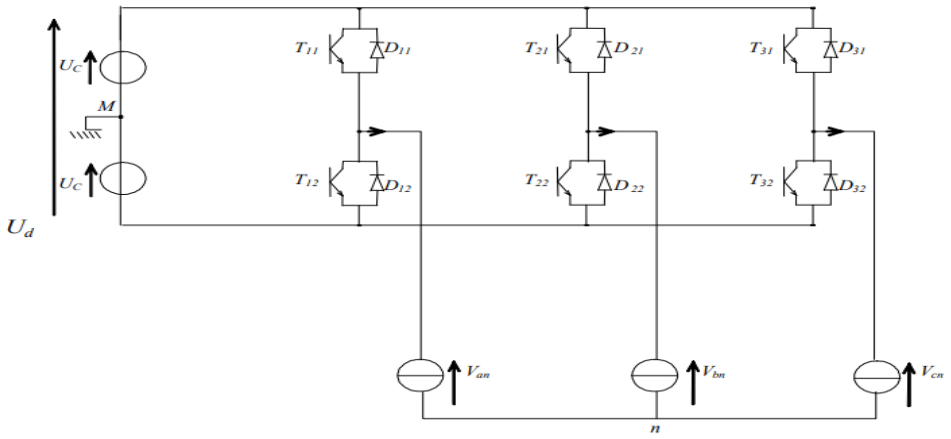


Figure II. 9: Two-level three-phase NPC inverter structure

The output composite voltages of the three-phase inverter are given by [16]:

$$\begin{cases} U_{ab=} V_{an0} - V_{bn0} \\ U_{bc=} V_{bn0} - V_{cn0} \\ U_{ca=} V_{cn0} - V_{an0} \end{cases} \quad \text{(II.33).}$$

The individual phase voltages of the load derived from the composite voltages have a zero sum, therefore:

$$\begin{cases} V_{an} = \frac{1}{3}[U_{ab} - U_{ca}] \\ V_{an} = \frac{1}{3}[U_{bc} - U_{ab}] \\ V_{an} = \frac{1}{3}[U_{ac} - U_{bc}] \end{cases} \quad \text{(II.34).}$$

They can be written based on the output voltages of the inverter by introducing the voltage of the load's neutral relative to the reference point n_0.

$$\begin{cases} V_{an} + V_{nn0} = V_{an0} \\ V_{bn} + V_{nn0} = V_{bn0} \\ V_{cn} + V_{nn0} = V_{cn0} \end{cases} \quad \text{(II-35)}$$

So, we can deduce that:

$$V_{nn0} = \frac{1}{3}[V_{an0} + V_{bn0} + V_{cn0}] \quad \text{(II-36)}$$

The state of the assumed perfect switches ↔ if (i = a, b, c), we have:

$$V_{in0} = F_i U_i \frac{U_0}{2} \quad \text{(II-37)}$$

So we have:

$$\begin{cases} V_{an0} = (S_a - 0.5)U_0 \\ V_{bn0} = (S_b - 0.5)U_0 \\ V_{cn0} = (S_c - 0.5)U_0 \end{cases} \quad \text{(II-38)}$$

By replacing, we obtain:

$$\begin{cases} V_{an} = +\frac{1}{3}V_{an0} - \frac{1}{3}V_{bn0} + \frac{1}{3}V_{cn0} \\ V_{bn} = -\frac{1}{3}V_{bn0} + \frac{1}{3}V_{bn0} - \frac{1}{3}V_{cn0} \\ V_{cn} = -\frac{1}{3}V_{cn0} - \frac{1}{3}V_{bn0} + \frac{1}{3}V_{cn0} \end{cases} \quad \text{(II-39)}$$

The individual load voltages are given by the following system:

$$\begin{bmatrix} \mathrm{V_{an}} \\ \mathrm{V_{bn}} \\ \mathrm{V_{cn}} \end{bmatrix} = \frac{\mathrm{U_0}}{3} \begin{bmatrix} 2 & -1 & -1 \\ -1 & 2 & -1 \\ -1 & -1 & 2 \end{bmatrix} \begin{bmatrix} \mathrm{F_a} \\ \mathrm{F_b} \\ \mathrm{F_c} \end{bmatrix} \quad \text{(II-40)}$$

II.6.4 Double-fed asynchronous machine simulation with the inverter struchure:

To simulate our machine, we used the MATLAB/SIMULINK software. The parameters of the machine are given in the appendix.

The obtained results are represented by the following figures:

The initial excitation voltage of the DFIG at t=0 on the stator side is the voltage from the electrical grid at a constant frequency and voltage (Vr=220 V; fr=50 Hz). On the rotor side, two cases are being studied:

- 1st case: constant voltage and variable frequency.
- 2nd case: variable voltage and constant frequency.

Vdr =0 AND Vqr =30

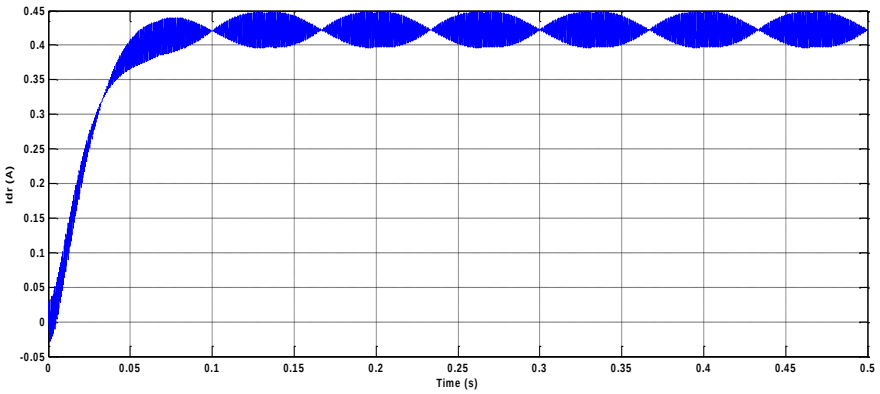


Fig.II.10: The rotor current along the d-axis

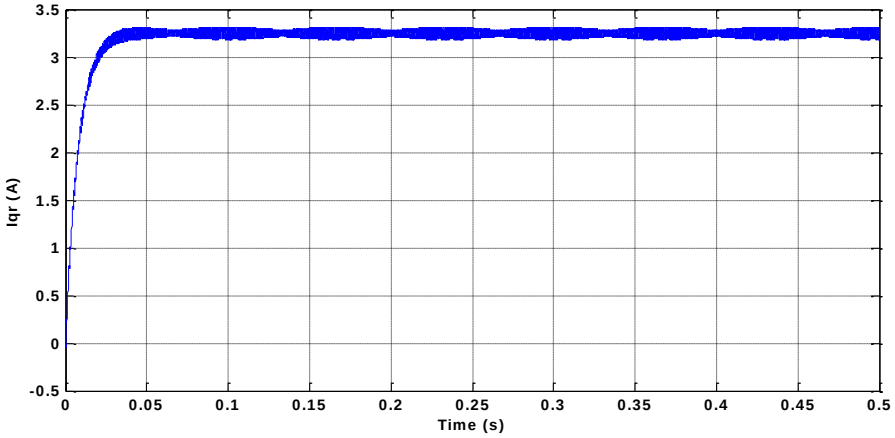


Fig.II.11: The rotor current along the q-axis

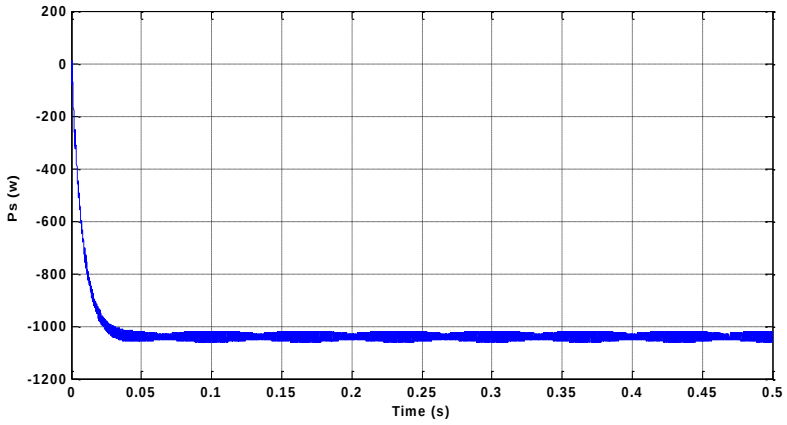


Fig.II.12: active power of the stator

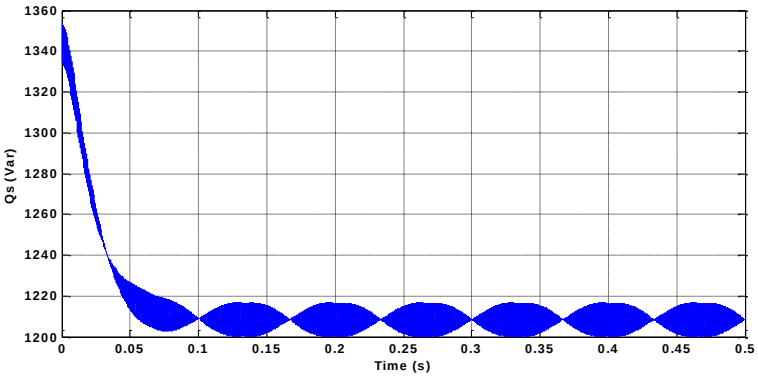


Fig.II.13:reactive power of the stator.

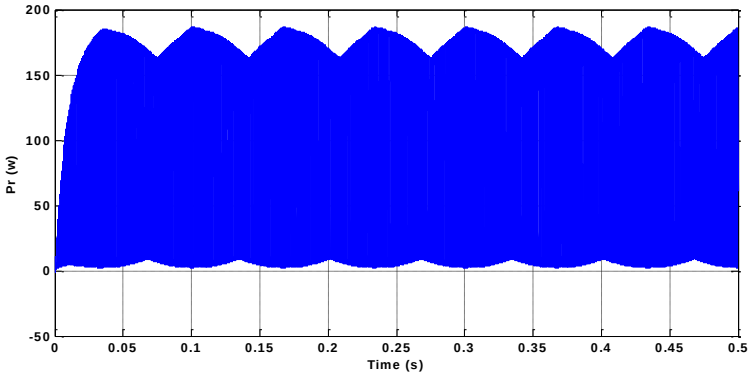


Fig.II.14: Active power of the rotor.

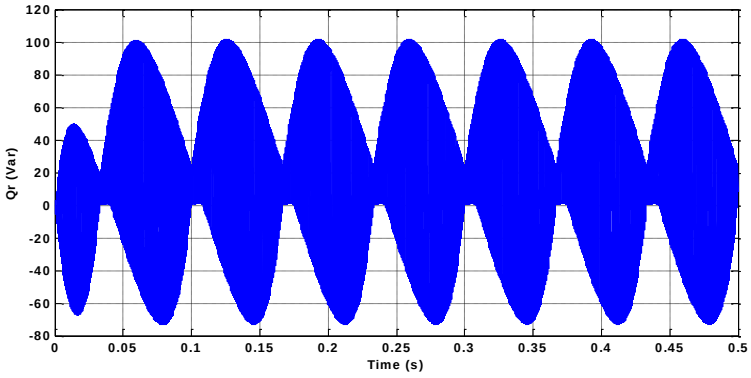


Fig.II.15: reactive power of the rotor.

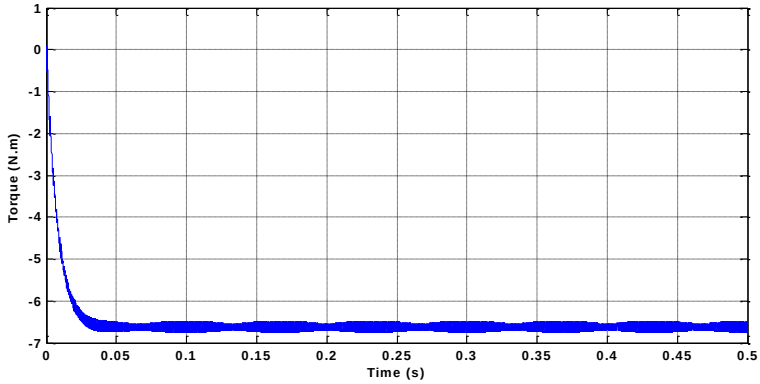


Fig.II.16: Electromagnetic torque

Vdr=0 AND Vqr=-30

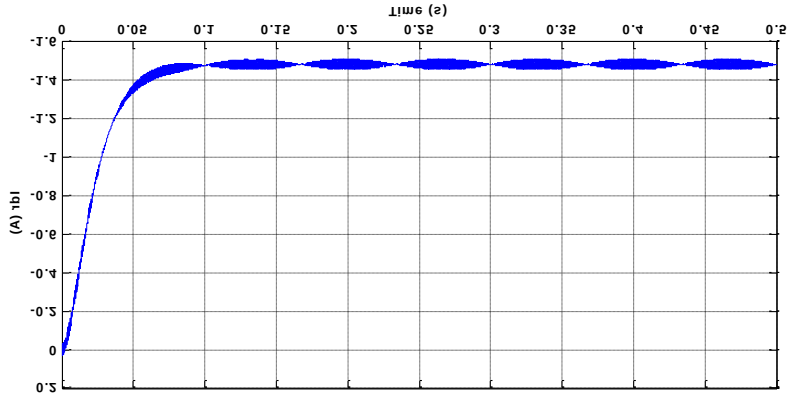


Fig.II.17: The rotor current along the d-axis

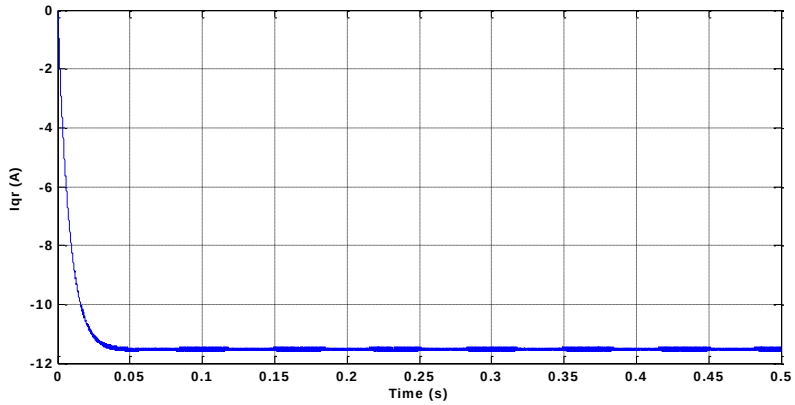


Fig.II.18: The rotor current along the q-axis

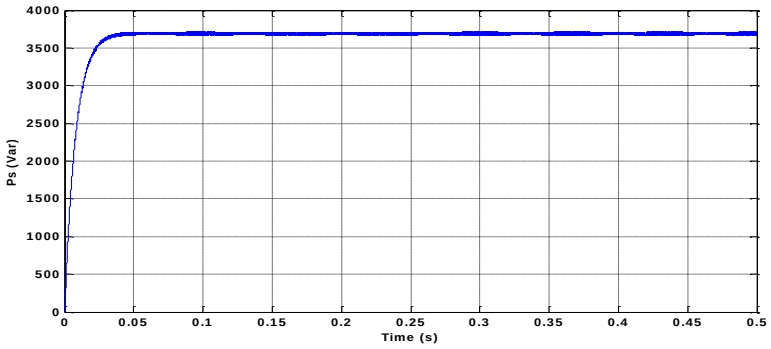


Fig.II.19: active power of the stator.

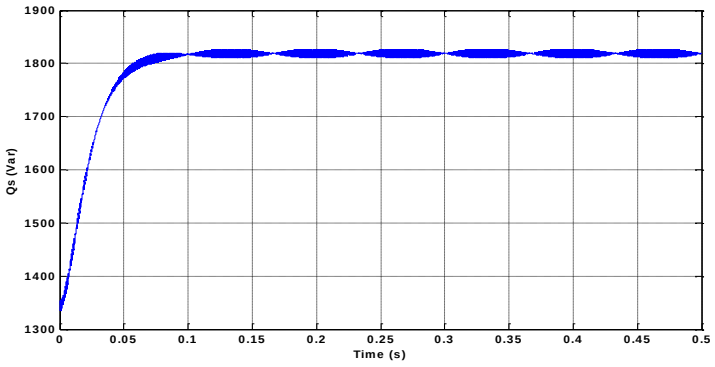


Fig.II.20:reactive power of the stator.

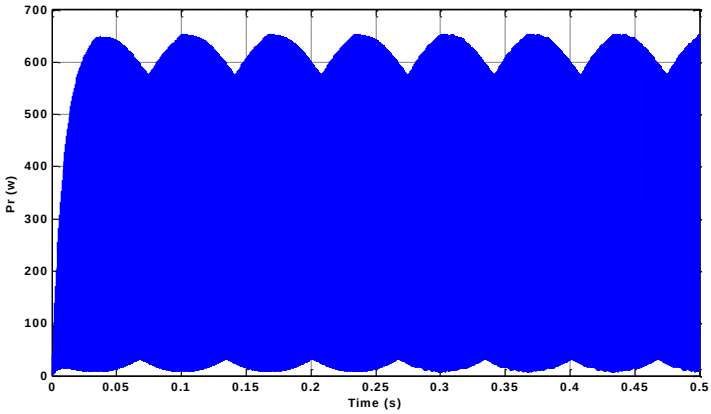


Fig.II.21: Active power of the rotor.

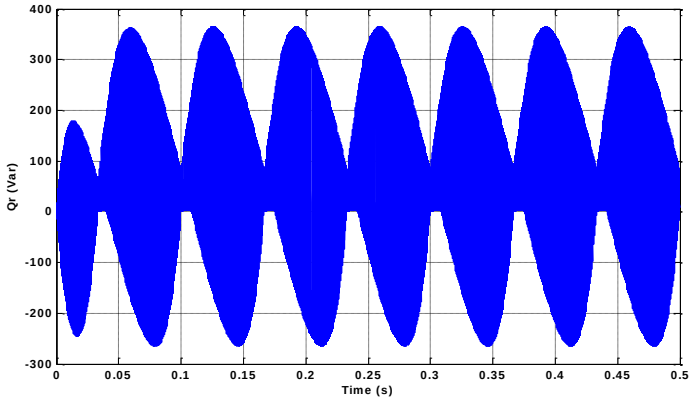


Fig.II.22: reactive power of the rotor.

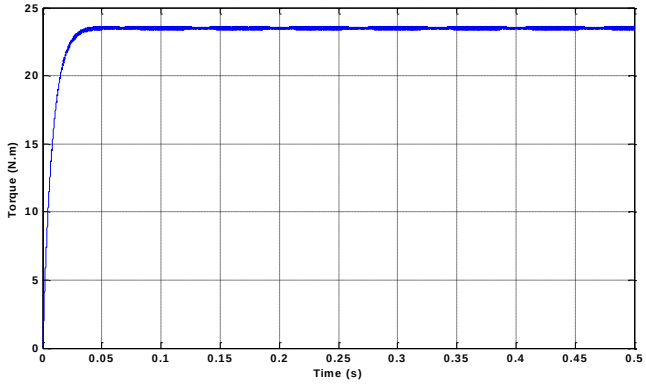


Fig.II.23: Electromagnetic torque

Vdr=30 AND Vqr=0

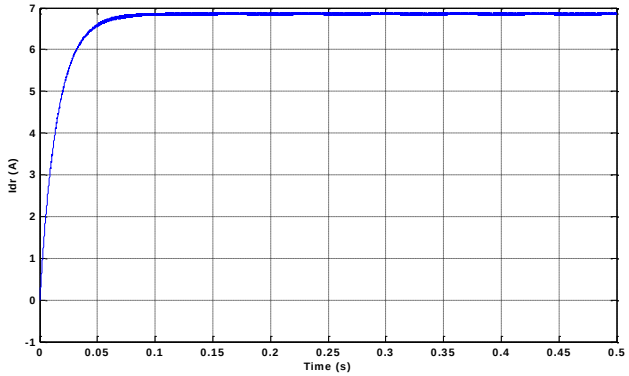


Fig.II.24: The rotor current along the d-axis

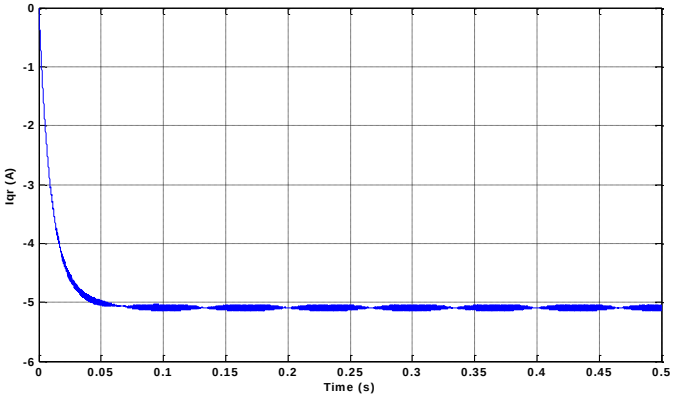


Fig.II.25: The rotor current along the q-axis

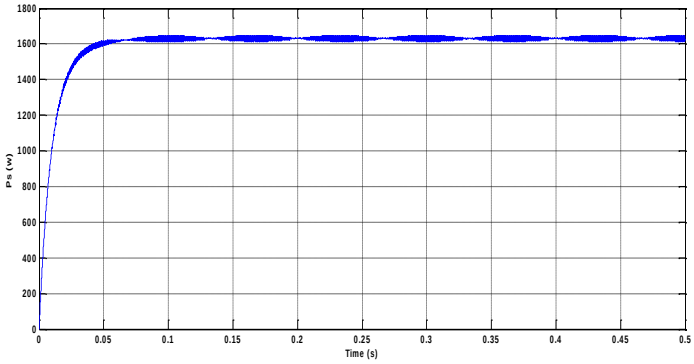


Fig.II.26: active power of the stator

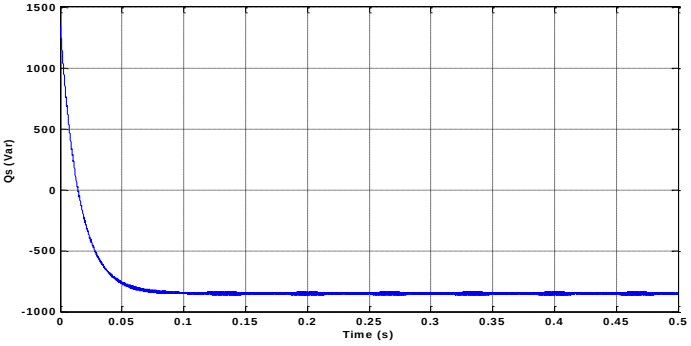


Fig.II.27:reactive power of the stator

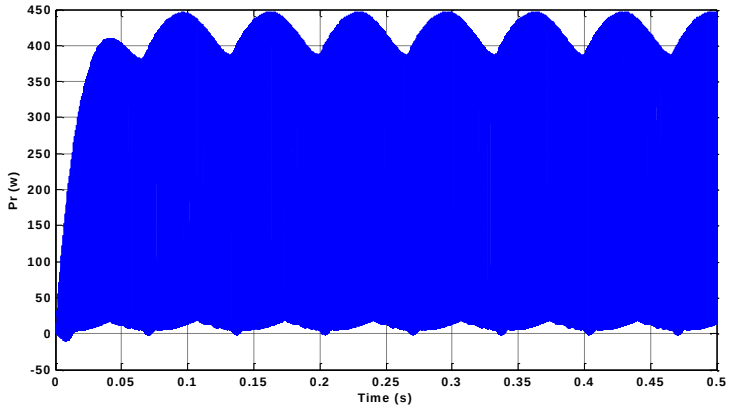


Fig.II.28: Active power of the rotor.

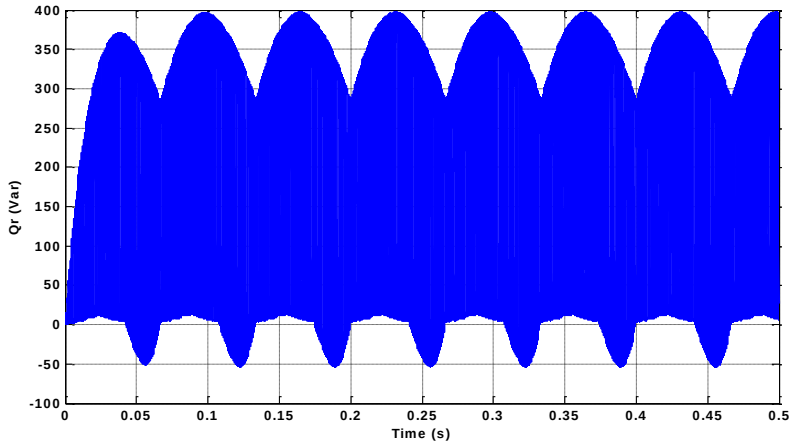


Fig.II.29: reactive power of the rotor.

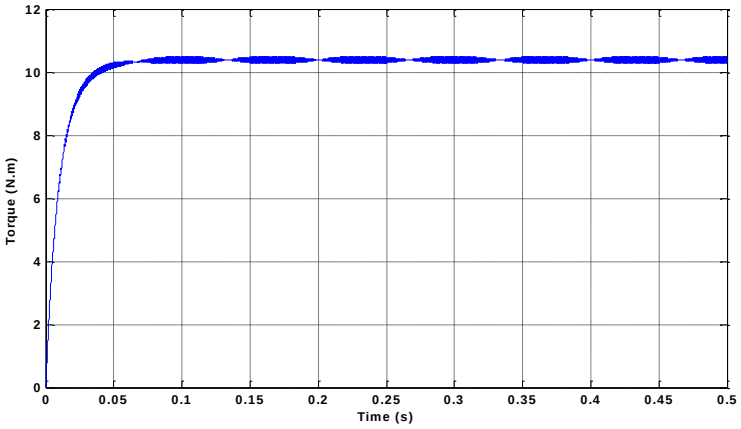


Fig.II.30: Electromagnetic torque

Vdr=-30 AND Vqr=0

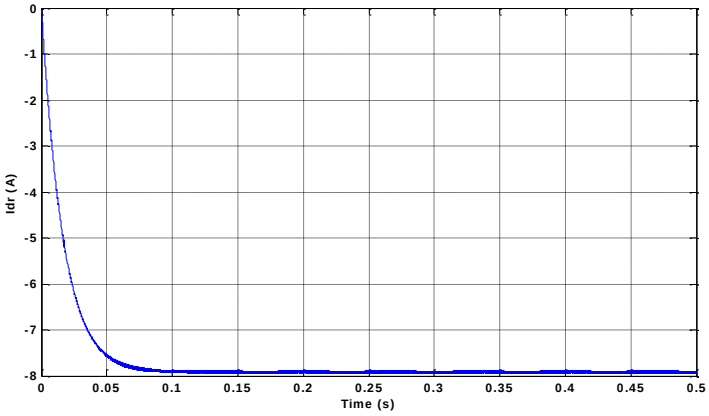


Fig.II.31: The rotor current along the d-axis

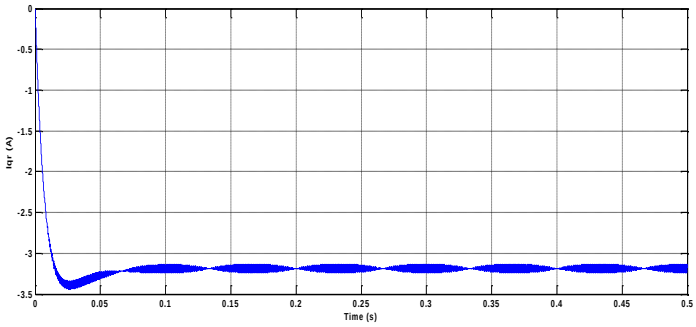


Fig.II.32: The rotor current along the q-axis

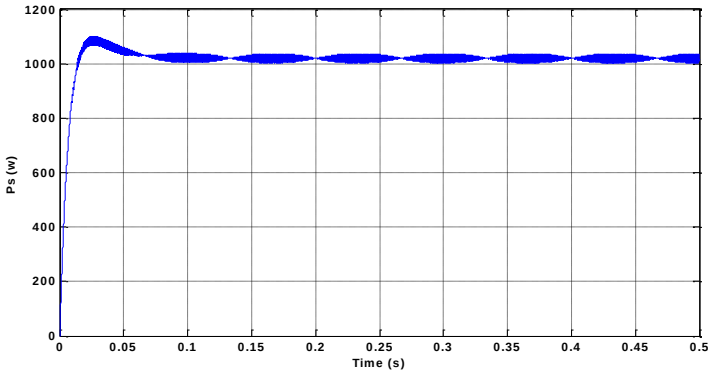


Fig.II.33: active power of the stator

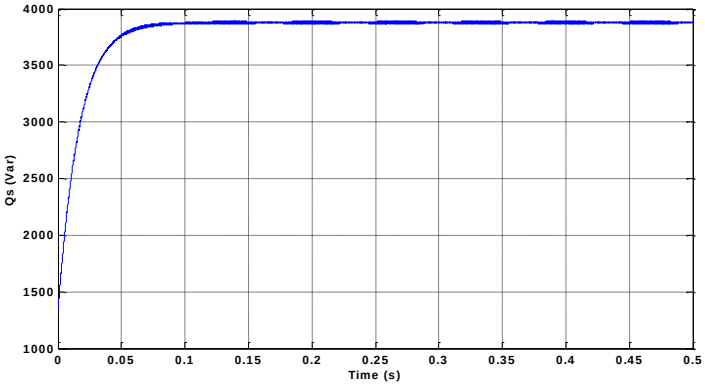


Fig.II.34:reactive power of the stator

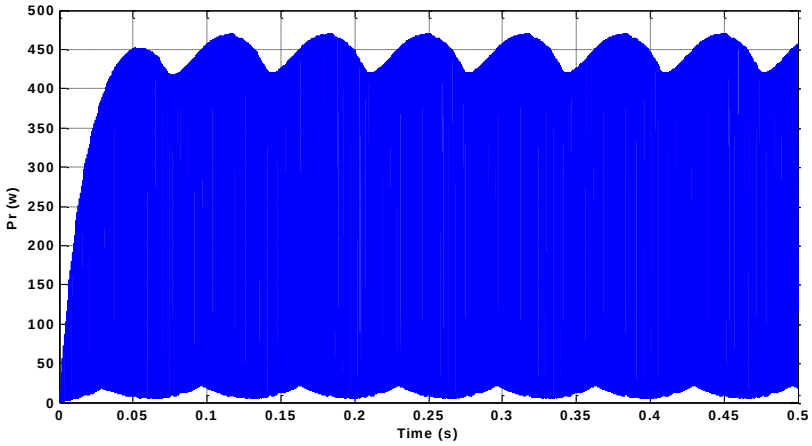


Fig.II.35: Active power of the rotor

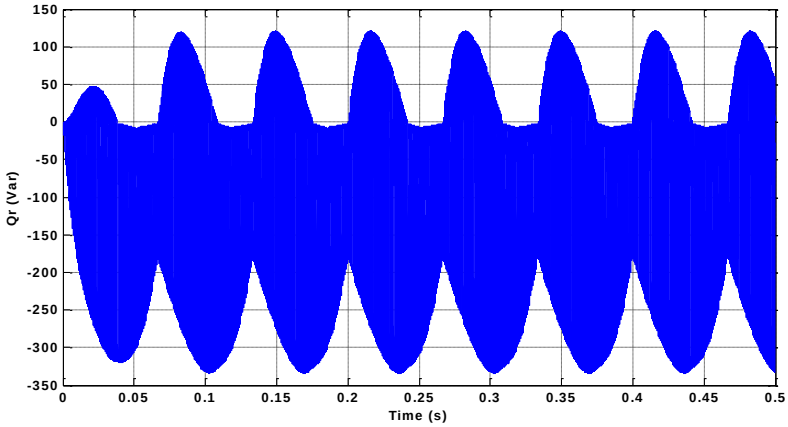


Fig.II.36: reactive power of the rotor

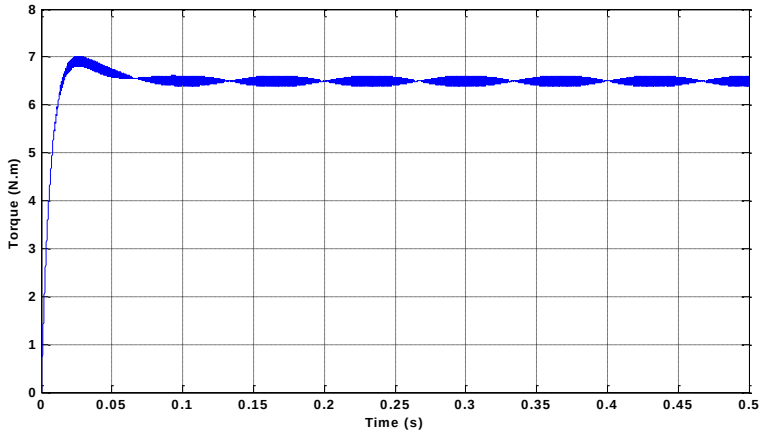


Fig.II.37: Electromagnetic torque

By employing simulations, I can demonstrate that after assigning specific values to Vdr and Vqr, I can effectively control the power system, achieving the desired outcomes precisely as intended. Simulations allow me to observe the system's response and behavior based on the assigned Vdr and Vqr values, providing a clear indication of the control achieved.

Through iterative adjustments and fine-tuning of these voltage parameters, I can optimize the control algorithms to ensure the system operates flawlessly according to my requirements. The ability to witness this control and its flawless performance in the simulated environment provides strong evidence that by manipulating Vdr and Vqr, I can exert perfect control over the power system.

II.7. Conclusion:

In this chapter, we have immersed ourselves in the fascinating world of the doubly fed asynchronous machine, conducting a thorough analysis that covers its intricate structure, working principle, diverse control strategies, and wide-ranging application domains. Our goal has been to provide a concise yet comprehensive understanding of this remarkable machine, shedding light on its multifaceted nature.

One of the pivotal aspects we have explored is the machine's model in the (a, b, c) reference frame. By employing the Park transformation, we have skillfully transformed the model into a linear format, making it more easily controllable. This transformation holds the key to implementing control techniques with greater efficiency, thereby paving the way for improved performance and operational adaptability.

The overarching objective behind this modeling endeavor has been to unlock the potential of vector control, which we will delve into further in the upcoming second chapter. Vector control represents a sophisticated and powerful technique that empowers us to finely manipulate the machine's operation, ushering in benefits such as enhanced efficiency, superior power quality, and dynamic response.

By immersing ourselves in the intricacies of the doubly-fed asynchronous machine, examining its model in the (a, b, c) reference frame, and elucidating the modeling of the power system, our aim is to equip readers with the foundational knowledge necessary to grasp and harness the true potential of vector control. This cutting-edge approach lies at the very core of optimizing the performance of the doubly fed induction generator, making it an indispensable area of study for those seeking to unlock the machine's full capabilities.

CHAPTER III
VECTOR CONTROL
OF THE DFIG

III.1 Introduction:

A good control of variable-speed alternating current machines is ensured if we guarantee a good decoupling between their electromagnetic variables. This is achieved by orienting them in a rotating reference frame (d, q) at the rotating field speed. If this is achieved, we can approximate its behavior to that of a separately excited direct current motor, where we find a natural decoupling between the excitation current that creates the flux and the armature current providing the necessary electromagnetic torque to make it rotate.

The vector control by flux orientation offers an attractive solution for achieving better performance in variable-speed applications for both generator and motor operation of the doubly-fed asynchronous machine.

In this context, we have proposed a control law for the doubly-fed asynchronous machine (DFIG) based on stator flux orientation, used to operate it as a generator. This control law highlights the relationships between the stator and rotor variables. These relationships will allow us to act on the rotor signals in order to control the exchange of active and reactive power between the machine's stator and the power grid.

III.2 Vector Control:

Vector control, or field-oriented control, is a control technique that involves transforming the three-phase currents and voltages of an electric motor into a rotating reference frame. In this reference frame, the stator currents can be separated into two components: the torque-producing component (direct axis or d-axis) and the magnetizing component (quadrature axis or q-axis). By independently controlling the d-axis and q-axis currents, vector control enables precise control of the motor's torque and flux.

III.2.1 Advantages of vector control:

- High performance: Vector control allows for precise control of motor torque and flux, resulting in high-performance motor drives with improved efficiency and dynamic response.
- Wide speed range: Vector control enables operation of electric motors over a wide speed range with good torque control, including low-speed and high-speed operation.
- Efficient torque production: Vector control optimizes torque production by effectively controlling the magnetizing current and the torque-producing current, resulting in efficient motor operation.
- Improved stability: The decoupling of torque and flux control in vector control improves the stability of the motor drive system, reducing disturbances and enhancing overall system performance.

III.2.2 Disadvantages of vector control:

- Complex implementation: Vector control requires complex control algorithms and calculations for transforming the currents and voltages into the rotating reference frame.

Implementing these algorithms can be challenging and may require advanced control techniques.

- Sensor requirements: Vector control often relies on accurate measurement of motor parameters such as rotor position and speed. This may require additional sensors, such as encoders or resolvers, which can increase system complexity and cost.
- Sensitivity to parameter variations: Vector control performance can be affected by variations in motor parameters, such as stator resistance and inductance. Proper calibration and compensation methods are needed to account for these parameter variations.

Overall, despite the complexities involved in implementation and sensor requirements, vector control offers significant advantages in terms of motor performance, efficiency, and dynamic response, making it a widely used technique in modern electric motor drives.

III.3 Principle of vector control:

The principle of vector control, also known as field-oriented control (FOC), involves controlling an electric motor by decoupling and independently controlling the torque-producing and magnetizing components of the motor's stator current. Here are the key principles of vector control:

- Coordinate Transformation: The first step in vector control is transforming the three-phase currents and voltages of the motor from the stationary reference frame (abc) to a rotating reference frame (d-q) aligned with the rotor flux. This transformation allows for decoupling the torque-producing and magnetizing components.
- Flux Orientation: In vector control, the stator current is controlled such that it aligns with the rotor flux, which results in improved torque production. The torque-producing component (direct axis or d-axis current) is aligned with the rotor flux, while the magnetizing component (quadrature axis or q-axis current) is orthogonal to the rotor flux.
- Independent Control: By controlling the d-axis and q-axis currents independently, vector control achieves precise control of the motor's torque and flux. The d-axis current controls the motor torque, while the q-axis current controls the motor flux. This decoupling allows for optimal control of both parameters.
- Current Regulators: Current regulators are used to track and control the desired d-axis and q-axis current references. These regulators adjust the stator current by comparing the actual currents with the reference values and generating appropriate control signals.
- Rotor Position Estimation: To implement vector control, accurate knowledge of the rotor position is required. Various methods are used to estimate the rotor position, such as sensor-based methods (encoders, resolvers) or sensor less methods
- Inverter Control: The final stage of vector control involves generating the appropriate voltage signals to the motor's stator windings through the inverter. The inverter control algorithm takes into account the desired torque and flux references, along with the rotor position information, to generate the necessary voltage signals.

- By employing these principles, vector control enables precise and efficient control of electric motor drives, providing high-performance operation with improved efficiency, wide speed range, and excellent dynamic response.

The figure (III.1) illustrates the equivalence between the torque expression achieved with the classical decoupled control of a direct current machine and the vector control of a doubly-fed asynchronous machine (DFIG).

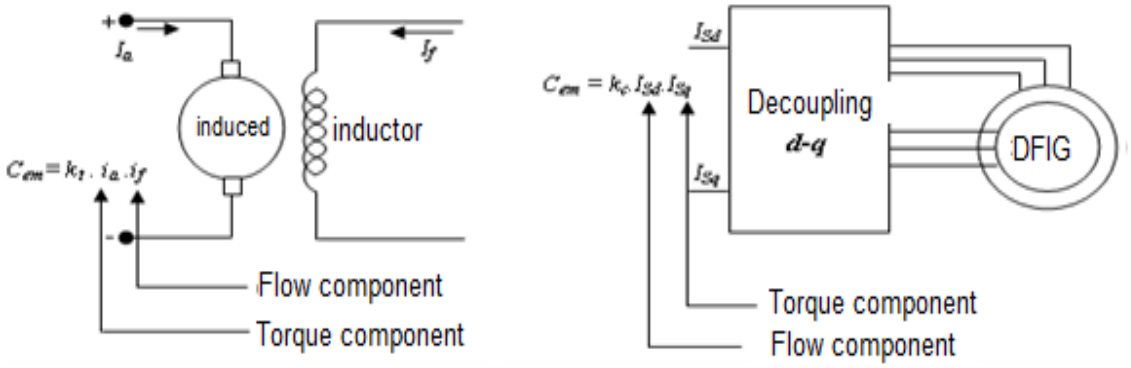


Figure III. 1 : Principle of vector control

III.4 Model for independent power control:

In order to easily control the electricity generation of the wind turbine, we will implement independent control of active and reactive powers by establishing equations that relate the values of rotor voltages, generated by a multi-level inverter, to the stator active and reactive powers [19], [20], [21], [22], [23],

We employ a two-phase model of the machine. The reference frame (d, q) is oriented such that the d-axis aligns with the stator fluxΨ_{ds}.

Hence:

$$\Psi_{ds} = \Psi_s; \Psi_{qs} = 0.$$

The expression for the electromagnetic torque then becomes:

$$C_e = n_p \frac{M}{L_s} \psi_{ds} . I_{qr} \qquad \text{(III.1)}$$

In the three-phase reference frame, denoted as a, b, c, the voltage across a phase n of the stator can be expressed by the general relationship:

$$V_{sn} = R_s I_{sn} + \frac{d\Psi_{sn}}{dt}$$

If we neglect the resistance of the stator winding Rs, this relationship becomes:

$$V_{sn} = \frac{d\Psi_{sn}}{dt} \qquad \text{(III.2)}$$

The relationship (III.2) shows that a reference frame aligned with the stator flux rotates at the same angular velocity as the stator voltage vector and is leading by π/2 radians. In this case of assuming a constant stator flux, we can then write:

$$V_{ds} = 0 \; et \; V_{qs} = V_s \tag{III.3}$$

we can simplify the voltage equations as follows:

$$\begin{cases} \mathrm{V_{ds}} = 0 \\ \mathrm{V_{qs}} = \mathrm{V_s} = \omega_s \Psi_{ds} \end{cases} \tag{III.4}$$

And the flux equations (II.21) become:

$$\begin{cases} \Psi_s = L_s I_{ds} + M I_{dr} \\ 0 = L_s I_{qs} + M I_{qr} \end{cases} \tag{III.5}$$

From equation (III.5), we can then write the equations relating the stator currents to the rotor currents:

$$\begin{cases} I_{ds} = \dfrac{\Psi_s}{L_s} - \dfrac{M}{L_s} I_{dr} \\ I_{qs} = -\dfrac{M}{L_s} I_{qr} \end{cases} \tag{III.6}$$

The active and reactive stator powers, in the orthogonal reference, are written:

$$\begin{cases} Ps = V_{ds} I_{ds} + V_{qs} I_{qs} \\ Qs = V_{qs} I_{ds} - V_{ds} I_{qs} \end{cases} \tag{III.7}$$

Adapting these equations to the chosen axis system and the simplifying assumptions made in our case (Vds=0) yields:

$$\begin{cases} Ps = V_s I_{qs} \\ Qs = V_s I_{ds} \end{cases} \tag{III.8}$$

By substituting Ids and Iqs with their expressions given in equation (III.6), we obtain the following expressions for the active and reactive powers:

$$\begin{cases} Ps = -V_s \frac{M}{L_s} I_{qr} \\ Qs = \frac{V_s \Psi_s}{L_s} - \frac{V_s M}{L_s} I_{dr} \end{cases} \tag{III.9}$$

Therefore, the expression for the powers (III.9) can be simplified as follows:

$$\begin{cases} Ps = -V_s \dfrac{M}{L_s} I_{qr} \\ Qs = -\dfrac{V_s M}{L_s} I_{dr} + \dfrac{{V_s}^2}{L_s \omega_s} \end{cases} \quad \text{(III.10)}$$

We can express the rotor fluxes by substituting the stator currents with their expressions from equation (III.6):

$$\begin{cases} \Psi_{dr} = L_r \sigma I_{dr} + \frac{MV_s}{\omega_s L_s} \\ \Psi_{qr} = L_r \sigma I_{qr} \end{cases} \quad \text{(III.11)}$$

$$\sigma = (1 - \frac{M^2}{L_r L_r})$$

These expressions of the d-axis and q-axis rotor fluxes are then integrated into the expressions of the two-phase rotor voltages from equation (II.22). We obtain the following:

$$\begin{cases} V_{dr} = R_r I_{dr} + L_r \sigma \frac{dI_{dr}}{dt} - \mathrm{g}\omega_s L_r \sigma I_{qr} \\ V_{qr} = R_r I_{qr} + L_r \sigma \frac{dI_{qr}}{dt} + \mathrm{g}\omega_s L_r \sigma I_{dr} + \mathrm{g}\omega_s \frac{MV_s}{\omega_s L_s} \end{cases} \quad \text{(III.12)}$$

In steady-state conditions, the terms involving the derivatives of the two-phase rotor currents disappear, so we can write:

$$\begin{cases} V_{dr} = R_r I_{dr} - \mathrm{g}\omega_s L_r \sigma I_{qr} \\ V_{qr} = R_r I_{qr} + \mathrm{g}\omega_s L_r \sigma I_{dr} + \mathrm{g}\omega_s \frac{MV_s}{\omega_s L_s} \end{cases} \quad \text{(III.13)}$$

Vdr and Vqr are the two-phase components of the rotor voltages that need to be applied to the machine to achieve the desired rotor currents. The impact of the coupling terms between the two axes, such as (Lr - (M^2/Ls)), is negligible. Adequate synthesis of the regulators in the control loop will compensate for these terms.

However, the term (g.(M.VS/Ls)) represents an electromotive force that is dependent on the rotational speed. Its influence is significant as it causes a drag error. Therefore, the control of the system should consider this error [12].

By examining equations (III.11) and (III.13), we can construct the block diagram shown in Figure (III.2), which has the rotor voltages as inputs and the stator active and reactive powers as outputs [24].

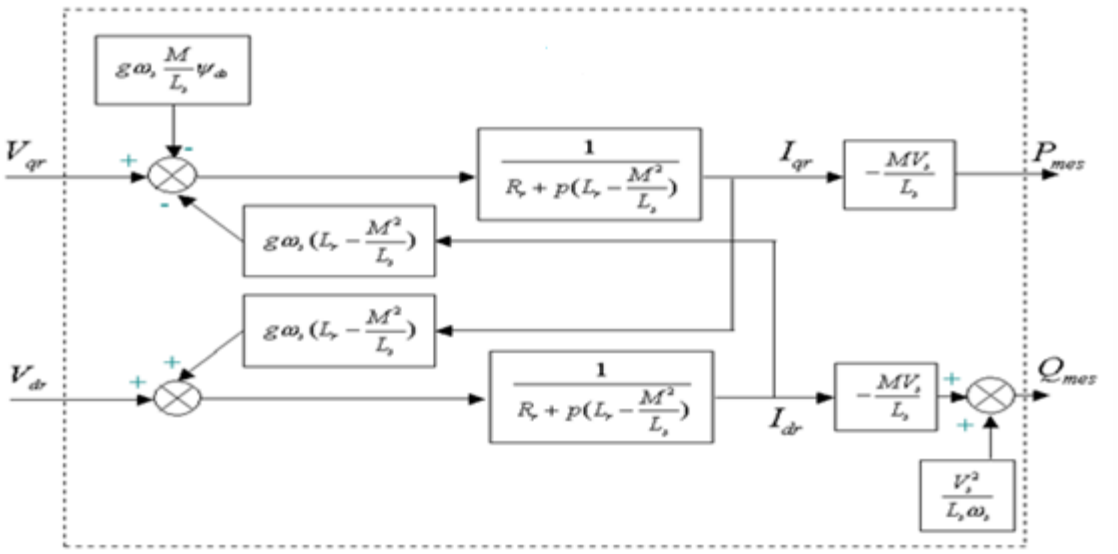


Figure III. 2 : Block diagram of the DFIG (Doubly-Fed Induction Generator)

The two-phase rotor voltages are the quantities to be imposed to control the rotor currents. $V_{dr}V_{qr}$Are thus considered as control variables, which are generated by the flux−oriented control block (Figure III.3), and the rotor currents $I_{dr}I_{qs}$ as state variables. The rotor voltages are thus a function of the set point values P_{ref}andQ_{ref}

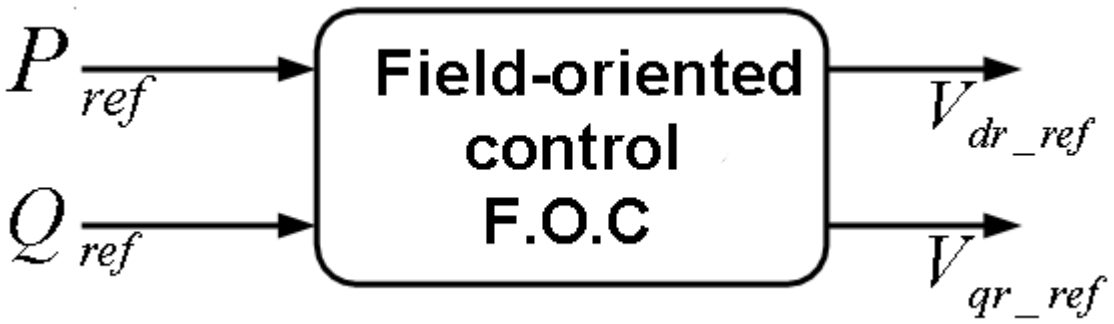


Figure III. 3 : Flux-oriented control block.

Note that the powers and voltages are interconnected through a first-order transfer function. The low coupling between the d and q axes (low slip) enables the straightforward implementation of a control system for this configuration. As a result, the two axes can be controlled separately using their respective regulators.

This control technique, known as the "P and Q command," utilizes the active and reactive powers as setpoints. In the subsequent part, we will study and simulate the latter method.

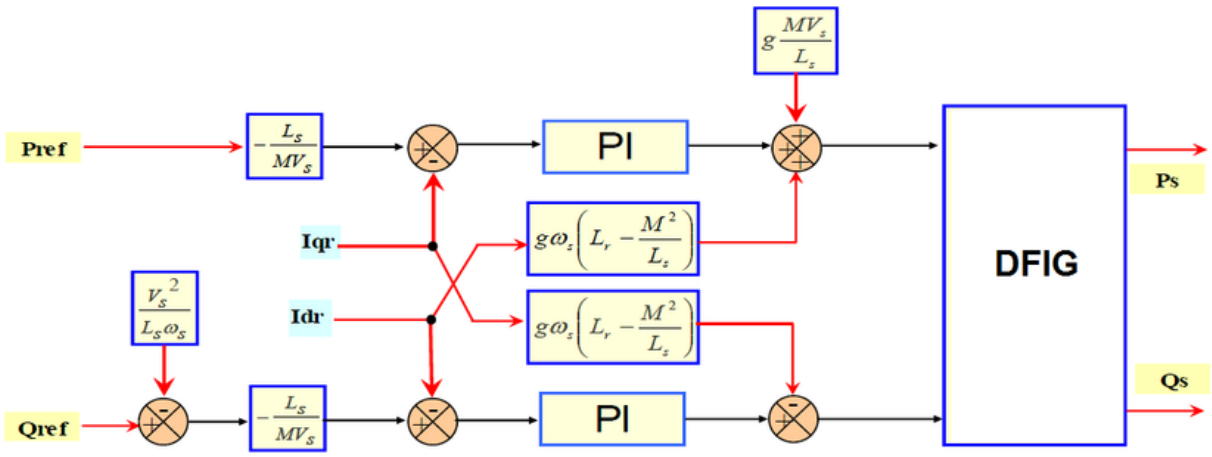


Figure III. 4 : Indirect control block diagram

III.5 Synthesis of current PI controllers:

For each control loop, we use a conventional PI (Proportional-Integral) controller. This control element is characterized by a proportional action to adjust the speed at which the regulation should be performed and an integral action whose purpose is to eliminate the steady-state error between the controlled variable and the set point.

For the direct and quadrature currents, we highlight two symmetric regulation loops equipped with controllers defined by the parameters (Kp, Ki).

Considering the direct axis, we can write:

$$\frac{I_{sd}}{V_{sd1}} = \frac{1}{R_S.(1+\sigma.T_S.s)} \text{(III. 14)}$$

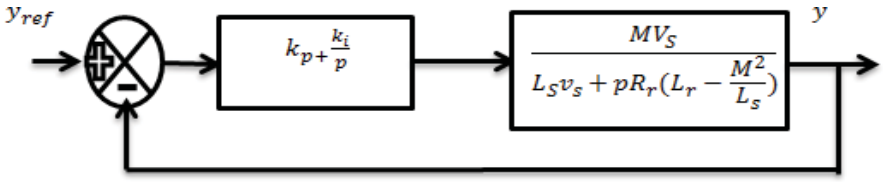


Figure III. 5 : Regulation loop of the direct component of the stator current**.**

Le The functional diagram of the regulation of the direct current is represented in Figure III.4. The open-loop transfer function is given by:

$$G_{dO}(s) = \frac{I_{Sd}}{I_{Sd}^*} = \frac{K_{pd}+\frac{K_{id}}{S}}{R_S+\sigma.L_S.s} \quad \text{(III.15)}$$

In closed-loop, we obtain a transfer function of the form:

$$G_{dF}(s) = \frac{I_{Sd}}{I_{Sd}^*} = \frac{\frac{K_{pd}.S+K_{id}}{\sigma.L_S}}{S^2+\left(\frac{R_S+K_{pd}}{\sigma.L_S}\right).s+\frac{K_{id}}{\sigma.L_S}} \quad \text{(III.16)}$$

Its characteristic polynomial highlights a second-order dynamics:

$$P_s = S^2 + \left(\frac{R_s + K_{pd}}{\sigma . L_s}\right) . s + \frac{K_{id}}{\sigma . L_S} \quad \text{(III.17)}$$

Let us impose two complex conjugate poles with negative real parts such that:

$$S_{1,2} = \rho_d(-1 \pm j) \quad \text{(III.18)}$$

The polynomial defining the desired dynamics takes the following form:

$$P_d(s) = s^2 + 2.\rho_d.s + 2.\rho_d^2 \quad \text{(III.19)}$$

By identifying term by term the two equations (III. 16)and(III. 18), we obtain the expressions for the regulator parameters:

$$K_{pd} = 2.\sigma.L_s.\rho_d - R_s \quad \text{(III.20)}$$

$$K_{id} = 2.\sigma.L_s.\rho_d^2 \quad \text{(III.21)}$$

III.6 Simulation of indirect power control

The first test consists of applying step changes in active and reactive power inputs while the machine is operating at a fixed speed of 1425 rpm.

• For active power:

- From t=0s to t=0.25s: a negative step of -1000 W.
- From t=0.25s to t=0.5s: a negative step of -500 W.
- From t=0.5s to t=0.75s: a negative step of -1500 W.
- From t=0.75s to t=1s: a negative step of -1500 W.

• For reactive power:

- From t=0s to t=0.25s: a negative step of -500 VAR.
- From t=0.25s to t=0.5s: a negative step of 500 VAR.
- From t=0.5s to t=0.75s: a negative step of 0 VAR.
- From t=0.75s to t=1s: a negative step of -500 VAR.

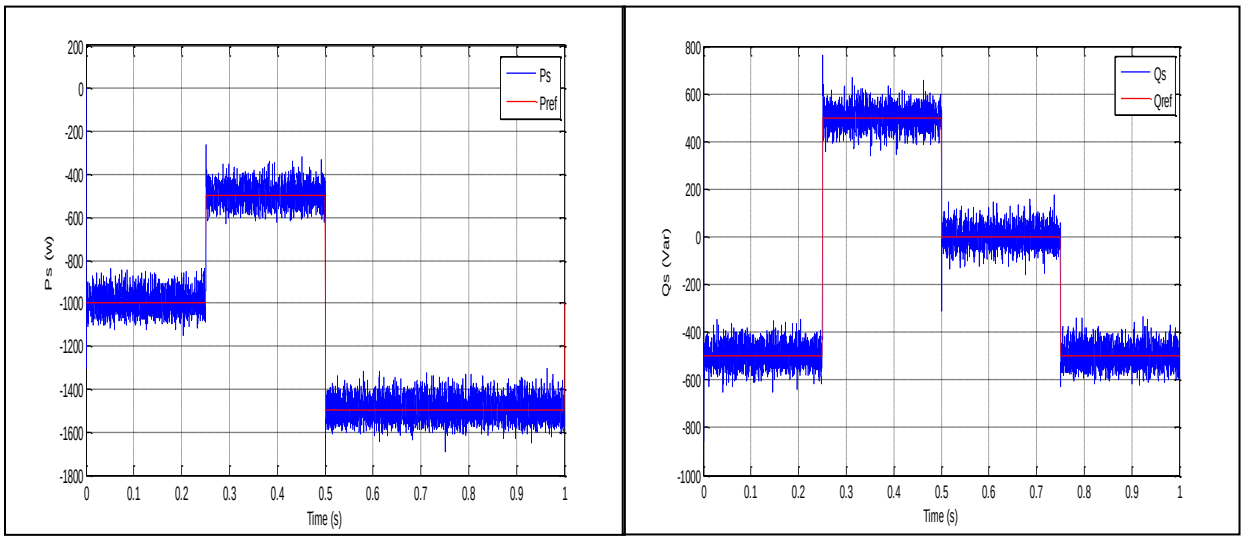


Figure III. 6 : Active and reactive power of the stator.

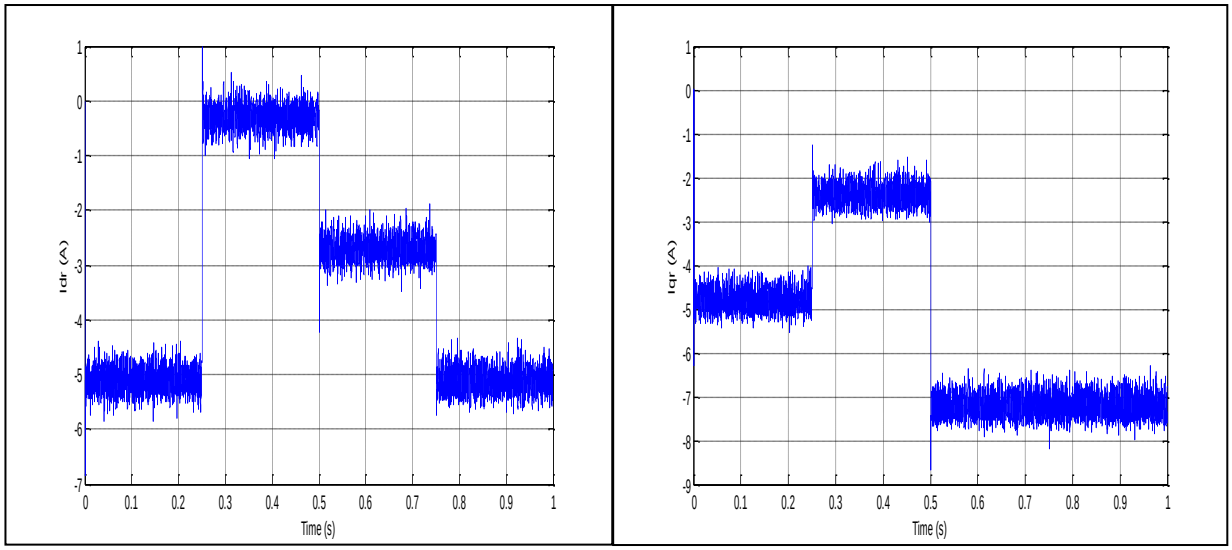


Figure III. 7 : The rotor current along the d-axis and q-axis

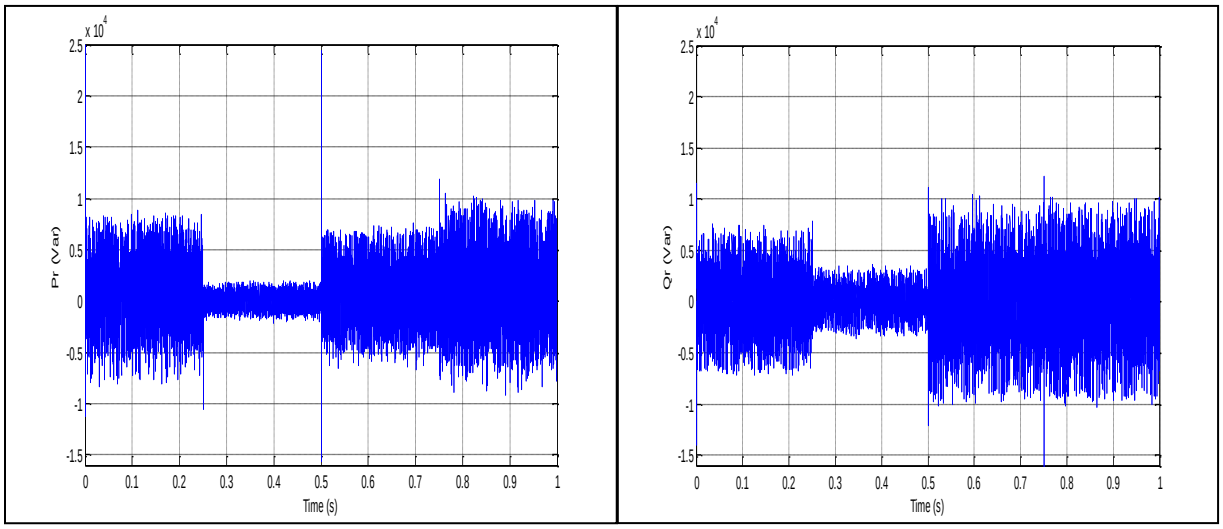


Figure III. 8 : Active and reactive power of the rotor**.**

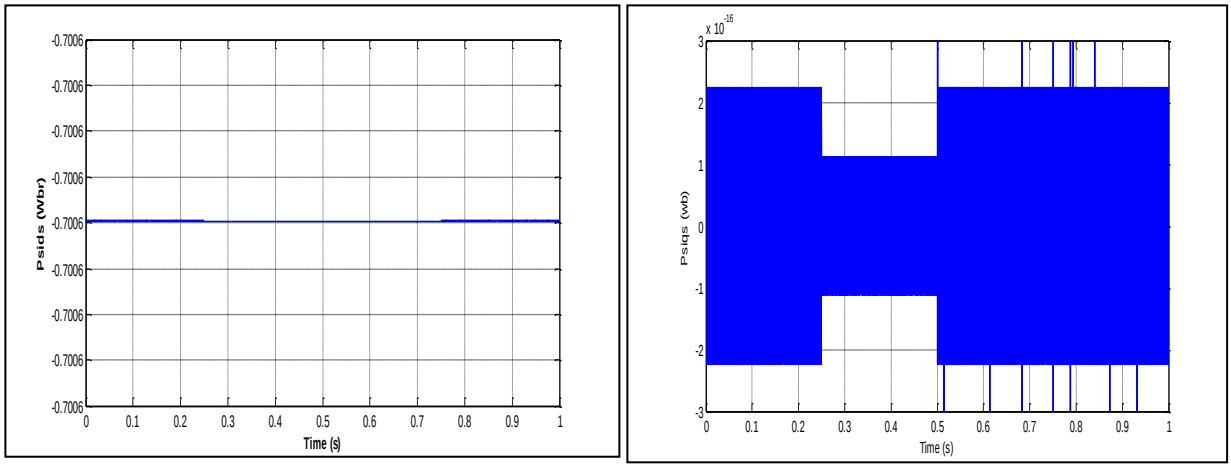


Figure III. 9 : The stator flux along the d and q axes**.**

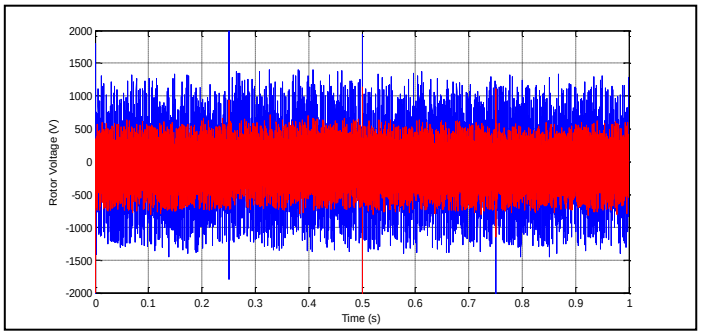


Figure III. 10 : Rotor voltages and currents**.**

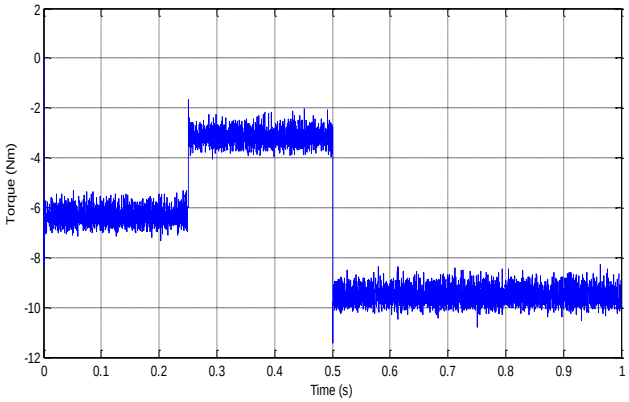


Figure III. 11 : Electromagnetic torque

By examining the preceding figures, we can draw several noteworthy observations. Firstly, the system demonstrates a desirable level of dynamism, accompanied by a minimal static error. In terms of active and reactive powers, there is a rapid and precise response without any overshoot. The system adeptly follows the desired power increments, resulting in accurate power measurements with no remaining errors. Moreover, the coupling between the two power components is exceptionally weak, barely perceptible in its influence.

A significant aspect of the system is the operation of reactive power control, which grants the ability to generate either negative reactive power, exhibiting capacitive behavior, or positive reactive power, displaying inductive behavior.

This control mechanism empowers the system to adapt and effectively manage the reactive power output, depending on the desired behavior and requirements of the systemThe values of active and reactive powers are directly proportional to the quadrature and direct components of the rotor current, respectively. The torque, on the other hand, primarily relies on the quadrature component of the rotor current (Iqr). The direct component of the stator flux remains nearly constant, while the quadrature component remains negligible.

III.9. Conclusion:

Integrating a PI (Proportional-Integral) controller into the vector control of a DFIG (Double Fed Induction Generator) is a crucial aspect of wind energy systems. This controller plays a vital role in ensuring precise regulation of torque and speed, which are essential for the smooth operation of the DFIG.

By combining proportional and integral actions, the PI controller responds swiftly to changes in operating conditions. It efficiently corrects any steady-state error, allowing for accurate energy conversion from mechanical power to electrical energy. This control technique not only guarantees precise energy conversion but also enables the DFIG system to perform dynamically, swiftly adapting to varying wind conditions and electrical load demands.

One notable advantage of the PI controller is its adjustability. By carefully fine-tuning the controller's parameters, the DFIG system can be customized to meet specific requirements. This adaptability ensures optimal performance under different wind speeds and load conditions, enhancing the system's efficiency and overall performance.

The effectiveness of the PI controller in practical applications has been proven time and again. Many wind energy systems employ the DFIG with a PI controller to achieve precise control and reliable energy conversion. This real-world implementation highlights the viability and practicality of using the PI controller in current energy systems.

In summary, the integration of a PI controller into the vector control of a DFIG is crucial for precise torque and speed regulation in wind energy systems. This controller's ability to swiftly respond, eliminate steady-state error, and ensure accurate energy conversion contributes to the system's dynamic performance and overall stability. The adjustability of the PI controller allows for customization, making it a practical and effective solution for DFIG systems in real-world applications within the current energy landscape.

CHAPTER IV

Backstepping Control of the DFIG

IV.1.Introduction:

Control design for nonlinear systems is a difficult task due to the complexity and nonlinearity of the dynamics. Conventional linear control techniques may not be effective in achieving the stability and desired performance of such systems. Nonlinear control techniques are designed to address these challenges and provide effective control strategies.

Backstepping is a control method specifically designed for stabilizing and controlling nonlinear systems. It is based on a recursive design approach that allows for systematic and structured control design. Backstepping divides the control problem into a series of steps, each corresponding to a specific aspect of the system dynamics. By constructing virtual tax inputs and corresponding tax laws, Backstepping stabilizes and tracks performance.

Overall, backstepping provides a powerful and systematic approach to control design for nonlinear systems. Its ability to handle complexity, achieve stability, and eliminate uncertainty has made it a valuable tool in modern control engineering. By understanding the principles and advantages of backstepping, researchers and engineers can effectively apply this methodology to a wide range of difficult control problems.[25]

IV.2.Basic Concepts and Principles:

Backstepping control is based on several fundamental principles that form the foundation of its design approach. These principles include the concept of virtual control and the use of stabilizing functions. Let's explore these concepts in more detail:

IV.2.1. Virtual Control:

The concept of virtual control is central to backstepping control. It involves introducing a set of intermediate control inputs, called virtual control inputs, to facilitate the control design process. These virtual control inputs are not physically implemented but serve as intermediate control targets to achieve desired system behavior.

Virtual control inputs are designed in a recursive manner, where each control input is constructed to stabilize the dynamics associated with the previous control input. This recursive design allows for a systematic and layered approach to address the complexity of nonlinear systems.

By constructing virtual control inputs, backstepping breaks down the control problem into a series of simpler sub-problems. This enables the design of control laws that stabilize each virtual control input, leading to overall system stability and desired tracking performance.

IV.2.2. Stabilizing Functions:

Stabilizing functions play a crucial role in achieving stability and tracking performance in backstepping control. A stabilizing function is a Lyapunov-like function that quantifies the stability properties of the system and guides the design of control laws.

Stabilizing functions are typically constructed based on the error between the system outputs and their desired values. They are chosen to be positive definite functions with negative definite time derivatives. The specific form of the stabilizing function depends on the system dynamics and desired performance objectives.

The stabilizing function is used to derive control laws that stabilize the virtual control inputs. By analyzing the time derivative of the stabilizing function along the system trajectories, stability can be proven. The control laws are designed such that they drive the system states towards the desired values, while ensuring the decrease of the stabilizing function.

Stabilizing functions provide a means to incorporate stability analysis into the control design process. They enable the assessment of stability and tracking performance and guide the selection of suitable control laws for achieving the desired system behavior.

In summary, the concept of virtual control and the use of stabilizing functions are fundamental principles in backstepping control. By constructing virtual control inputs and designing control laws based on stabilizing functions, backstepping provides a systematic approach to address the complexity of nonlinear systems and achieve stability and desired tracking performance.

IV.3. Backstepping Control [26]

From the equations (III. 10) and (III.12) we can establish the block diagram of the regulation loops of the rotor currents 'axes 'dq' thus giving the desired stator powers (Figure IV.1).

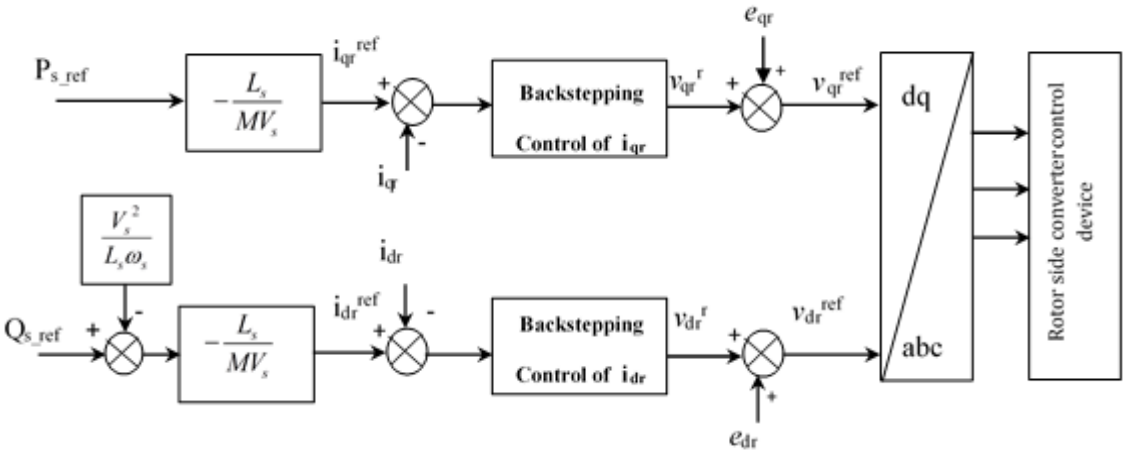


Figure IV. 1 : Diagram of the indirect control of the stator powers of the DFIG,

In the d-q reference frame, the electrical equations of the Dual FeedAsynchronous Machine (DFIG) can be represented as follows:

$$\begin{cases} v_{dr} = v_{dr}^{r} + e_{dr} & \text{with: } v_{dr}^{r} = R_r i_{dr} + \sigma L_r \dfrac{d}{dt} i_{dr} \ , \ e_{dr} = -\sigma L_r g \omega_s i_{qr} \\ v_{qr} = v_{qr}^{r} + e_{qr} & \text{with: } v_{qr}^{r} = R_r i_{qr} + \sigma L_r \dfrac{d}{dt} i_{qr} \ , \ e_{qr} = \sigma L_r g \omega_s i_{dr} + g \dfrac{M V_s}{L_s} \end{cases} \quad \text{(IV.1)}$$

withe : e_{dr} and e_{qr} are the coupling terms.

$$\begin{cases} v_{dr}^{r} = R_r i_{dr} + \sigma L_r \dfrac{d}{dt} i_{dr} \\ v_{qr}^{r} = R_r i_{qr} + \sigma L_r \dfrac{d}{dt} i_{qr} \end{cases} \quad \text{(IV.2)}$$

$$\begin{cases} i_{qr}^{ref} = -\dfrac{L_s}{M V_s} P_{s_ref} \\ i_{dr}^{ref} = -\dfrac{L_s}{M V_s} Q_{s_ref} + \dfrac{V_s}{M \omega_s} \end{cases} \quad \text{(IV.3)}$$

$\sigma=(1-M^2/(L_rL_s))$: is the dispersion coefficient.

IV.3.1. Lyapunov Method:

Control of nonlinear systems relies on two possible approaches. The first approach aims to linearize the system to be controlled in order to leverage techniques developed for linear systems. The second approach involves finding a Lyapunov control function that guarantees certain performance criteria for the closed-loop system. Such functions can be challenging to find for high-order nonlinear systems.

The Backstepping technique effectively reduces this complexity. Stability analysis in the context of Backstepping is based on Lyapunov methods, which are a powerful tool for testing and finding sufficient conditions for the stability of dynamic systems without explicitly solving the differential equations describing them. Lyapunov introduced a similar function with properties analogous to mechanical energy, which allows for more convenient stability analysis. A system is considered stable if its total mechanical energy decreases over time. Lyapunov's function captures similar properties, facilitating stability analysis.

a- The first method proposed by Lyapunov allows for the analysis of system stability by examining its local stability through the linearization of dynamics around an equilibrium point. However, this method has limited significance as it only focuses on local stability and does not provide information about the overall stability of the system. Additionally, due to the linearization approximations, it cannot account for all types of nonlinear phenomena. If the linearized system is found to be unstable, it implies that the nonlinear system will also be unstable.

b- The second method introduced by Lyapunov is based on the concept of energy within a system. This approach analyzes system stability without the need to solve the governing nonlinear differential equations. Instead, it relies on studying the variations (sign of the derivative) of energy or an equivalent function along the system's trajectory. To assess the stability of a system characterized by a state vector X, the goal is to find a function $V(x)$ (representing energy) with a definite sign, where its derivative dV/dt is semi-definite and of opposite sign within the same domain.[27].

IV.3.2. Rotor currents control:

The rotor currents errors are defined by:

$$\begin{cases} e_1 = i_{qr}^{ref} - i_{qr} \\ e_2 = i_{dr}^{ref} - i_{dr} \end{cases} \quad \text{(IV.4)}$$

The derivative of error gives:

$$\begin{cases} \dot{e}_1 = \dot{i}_{qr}^{ref} - \dot{i}_{qr} \\ \dot{e}_2 = \dot{i}_{dr}^{ref} - \dot{i}_{dr} \end{cases} \quad \text{(IV.5)}$$

We can choose the Lyapunov function *V*associated to the currents errors, such us:

$$V = \frac{1}{2}e_1^2 + \frac{1}{2}e_2^2 \quad \text{(IV.6)}$$

The derivation of equation IV.6 is given by:

$$\dot{V} = e_1\dot{e}_1 + e_2\dot{e}_2 \quad \text{(IV.7)}$$

According to Lyapunov theory, function $\dot{V}$ must be negative defined, and that can be rewritten as follows:

$$\dot{V} = -k_1e_1^2 - k_2e_2^2 \quad \text{(IV.8)}$$

Where k_1, k_2 shold be positive constants, to ensure a negative value.

Using equations (IV.7) and (IV.8) and (IV.5) we can have:

$$\begin{cases} \dot{e}_1 = -k_1e_1 = \dot{i}_{qr}^{ref} - \dot{i}_{qr} \\ \dot{e}_2 = -k_2e_2 = \dot{i}_{dr}^{ref} - \dot{i}_{dr} \end{cases} \quad \text{(IV.9)}$$

Using equations (IV.9) and (IV.2) we obtain:

$$\begin{cases} v_{dr}^{r} = \sigma L_r \dot{i}_{dr}^{ref} + R_r i_{dr} + \sigma L_r k_1 (i_{dr}^{ref} - \mathrm{i}_{\mathrm{dr}}) \\ v_{qr}^{r} = \sigma L_r \dot{i}_{qr}^{ref} + R_r i_{qr} + \sigma L_r k_2 (i_{qr}^{ref} - \mathrm{i}_{\mathrm{qr}}) \end{cases} \quad \text{(IV.2)}$$

Where, i_{dr}^{ref} , i_{qr}^{ref} are given by equation (IV.2).

The figure IV.2 show the structure of the Backstepping control.

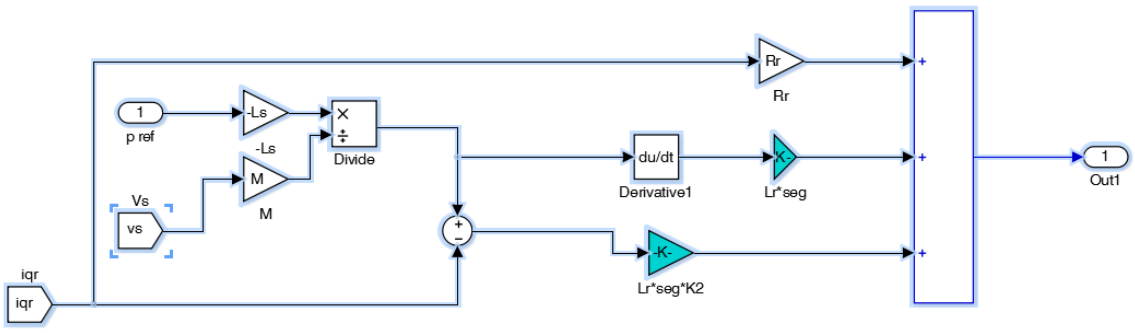


Figure IV. 2 : Bloc diagram of the Backstepping iqrcurrent controller

IV.4. simulation results:

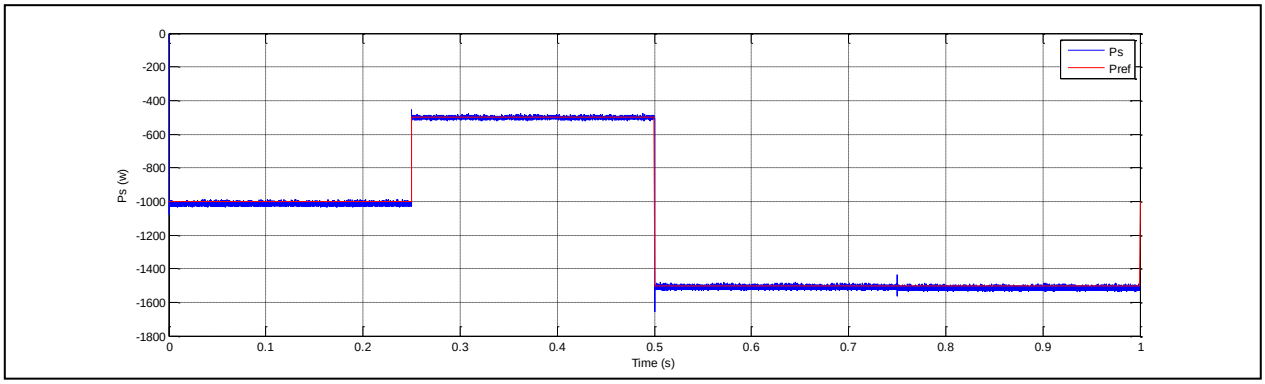
The first test consists of applying step changes in active and reactive power inputs

• For active power:

- From t=0s to t=0.25s: a negative step of -1000 W.
- From t=0.25s to t=0.5s: a negative step of -500 W.
- From t=0.5s to t=0.75s: a negative step of -1500 W.
- From t=0.75s to t=1s: a negative step of -1500 W.

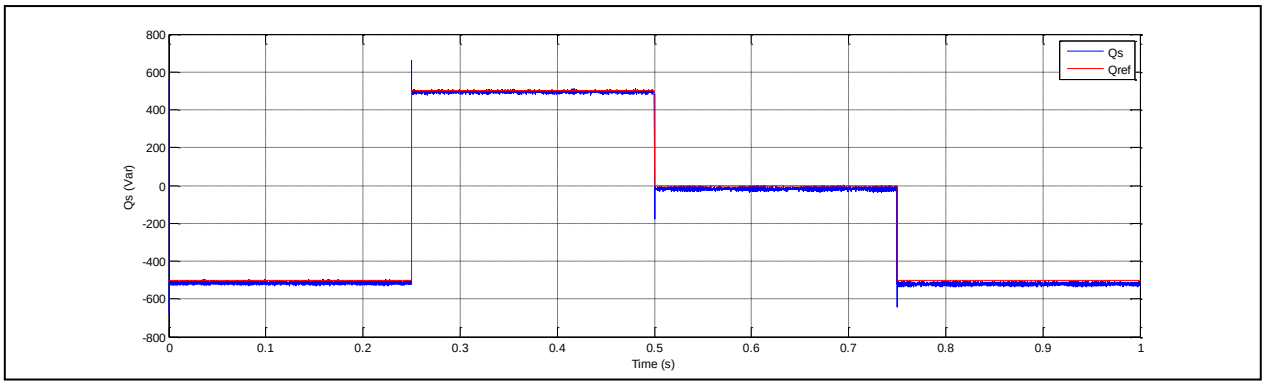
• For reactive power:

- From t=0s to t=0.25s: a negative step of -500 VAR.
- From t=0.25s to t=0.5s: a positive step of 500 VAR.
- From t=0.5s to t=0.75s: zerovalue0 VAR.
- From t=0.75s to t=1s: a negative step of -500 VAR.



.

Figure IV. 3 : Active power of the stator.



.

Figure IV. 4 : Reactive power of the stator**.**

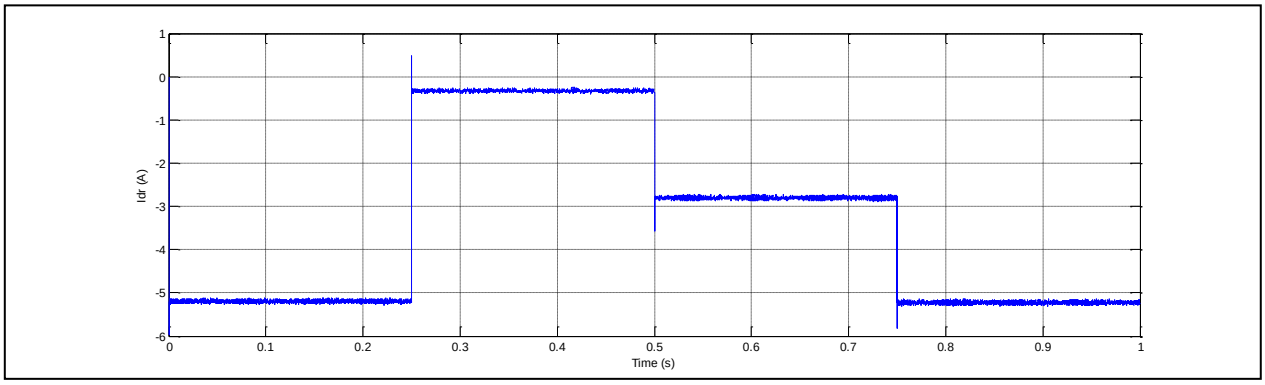


Figure IV. 5 : Rotor current along the d-axis.

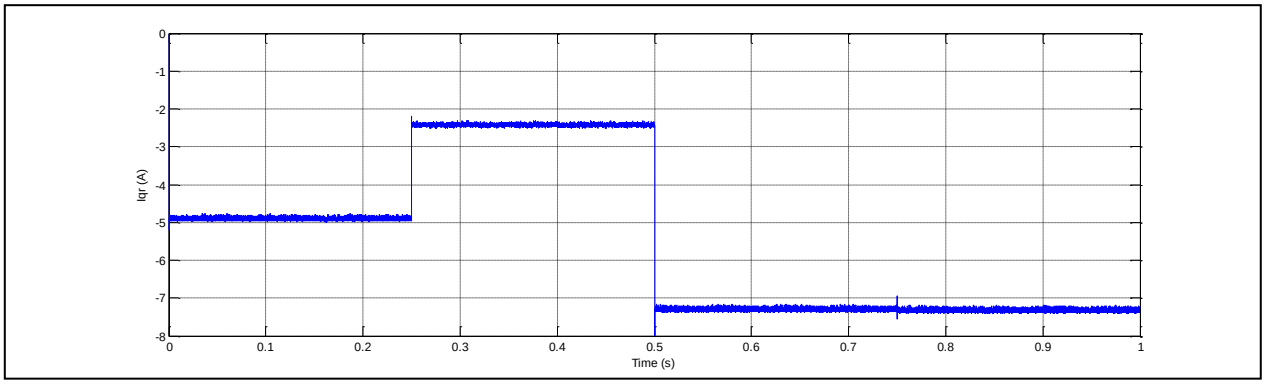
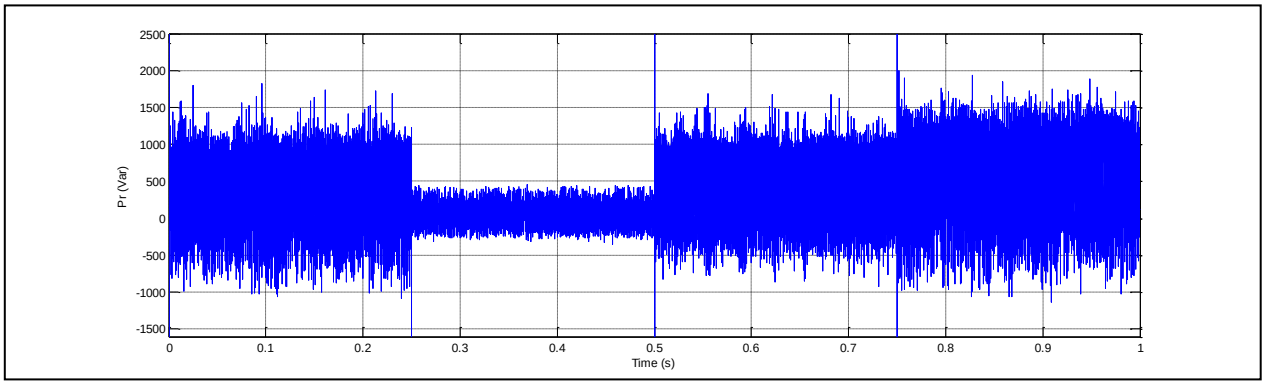


Figure IV. 6 : Rotor current along the q-axis.



.

Figure IV. 7 : Active power of the rotor.

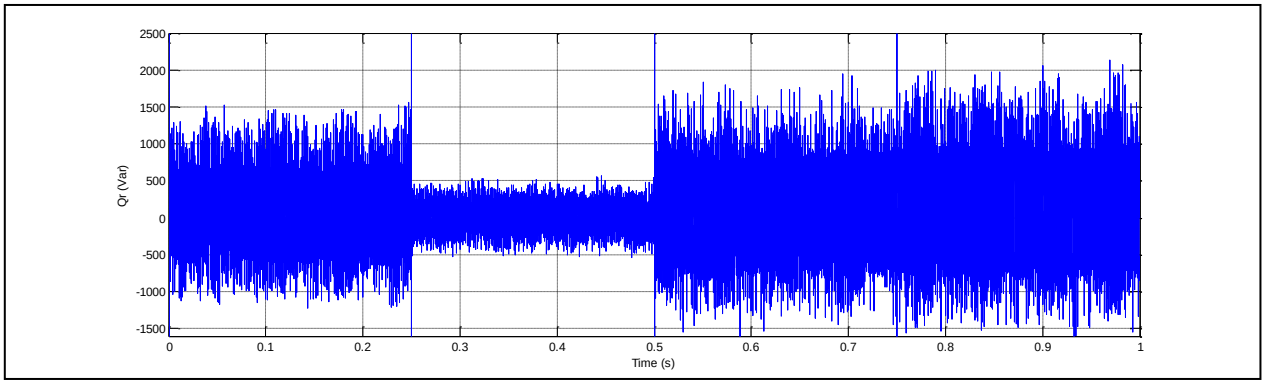
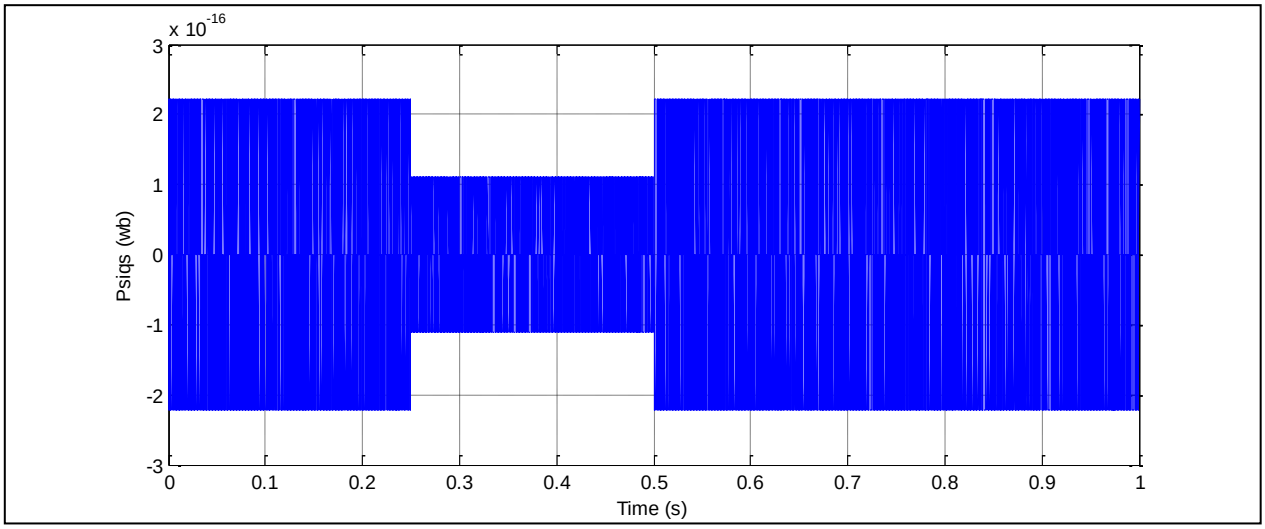


Figure IV. 8 : Reactive power of the rotor.



.

Figure IV. 9 : Stator flux along the q-axis.

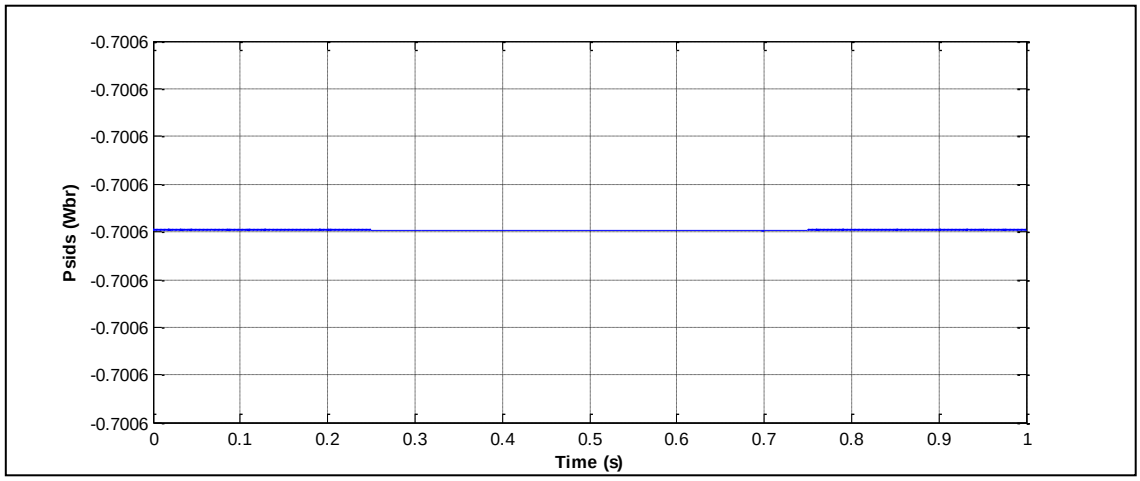


Figure IV. 10 : Stator flux along the d-axis.

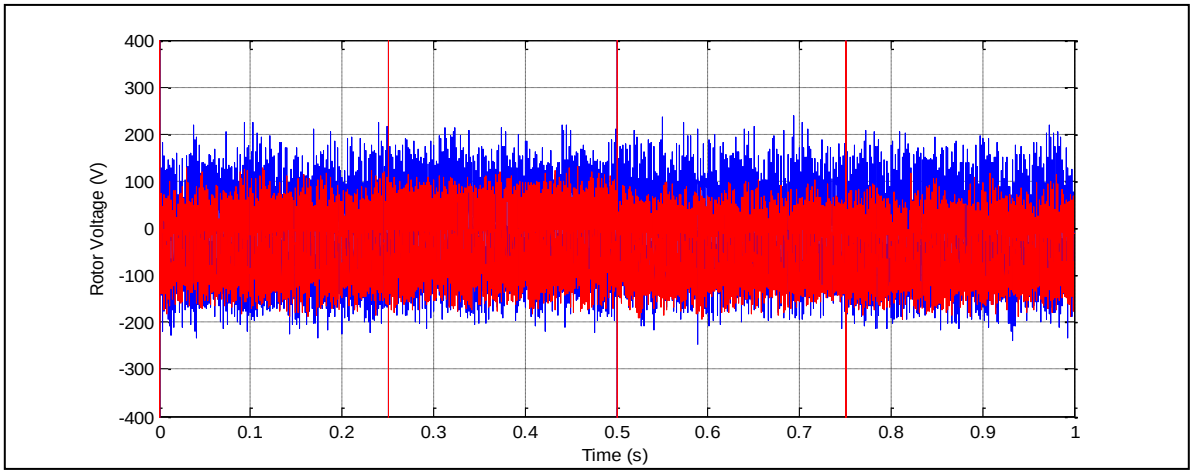


Figure IV. 11 : Rotor Voltages.

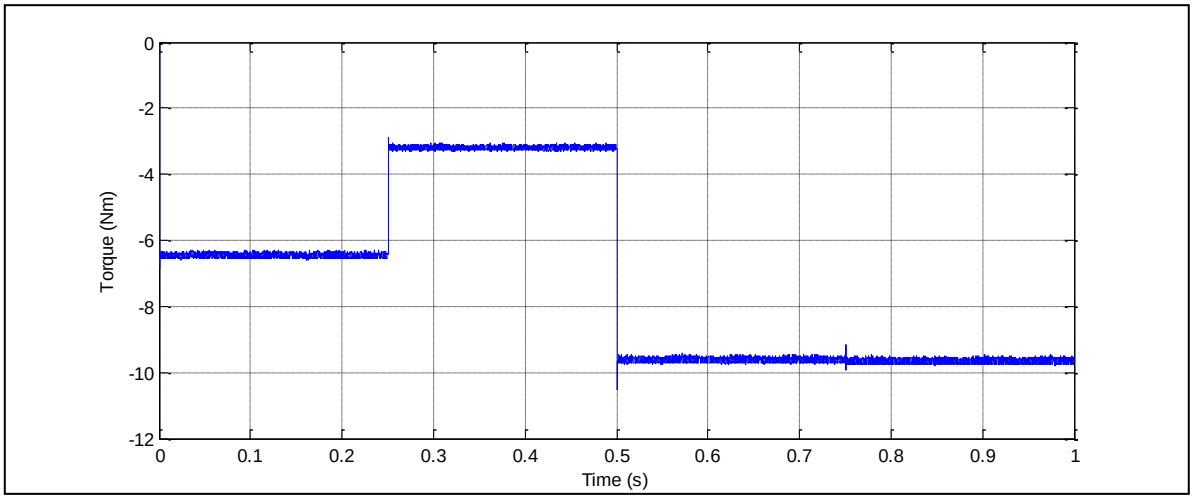


Figure IV. 12 : Electromagnetic torque

.

The power-based responses generated in accordance with instructions are graphically depicted in Figures (IV.4 and IV.5). These figures illustrate the system's dynamic behavior when controlled using the assigned values of Vdr and Vqr. The results clearly demonstrate that the system accurately follows the provided instructions. Notably, when comparing the performance of the backstepping command, as discussed in Chapter IV, to the previously presented PI controller in Chapter III, it is evident that the backstepping command outperforms the PI controller in terms of tracking performance. The backstepping command exhibits a remarkable absence of overshoot, showcases a rapid transient response, and consistently converges to a steady-state error approaching zero. These observations highlight the superior control capabilities attained through the manipulation of Vdr and Vqr, indicating the potential for achieving perfect control over the power system.

IV.5.Comparison between Backstepping and the PI Controller:

The comparison between "backstepping" and the PI controller is often made in the field of control systems. They are two different approaches used to design controllers that enable tracking of a reference trajectory and disturbance rejection.

IV.5.1 Backstepping:

Backstepping is a method for designing nonlinear controllers for nonlinear dynamic systems. It involves dividing the system into several subsystems, called "virtual systems," and designing control laws for each virtual system sequentially. Each step in the backstepping design aims to make the tracking errors of each virtual system asymptotically zero. This ensures global stability of the overall system. Backstepping is often used for complex systems with nonlinear models

IV.5.2 PI Controller (Proportional-Integral):

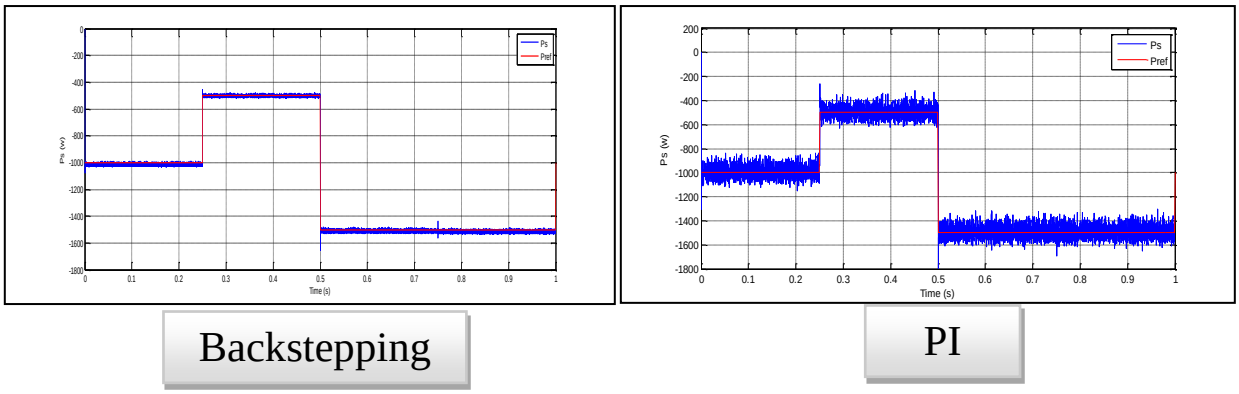


Figure IV. 13 : the active power of the stator using a PI controller and the backstepping command

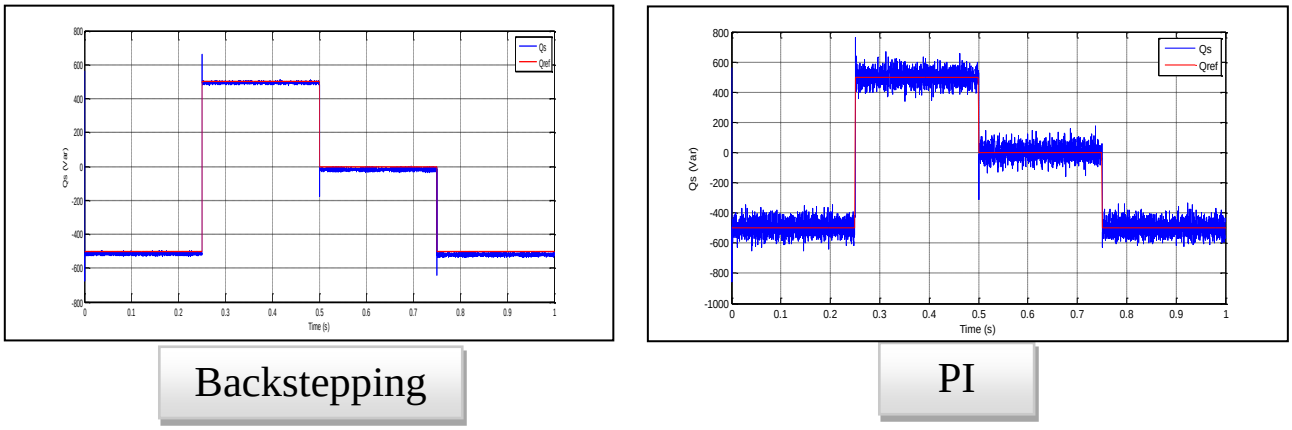


Figure IV. 14 : comparing the reactive power of the stator using a PI controller and the Backstepping command

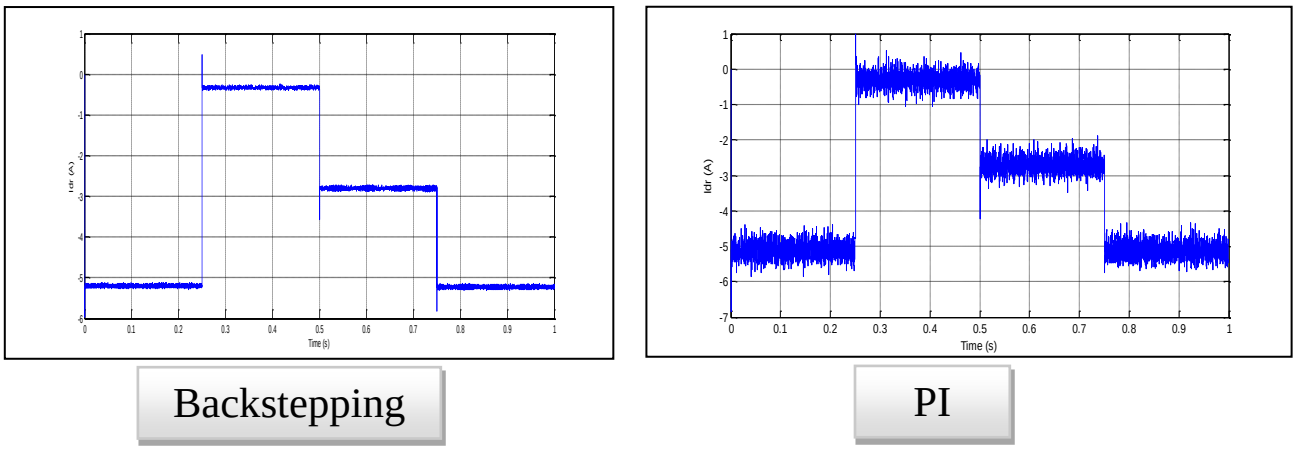


Figure IV. 15 : comparing the Rotor current along the d-axis.

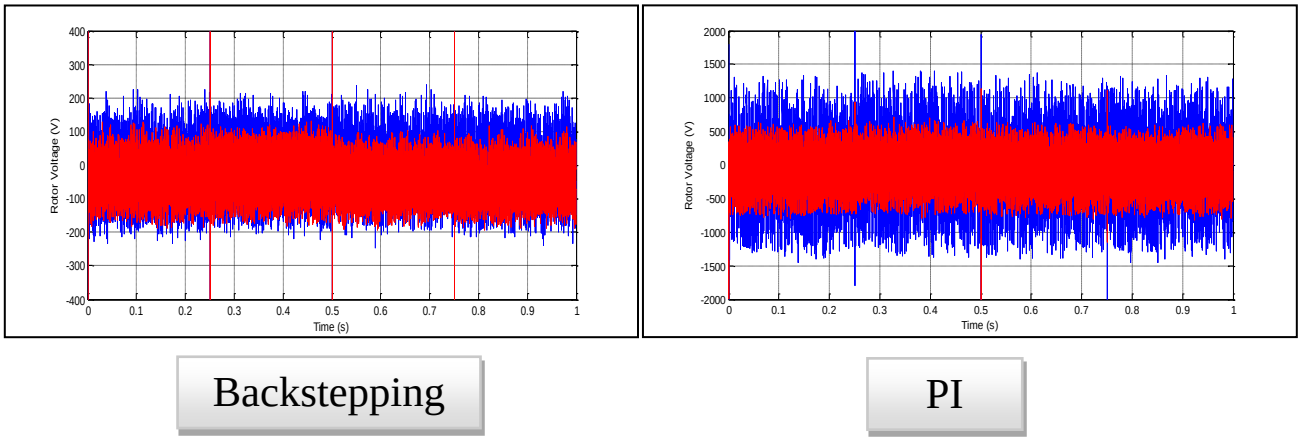


Figure IV. 16 : comparing the Rotor current along the q-axis.

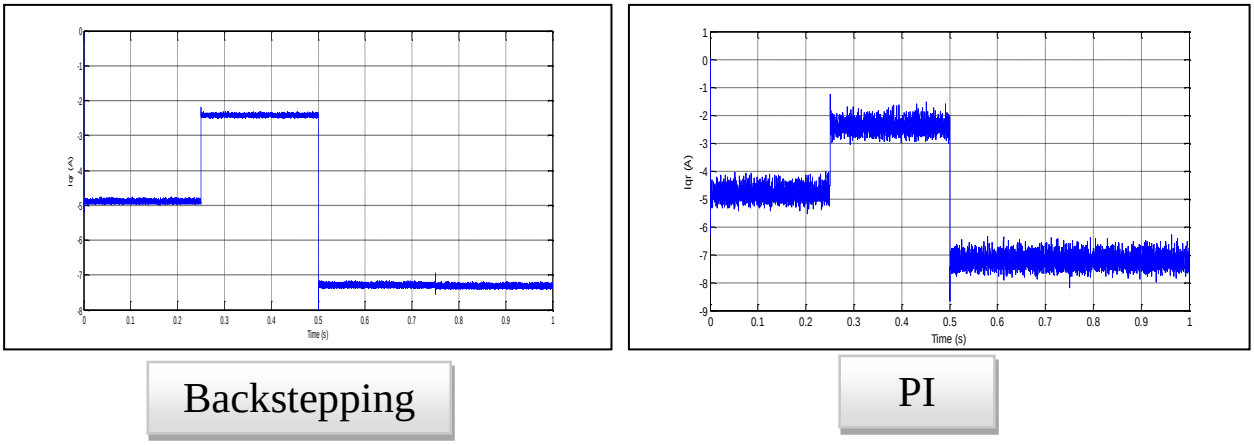


Figure IV. 17 : comparing The Rotor Voltages using a PI controller and the Backstepping Controller

The conclusion drawn from the simulation results is that the Backstepping controller exhibited superior performance and was more satisfactory compared to the classical PI controllers.

Backstepping control is a nonlinear control technique commonly used in control systems. It is designed to stabilize a system by recursively designing a series of controllers to drive the system's states to a desired state. This technique is particularly useful for controlling nonlinear systems or systems with uncertain dynamics.

On the other hand, a proportional-integral (PI) controller is a common type of linear controller widely used in various applications. It provides control action based on the proportional and integral terms of the error between the desired setpoint and the system output.

The simulation results that led to the conclusion could have been obtained by comparing various performance criteria, such as settling time, overshoot, steady-state error, or robustness to

disturbances. Backstepping control might have demonstrated better performance in terms of one or more of these criteria compared to the classical PI controllers.

IV.6.Conclusion:

In conclusion, controlling Doubly Fed Induction Generators (DFIGs) using the Backstepping controller has proven to be an effective approach. The Backstepping control method provides a robust and adaptive control strategy that addresses the complex dynamics and uncertainties associated with DFIG systems.

By employing the Backstepping controller, the control design is divided into multiple steps, allowing for a systematic and sequential approach to handling various control objectives. This control method enables the decoupling of the active and reactive power control loops, leading to improved tracking performance and enhanced transient response.

The backstepping controller leverages Lyapunov stability analysis to ensure the stability and convergence of the control system. This analysis helps in designing control laws that guarantee the desired performance and robustness in the presence of disturbances and parameter variations.

Moreover, the backstepping control approach facilitates the inclusion of advanced control features, such as rotor flux-oriented control and power optimization algorithms, which further enhance the overall system performance and efficiency. However, it is essential to consider certain challenges associated with implementing the Backstepping control strategy for DFIGs. These include the complexity of control design, the need for accurate system modeling, and the computational requirements for real-time implementation.

Overall, the Backstepping controller offers a promising solution for the control of DFIGs, enabling reliable operation, improved performance, and robustness in the face of uncertainties. Further research and development in this area can lead to advancements in renewable energy systems and the integration of DFIGs in various applications, including wind power generation and grid integration.

General Conclusion

General Conclusion:

Industrial systems that rely on control structures often exhibit complex and nonlinear behavior, necessitating the development of control methods tailored specifically for such nonlinear systems. The primary objective of this thesis is to synthesize efficient control laws for Doubly-Fed Induction Generators (DFIG) using the Backstepping control principle, which is based on Lyapunov's direct method.

To begin, a concise description of the DFIG structure and operational principles is provided. The model of the DFIG is then developed utilizing both fixed and rotating reference frames. Through simulations, the established model is validated to ensure its accuracy and reliability.

The theoretical aspects of the nonlinear Backstepping technique are then explored, outlining the step-by-step process involved in establishing control laws using different Backstepping approaches. In particular, Backstepping control based on the Lyapunov function is employed to generate control laws for the active and reactive powers of the DFIG.

Finally, the developed control laws are subjected to simulation-based validation, demonstrating their highly satisfactory performance. These results present a promising outlook for the practical implementation of the proposed control method in real-world scenarios, further highlighting its potential benefits for industrial systems utilizing DFIGs.

Annexe

Data of the double-fed induction machine
Valeurs nominales : 1.5KW ; 220V- 50Hz ; 15/8.6A ; 1425 tr/min.

Settings 1 :
Rs (Stator resistance) =1.2Ω
Rr (Rotor resistance) =1.8 Ω
Ls (Stator inductance) = 0.1554H
Lr (Rotor Inductance) = 0.1568H
M (Mutual Inductance) = 0.15H

Settings 2 :
Rs (Stator resistance) =4.85
Rr (Rotor resistance =3.805
Ls (Stator inductance) =0.274
Lr (Rotor Inductance) =0.274
(Mutual Inductance) =0.258
Ws (electrical frequencies respectively of the stator) =314
g (slip of the machine)=0.05
wr (electrical frequencies respectively of the rotor) =15.7

Mechanical constants:
J (Moment of inertia) = 0.2 Kg.m2
f (Coefficient of friction) = 0.001N.m.s/rd

Bibliography

[1] BOLDEA I. “The Electric Generator Handbook: variable speed generators, CRC press Taylor & Francis group, 2006, New York, U.S.A.

[2] F. BONNET, « Contribution à l’Optimisation de la Commande d’une Machine Asynchrone à Double Alimentation utilisée en mode Moteur ». Thèse de Doctorat en Génie Électrique, Institut National Polytechnique de Toulouse, France, 2008

[3] AZAIZIZA.R, "Etude et commande d'une machine asynchrone à double alimentation alimentée par un convertisseur multi-niveaux", Mémoire de magister en génie électrique, Université de Boumerdes, Algérie, 2008.

[4] AKKARI.N, « Contribution à l’amélioration de la robustesse de la commande d’une machine asynchrone à double alimentation » ; thèse de doctorat. Université de Batna, Algérie 2010

[5] M.Hallouz, N.Kabache, etS.Moulahom, « DTC Backstepping Based control of Double Fed Induction Generator ». in 2019 Progress in applied Electrical Enggineering(PAEE), 2019,p.1-6 .

[6] L PENG, « Reconfiguration du dispositif de commande d’une éolienne en cas de creux de tension », thèses de doctorat, université de Lille, 2010

[7] L. Khettache «Etude et commande d’un système Eolien à base d’une Machine Electrique Double Alimentée » thèse de magister université de Batna

[8] J. Martin, «Energies éoliennes», Techniques de l’Ingénieur, traité de Génie énergétique, pp. B 8 585 1- B 8 585 21.

[9] KHATTACHE.L.«Etude et commande d’un système éolienneà base d’une machine électrique double alimentée». Mémoire de Magister .Université de Batna.2007.

[10] I. HAMZAOUI, «Modélisation de la machine asynchrone à double alimentation en vue de son utilisation comme aérogénérateur», Mémoire Magister ,ENP.20/10/2008

[11] L. Khettache, ″Etude et Commande d’un Système Eolien à Base d’une Machine Electrique Double Alimentée″, Mémoire de Magister, Université de Batna,Algérie , 2007.

[12] F.POITIER, «Etude et commande de la génératrice asynchrone pour l’utilisation de l’énergie éolienne», thèse de doctorat, Université de Nantes, 19/11/ 2003.

[13] Y. BENCHERIF «Modélisation et commande d’une Machine Asynchrone à Double Alimentation pour la production de l’énergie éolienne» , Mémoire d’ingénieur d’état en Génie Electrique,ENP.2008

[14] A. Abdelli, ″Optimisation Multicritère d’une Chaîne Eolienne Passive″, Thèse de Doctorat en Génie Electrique, Institut National Polytechnique de Toulouse, France,2007.

[15] S. El Aimani, □Modélisation de Différentes Technologies d’Eoliennes Intégrées dans un Réseau de Moyenne Tension□, Thèse de Doctorat en Génie Electrique, Université des Sciences et Technologies de Lille, France, 2004.

[16] Jamal A. Baroudi, Venkata Dinavahi_, Andrew M. Knight, «a review of power converter topologies for wind generators», Renew Energy (2007),

[17] A. Chaiba, « commande de la machine asynchrone a double alimentation par des techniques de l'intelligence artificielle », thèse de doctorat, université de Batna, 2010.

[18] Y .Elbia, « commande floue optimisée d'une machine asynchrone à double alimentation et a flux oriente », Mémoire de magistère, université de Batna,2009.

[19] V .Paul-Etienne, « commande non-linéaire d'une machine asynchrone a double alimentation », thèses de doctorat, Institut polytechnique de Toulouse, 2004.

[20] S. El Aimani, B. François, F. Minne, B. Robyns « Modelling and Simulation of Doubly Fed Induction Generators for Variable Speed Wind Turbines integrated in a Distribution Network", EPE 2003, Toulouse.

[21] J.R. Saenz, A. Tapia, G. Tapia, X. Ostolaza, I. Albizu, F. Pérez-Hidalgo, M. Irizar, "Reactive Power Regulation in Wind Farms : Control Strategies", EPE 2001 –Graz.

[22] José Coto Aladro, Isabel Garcia Alvarez, Guzmán Diaz Gonzalez, Javier Gomez-Aleixandre, "Wind speed model design and dynamic simulation of a wind farm embedded on distribution networks", Dpt d'Ingeniera Electrica, Electronica, Computadores y de Sistemas Escuela Politecnica Superior de Ingenieros Uniyersidad de Oviedo Campus de Viesques

[23] J.P Caron, J.P Hautier, « Modélisation de la MAS, Commande vectorielle », éditions techniques, Paris, 1995.

[24] A .Boyette, « contrôle-commande d'un générateur asynchrone à double alimentation avec système de stockage pour la production éolienne », thèse de doctorat, université de Nancy, 2006.

[25] H. H. Lee, P. Q. Dzung, L. M. Phuong, L. D. Khoa, N. H. Nhan, "A New Fuzzy Logic Approach For Control System Of Wind Turbine With Doubly Fed Induction Generator", International Forum on Strategic Technology (IFOST 2010), Ulsan, South Korea, 13-15 octobre 2015.

[26] P. Andreas, "Analysis, Modeling and Control of Doubly-Fed Induction Generators for Wind Turbines", PhD Thesis, University of Technology, Goteborg, Sweden, 2005.

[27] Nonlinear Backstepping Control of a Double-Fed Induction Generator M. Doumi*, A.G. Aissaoui**, A. Tahour**, M. Abid**, and K. Tahir**